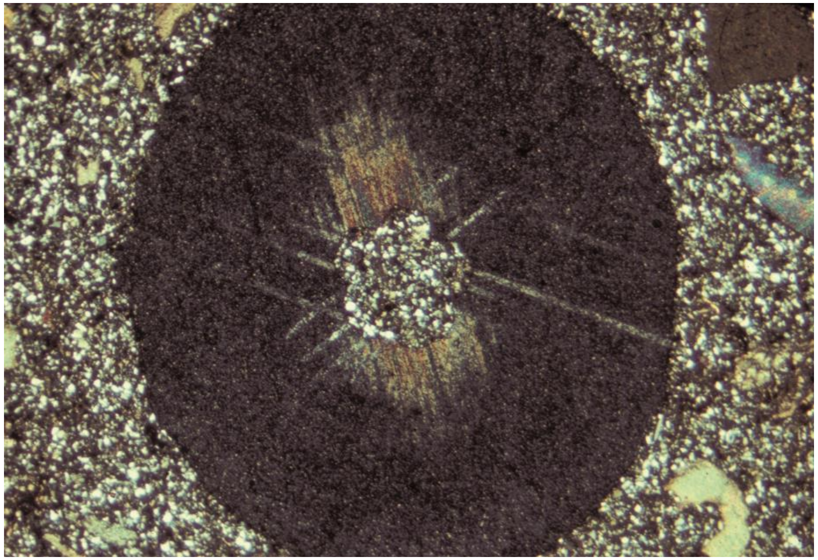

The Three Elements of Structural Geology

Sponsored by

Fourth Sessions

Terry Engelder

Professor of Geosciences, The Pennsylvania State University

Table of Contents

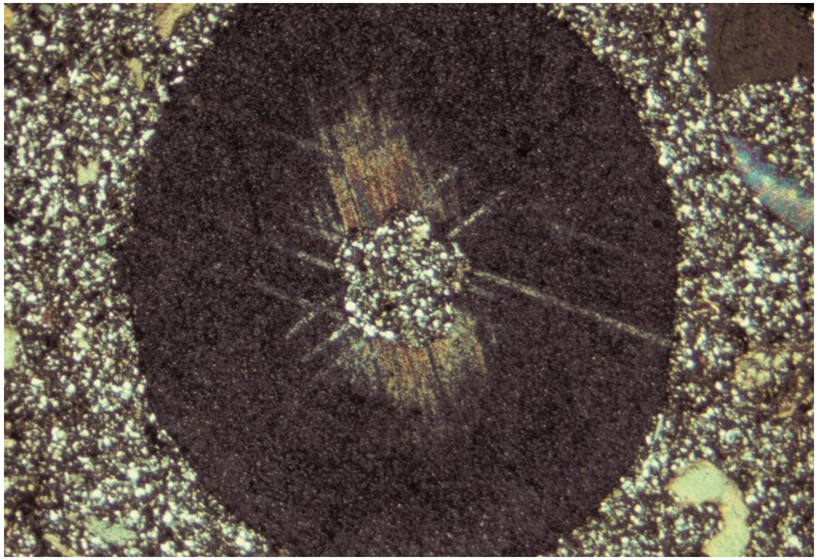

4.1.1 Properties of Faults

An AAPG Short Course by

Terry Engelder

Professor of Geosciences

The Pennsylvania State University

Faults

- Normal
- Reverse
- Strike-slip

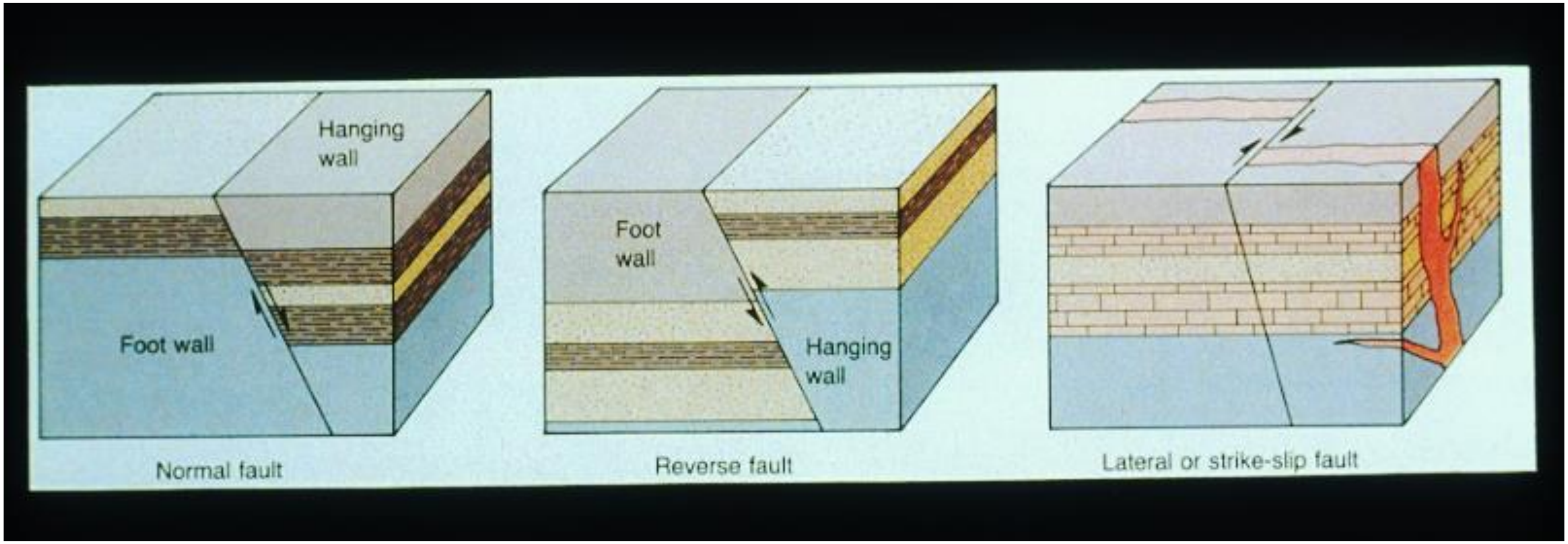

Reverse Fault to Detachment (Décollement)

Terry Engelder

Normal Fault

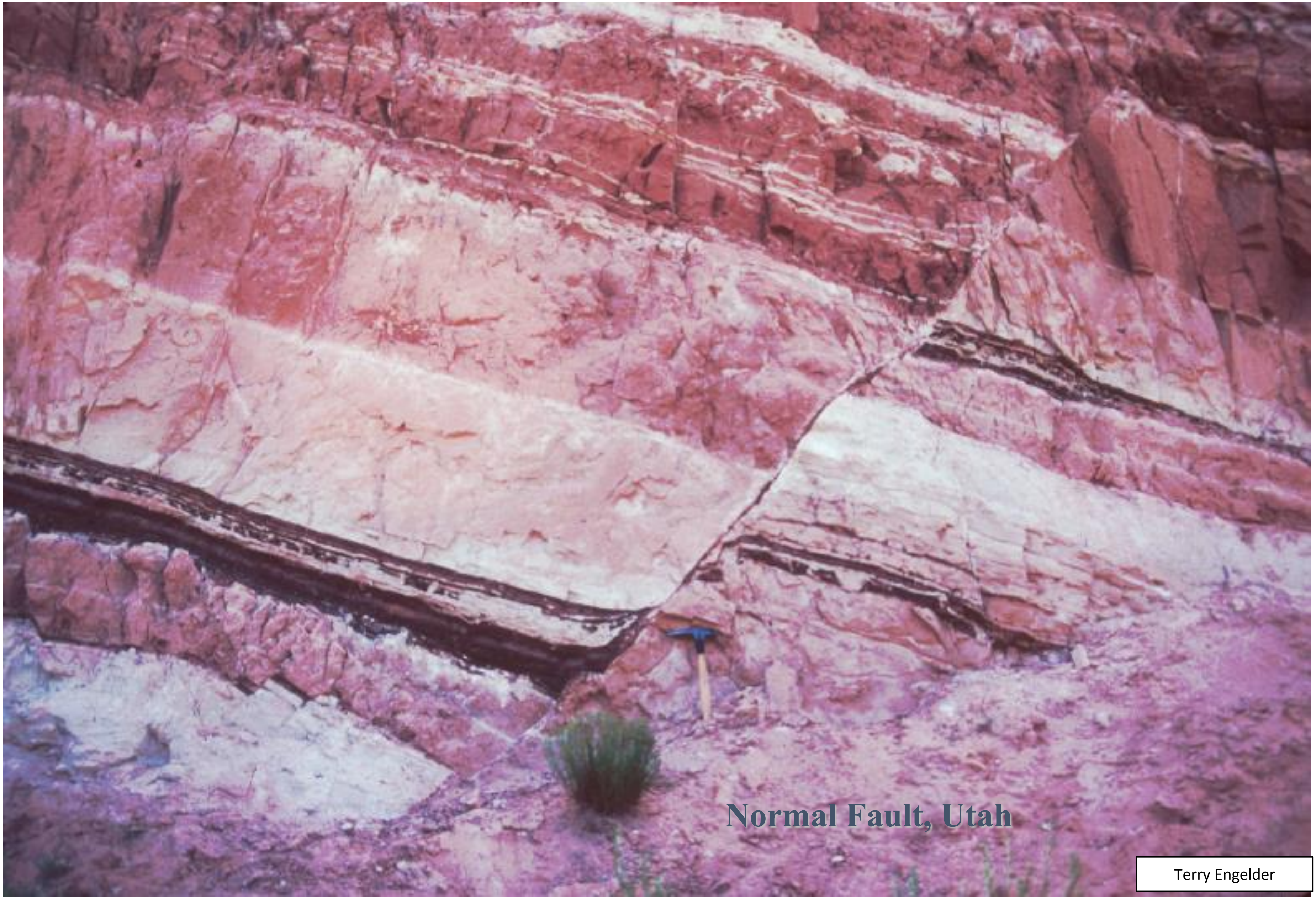

Terry Engelder

Strike-slip Fault

Andersonian Classification of Faults

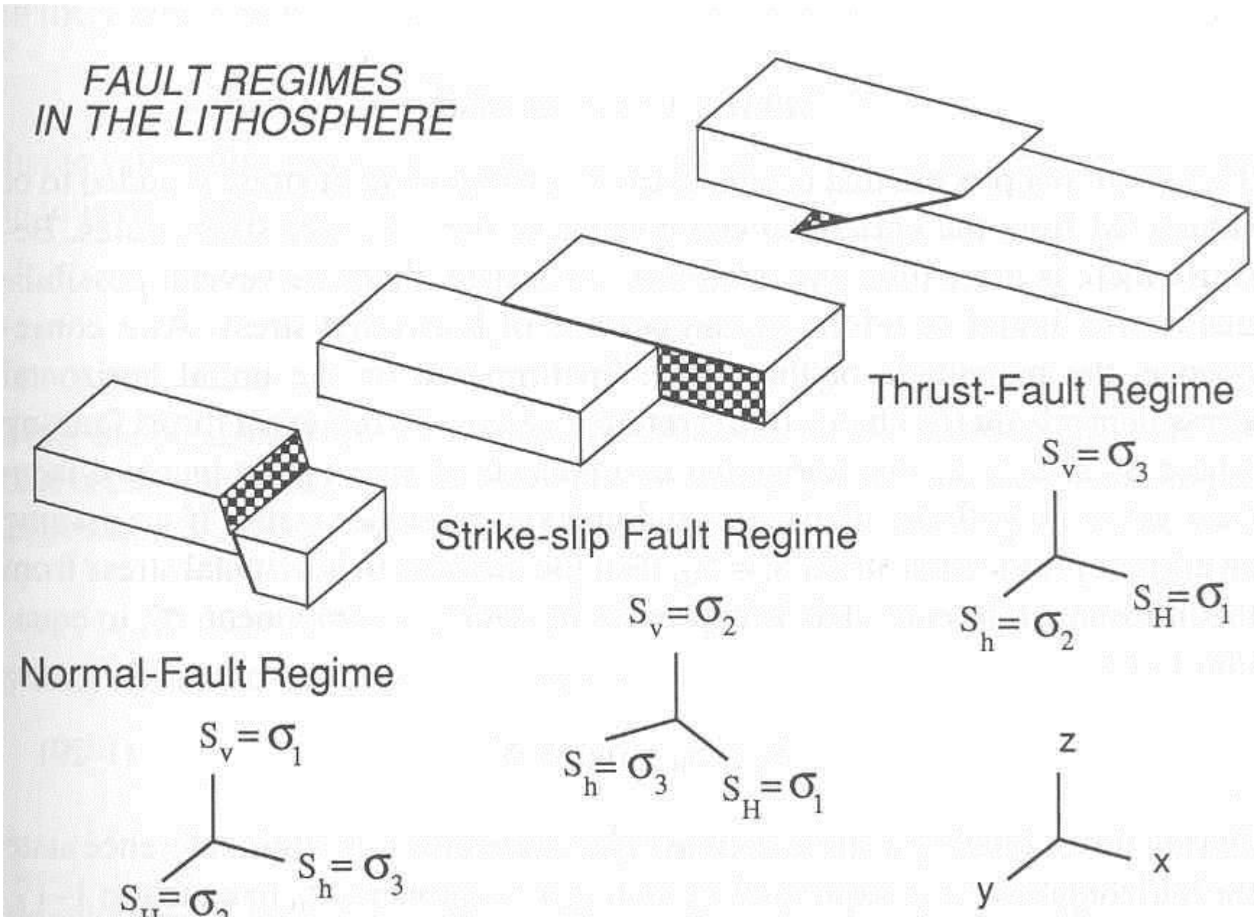

Terry Engelder

Fault-related rocks: A terminology

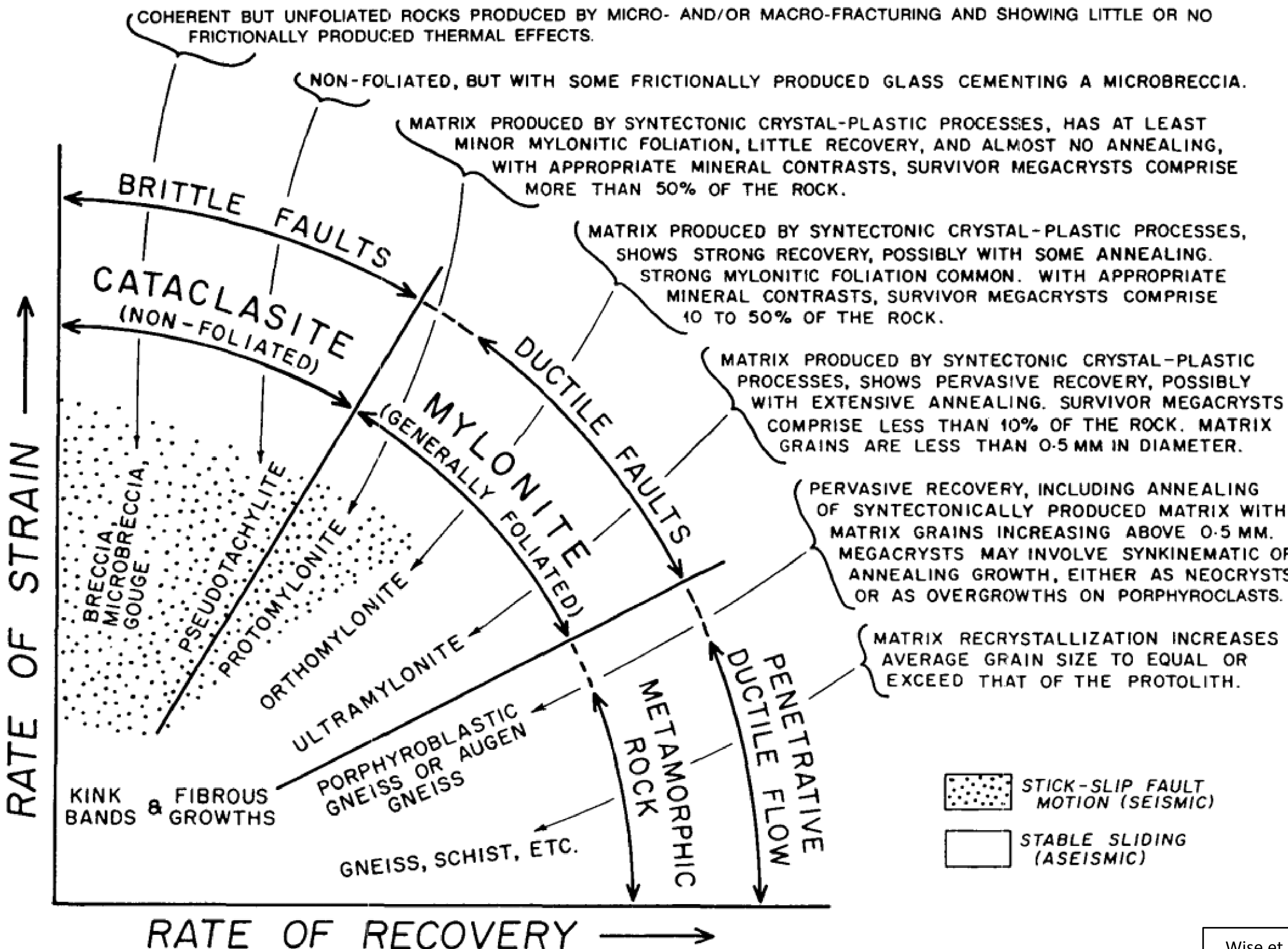

Wise et a., 1984

Fault-related rocks: A terminology

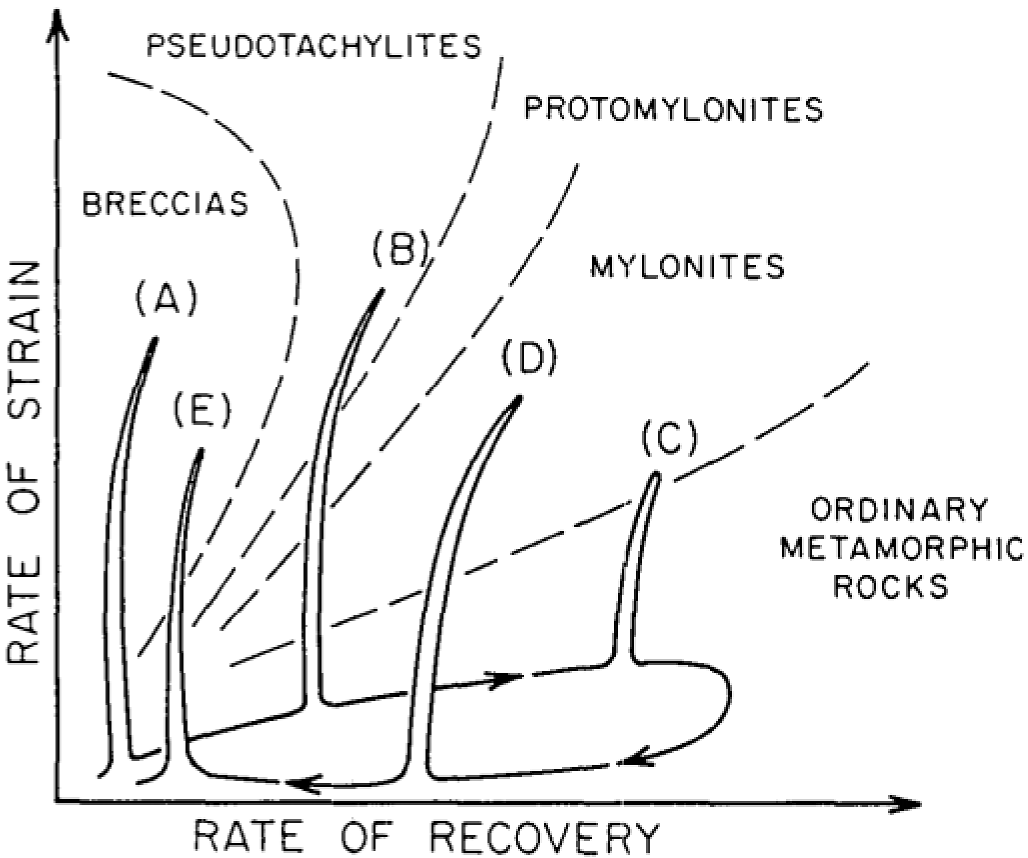

The evolutionary history of a rock in the vicinity of a major fault zone might follow the path illustrated here. The main rock mass might pass through a series of deformations involving generally low strain rates in going to high metamorphic grade and back to surface conditions. Superimposed on this general patten:. could be a number of brief pulses of high strain rates, as indicated by the spikes in Figure 2. Frictional heating at higher strain rates might cause temporary, slightly increased recovery rates, as suggested by curvature of the spikes to the right. Early-formed breccia and gouge (A) or mylonite (B) would be homogenized and in part camouflaged by later metamorphism and ductile flowage. Mylonitic and cataclastic rocks produced after the metamorphic peak would be much more likely to survive in recognizable form. Some of the early-formed mylonites (D) would be likely to have a variety of younger deformational features superimposed on them, such as foliation, kink bands, and passive and/or flexural folds, or they might be slickensided or brecciated by late fault motions (E). Thus, a typical mylonitic specimen should be considered the end result of a long history of these types of deformations and metamorphisms under a variety of pressure, temperature, and strain conditions.

Wise et a., 1984

Properties of Faults

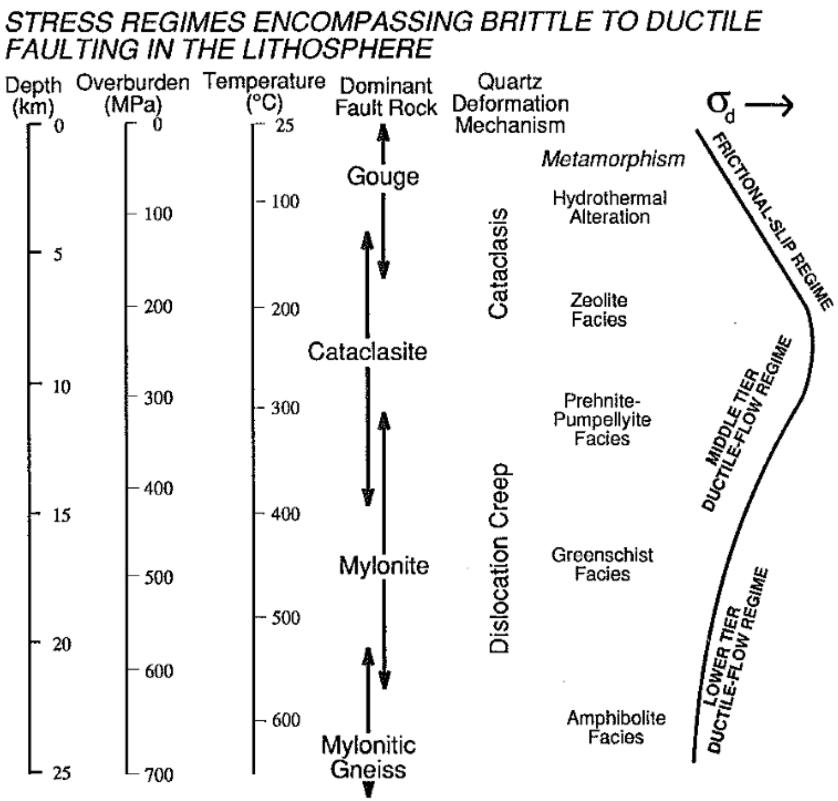

Faulting is affected by changes in mechanism from brittle to ductile behavior as evidenced by exhumed fault zones which were once active at great depths. Some famous examples include the Moine Thrust of Scotland, the Alpine Fault of New Zealand, the Outer Hebrides Thrusts of Scotland, the Greenland Shear Zones, and the mantled gneiss domes of the southwestern United States. A correlation is seen between depth of burial and several parameters including temperature, confining pressure, metamorphic grade, and general type of fault rock (Sibson, 1977, 1986). Fault rock is characterized by grain reduction through either brittle or ductile mechanisms with the three main types of fault rock being gouge, cataclasite, and mylonite. *Gouge,* a product of frictional slip, is a cataclastic material without fabric or cohesion; grain-size reduction is dominated by brittle fracture. A *cataclasite* is a nonfoliated faultzone material with cohesion, whereas a *mylonite* is a foliated fault-zone material with cohesion. Both cataclasites and mylonites are the product of semibrittle deformation with differences depending, in part, on strain rate versus recovery rate of grains. As a general rule, higher σ_d, is associated with higher strain rate.

Terry Engelder

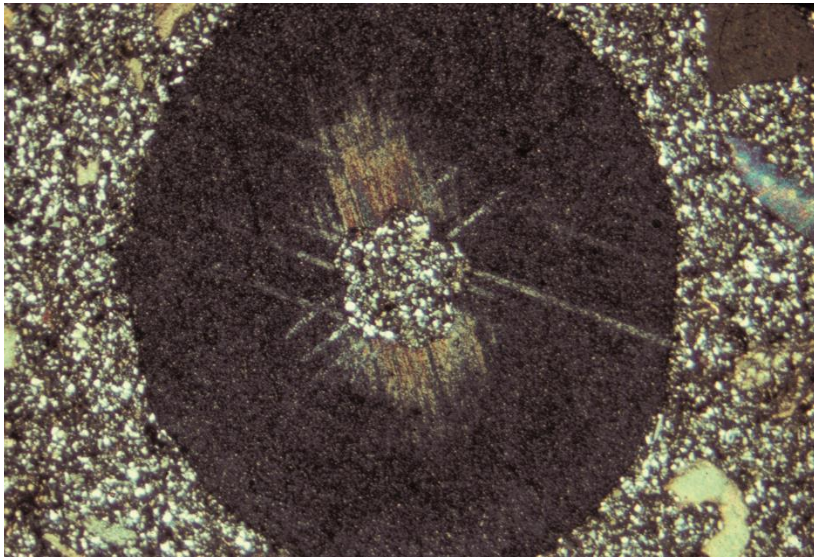

4.1.2 – Faulted Surfaces

An AAPG Short Course by
Terry Engelder
Professor of Geosciences
The Pennsylvania State University

Classification of faulted surfaces

- Means, 1987
- Petit, 1987

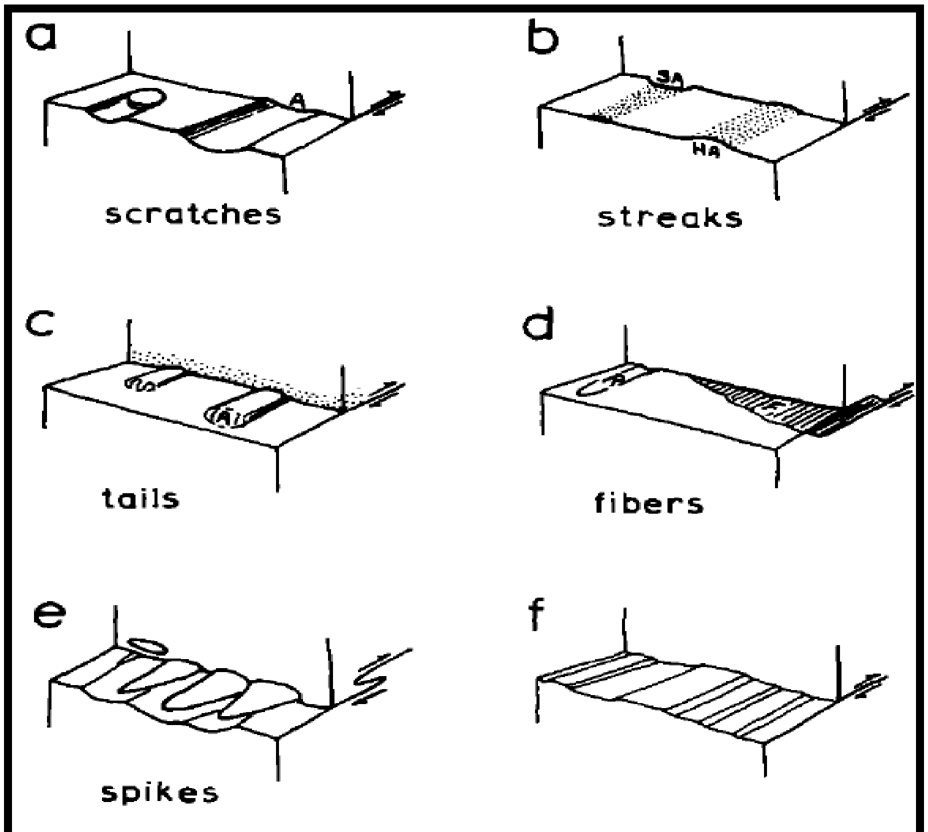

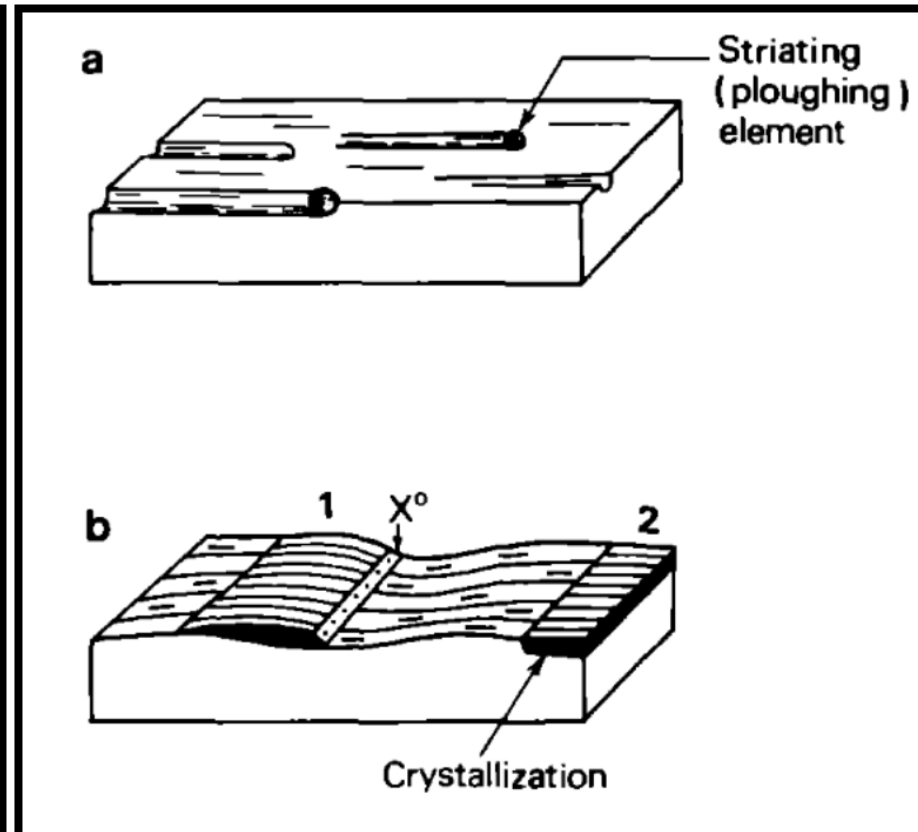

Classification of faulted surfaces

- Doblas, 1998

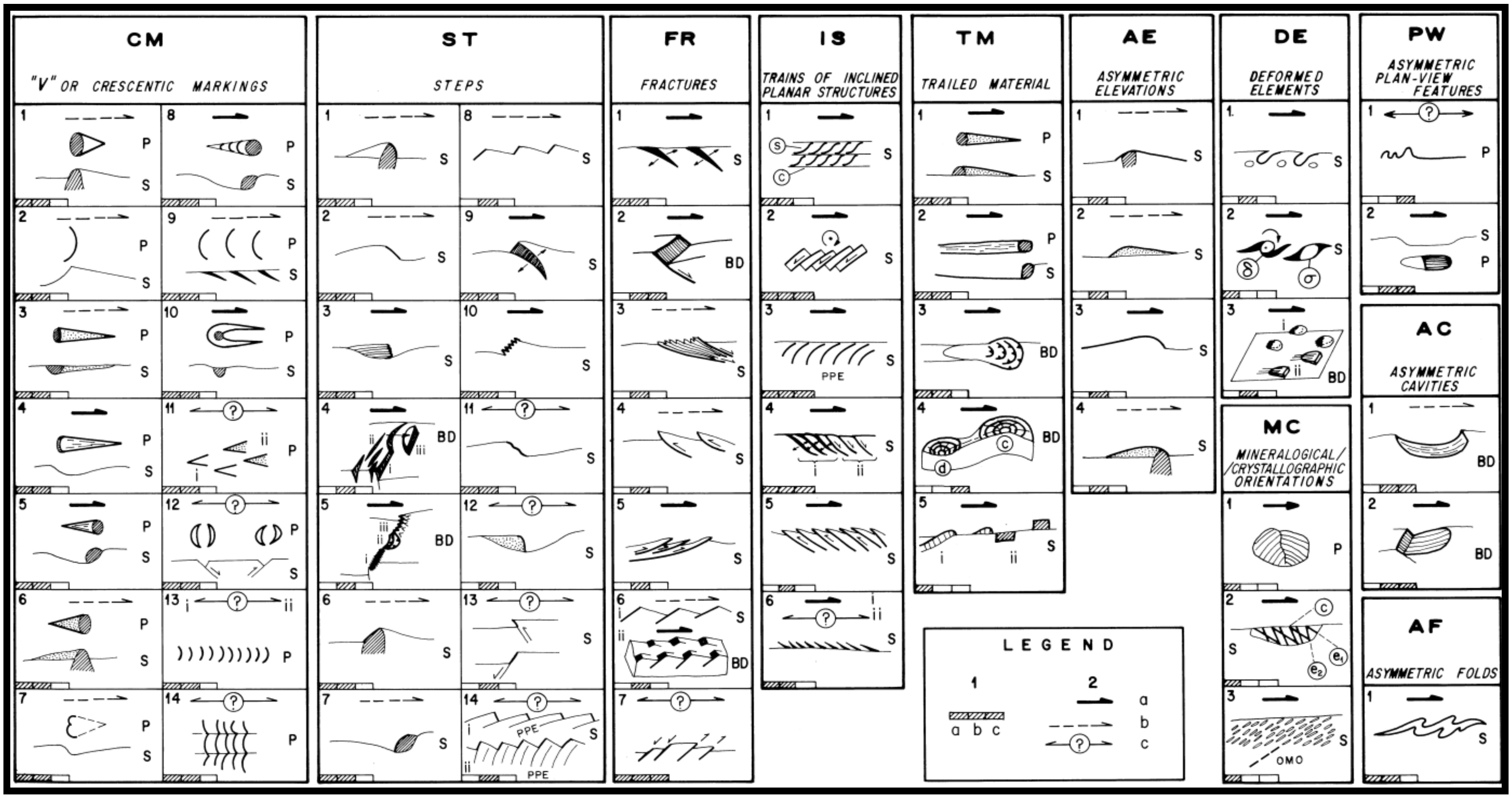

Classification of faulted surfaces

- Brittle:
  - Asperity ploughing
  - Debris ploughing
  - Step-like slip
- Ductile:
  - Fiber growth
  - Amorphous surfaces
  - Shiny surfaces

Aydin & Engelder, 2014

53 cm thick cleavage duplex 2 m above the Selinsgrove Limestone in the Marcellus Formation at Newtown Hamilton.

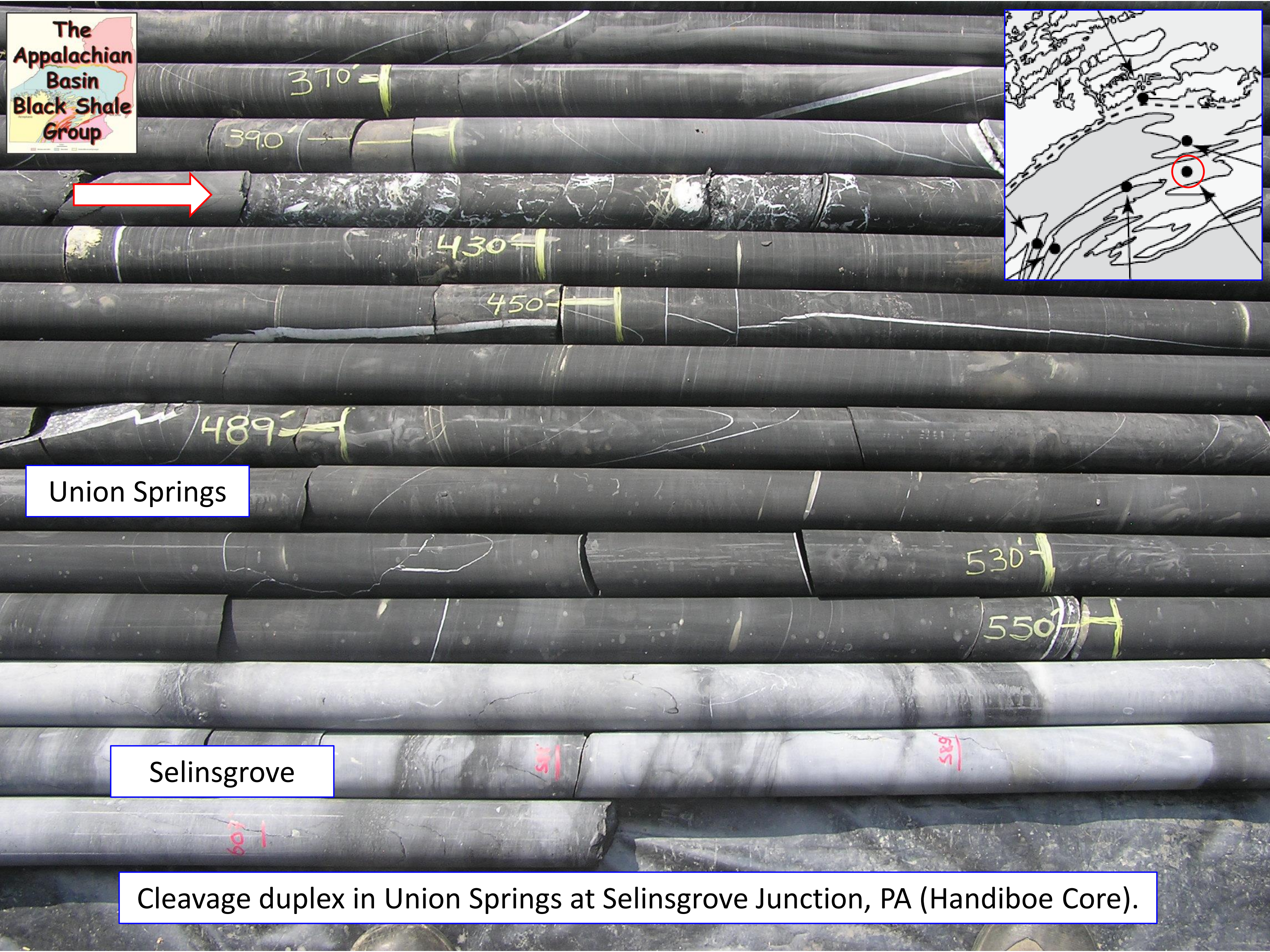

Cleavage duplex in Union Springs at Selinsgrove Junction, PA (Handiboe Core).

Cleavage duplexes in Utica = High pore pressure fluid (gas & water)

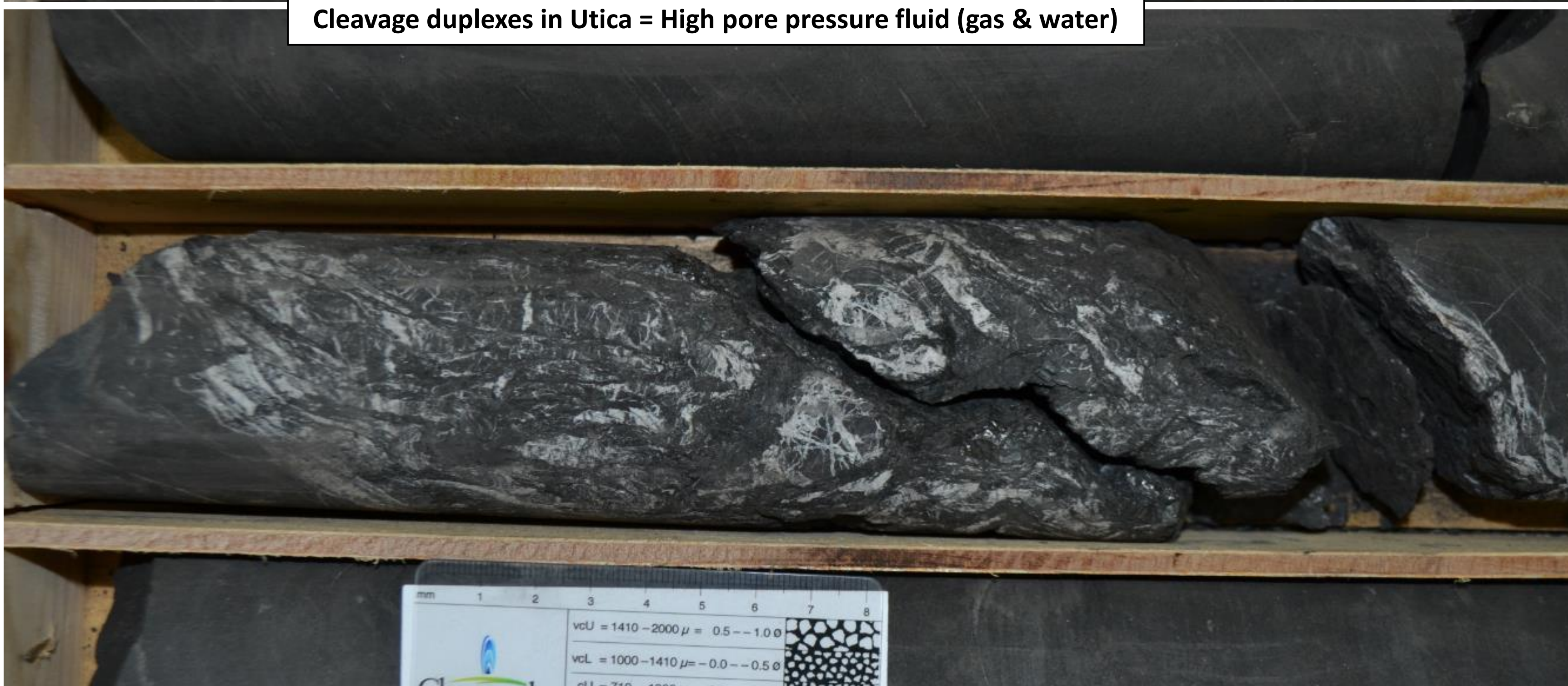

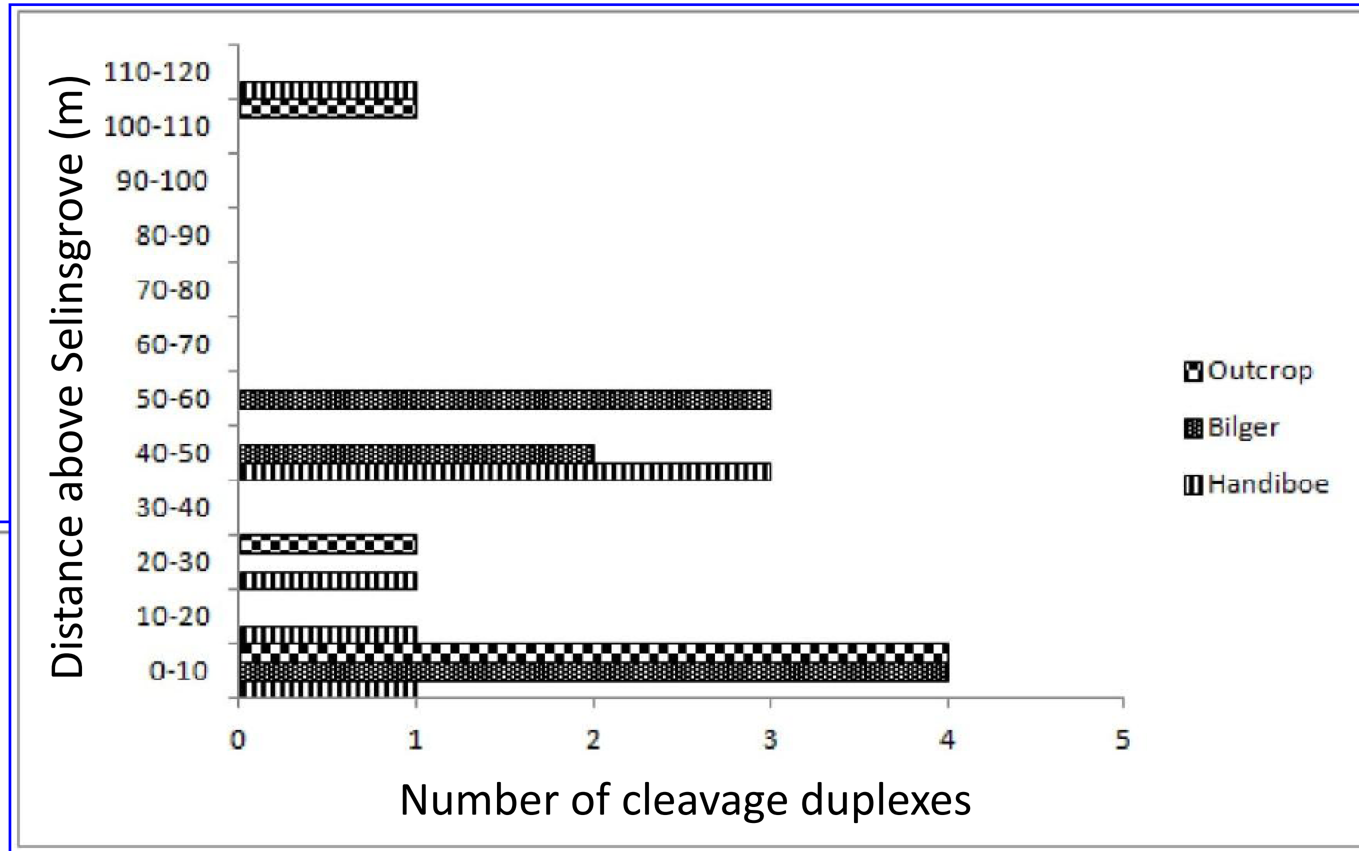
Distance above Selinsgrove (m)
110-120
100-110
90-100
80-90
70-80
60-70
50-60
40-50
30-40
20-30
10-20
0-10
0
1
2
3
4
5
Number of cleavage duplexes
Outcrop
Bilger
Handiboe

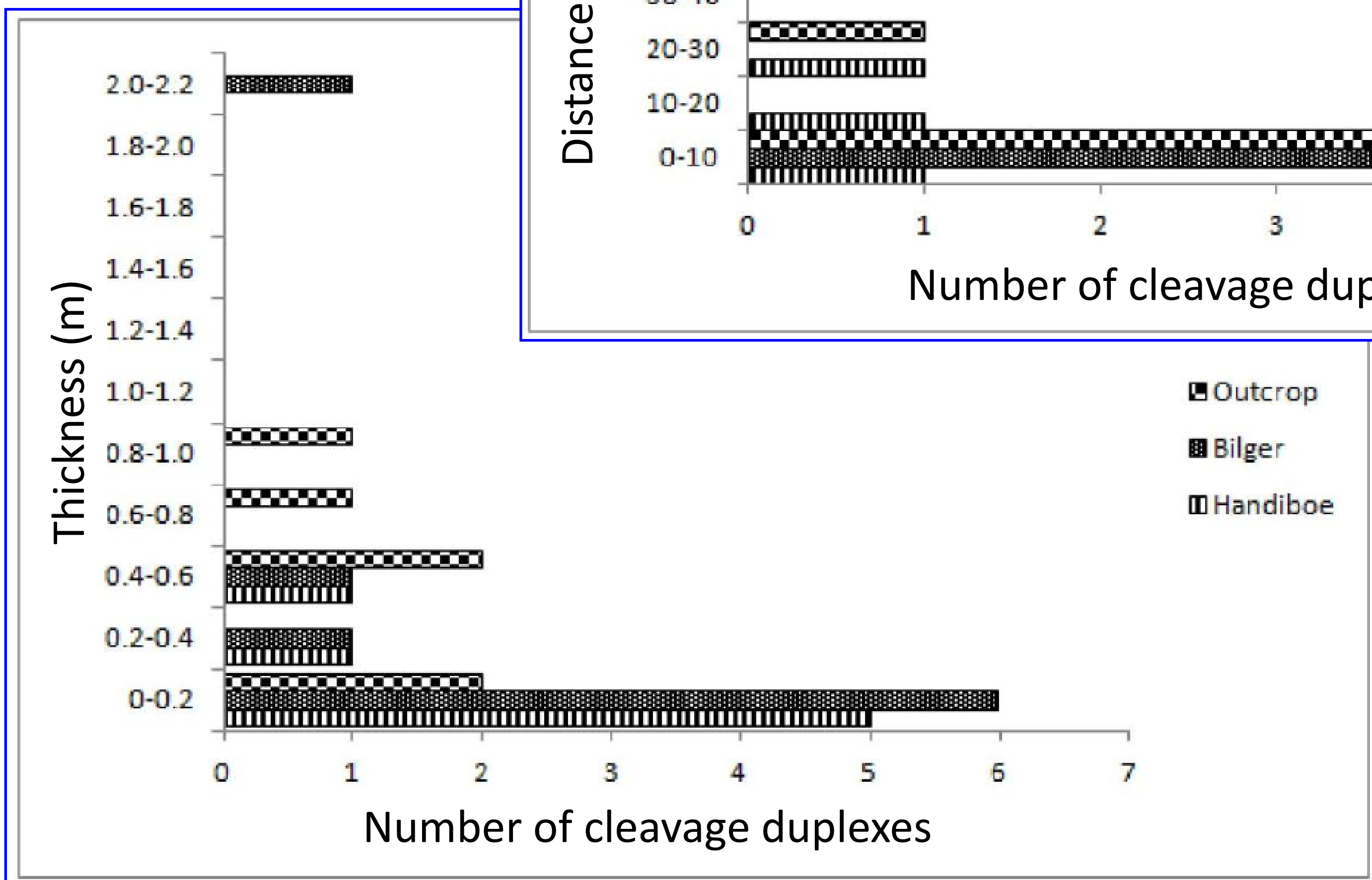
Thickness (m)
2.0-2.2
1.8-2.0
1.6-1.8
1.4-1.6
1.2-1.4
1.0-1.2
0.8-1.0
0.6-0.8
0.4-0.6
0.2-0.4
0-0.2
0
1
2
3
4
5
6
7
Number of cleavage duplexes
Outcrop
Bilger
Handiboe

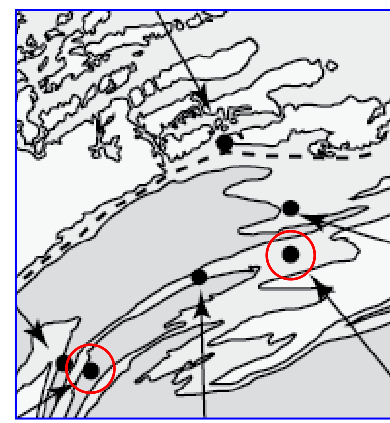

Bedding-parallel slip surfaces in the Lock Haven Formation north of Williamsport, PA.

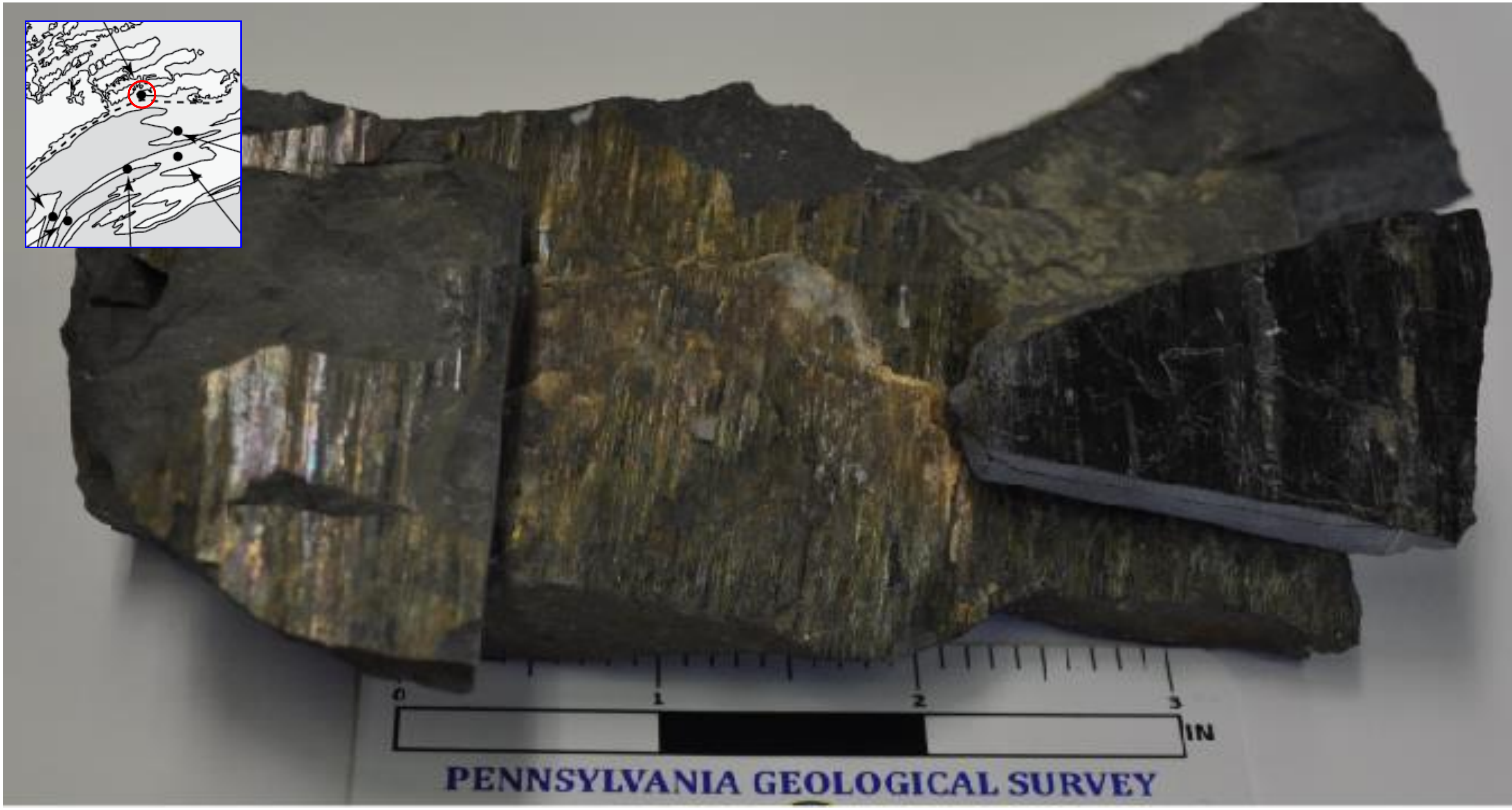

A mirror slip surface.

Green chlorite over white quartz over 'black' graywacke with ridge-in-groove striation.

A mirror slip surface that appears black when green chlorite sits directly on 'black' graywacke.

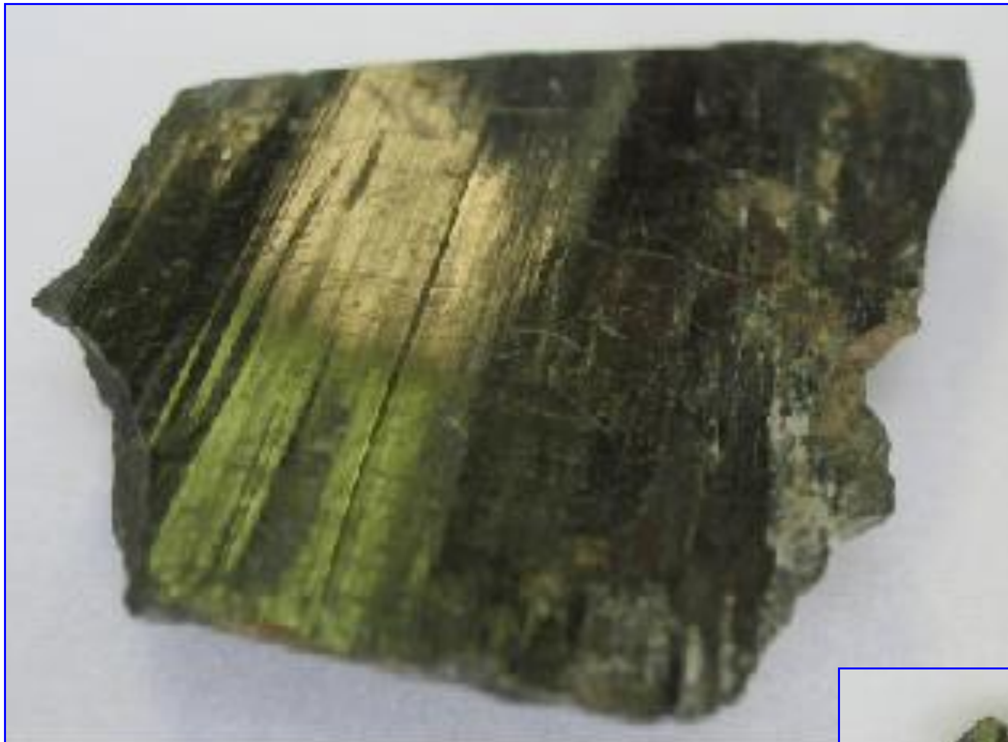

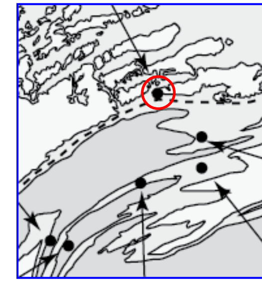

(Left) Mirror slip surface of a chlorite film on a greywacke matrix. Olive green light refracts from the mirror.

(Right) Ridge-in-groove striation on bedding slip surface in Lock Haven Formation showing the olive green color of a chlorite film on white quartz fibers.

The morphology of intraformational slip surfaces (ISS) in the Mahantango-Marcellus section

slip fibers

Mahantango (Bilger 117.49 m)

Oatka Creek (Handiboe 145.57 m)

Union Springs (Handiboe 2.36 m)

Union Springs (Erb 4.30 m)

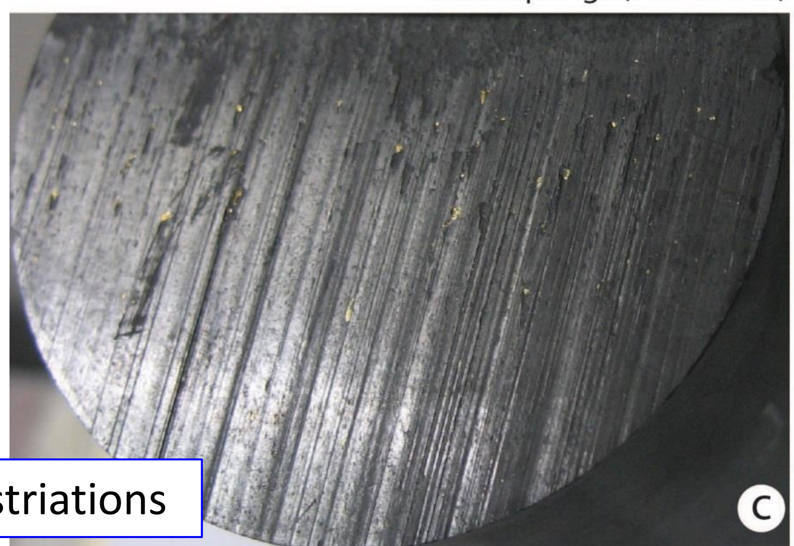

ridge-in-groove striations

Progressive mineral development on slip surfaces.

Mahantango (Bilger, 108.81 m)

Union Springs (Erb, 4.63 m)

Union Springs (Handiboe, 10.57 m)

Union Springs (Handiboe, 31.84 m)

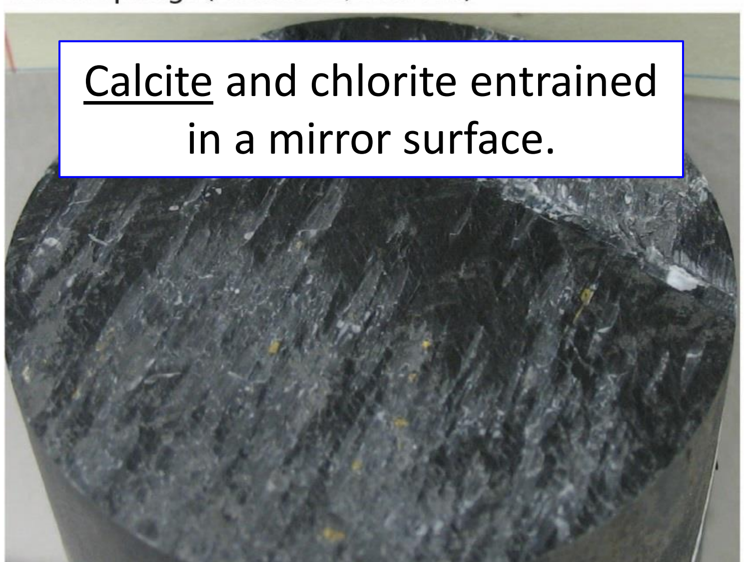

Distribution of ISS in four ABBSG cores

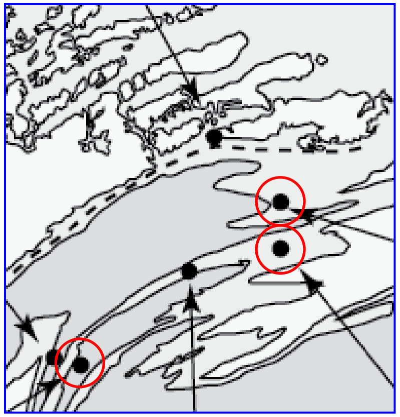

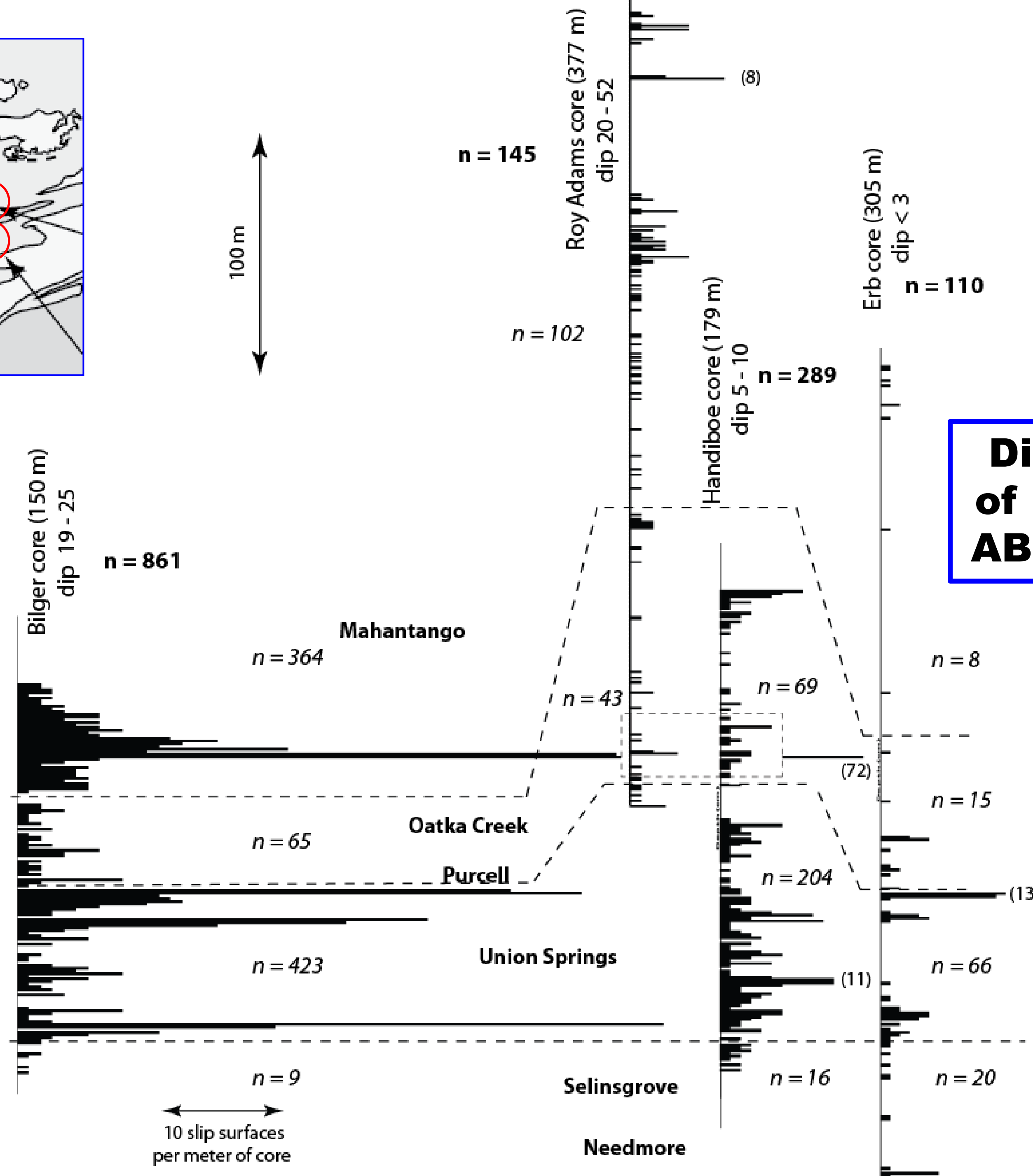

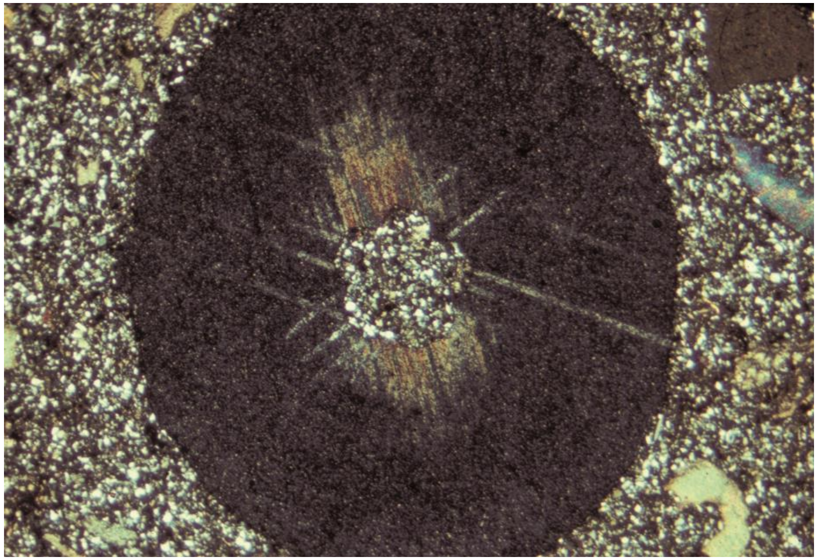

4.1.3 Fault Seals

An AAPG Short Course by
Terry Engelder
Professor of Geosciences
The Pennsylvania State University

Fault Terminology

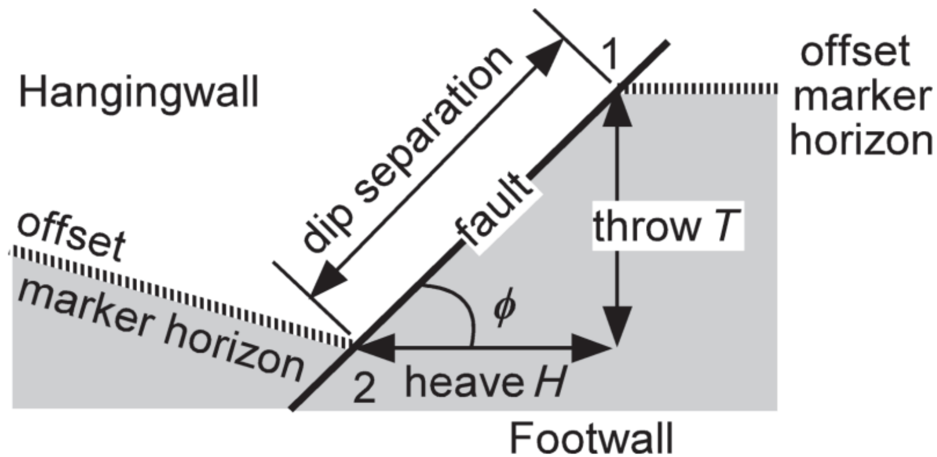

Terry Engelder

Allan Diagram

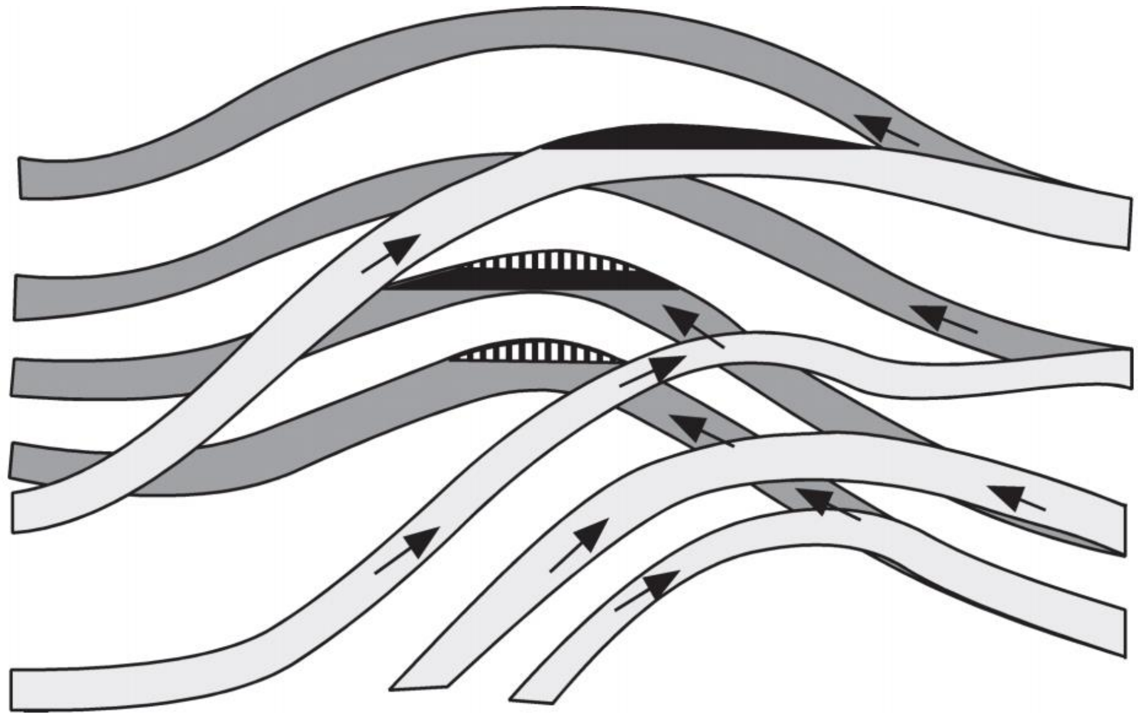

Allan diagram showing fluid migration pathways through permeable beds separated by impermeable beds; footwall *shaded*. *Arrows* give migration routes of fluids that are lighter than water. Oil accumulations are *solid black*; gas accumulation is indicated by *vertical lines*. (from Allan 1989)

Fault Properties

- Shale gouge ratio (SGR), i.e. the proportion of shale which has moved past each point on a fault
- Gouge ratio is an estimate of the proportion of fine-grained material entrained into the fault gouge from the wall rocks.
- Smear factor methods (including clay smear potential and shale smear factor) estimate the profile thickness of a shale drawn along the fault zone during faulting.

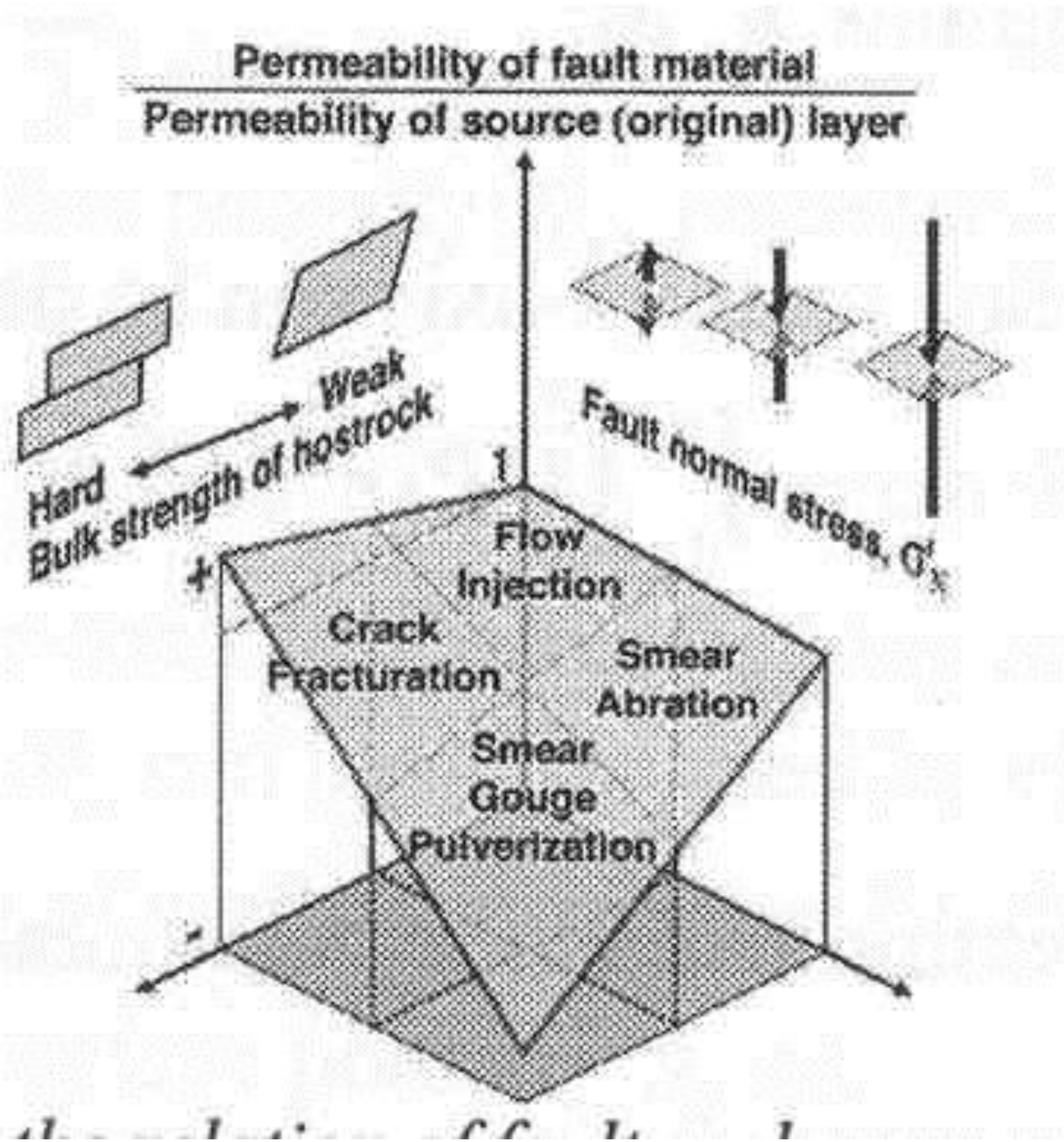

- Effect of rock properties and stress on relative permeability of fault zone rock.

Suzuki, 2003

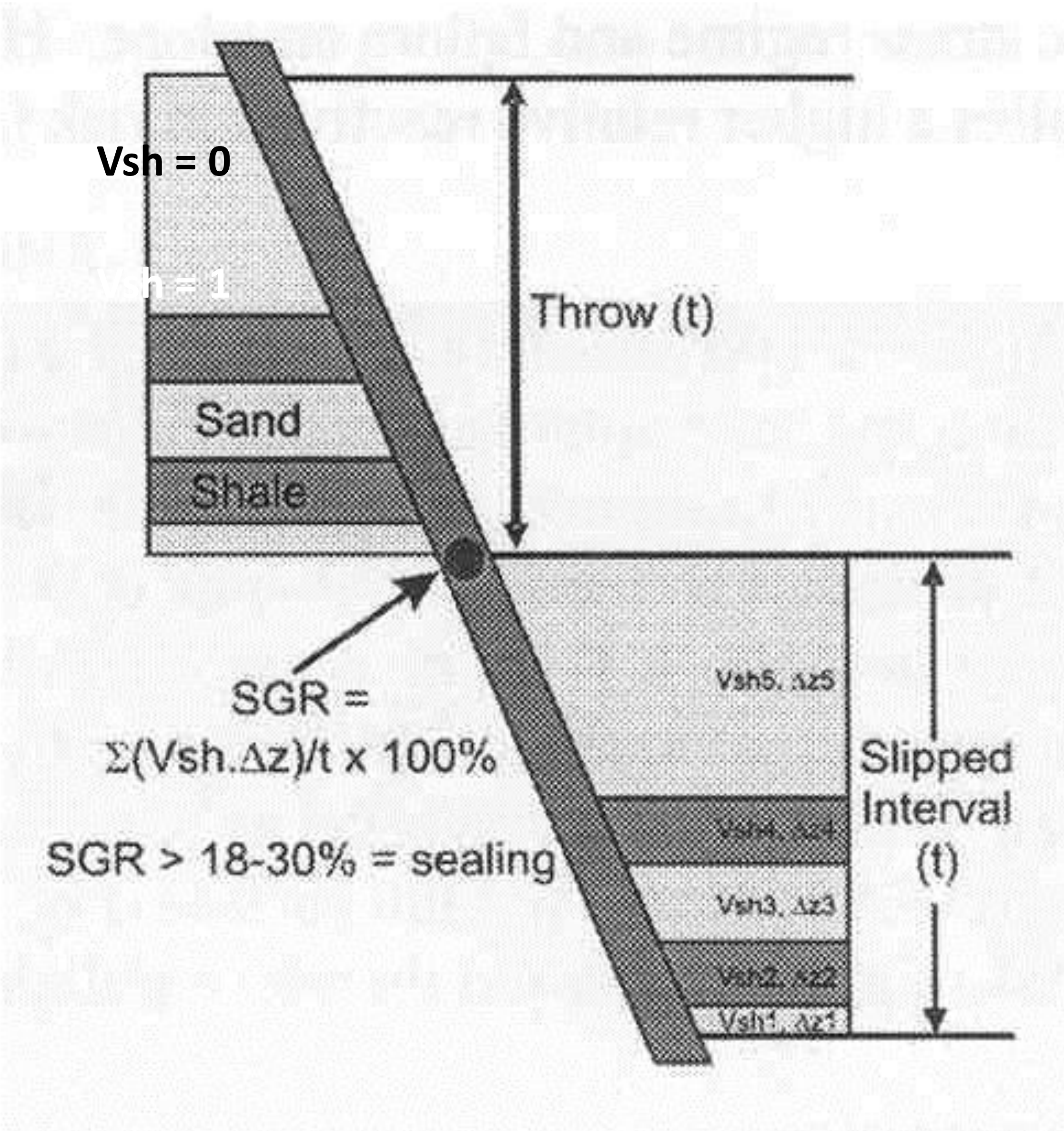

- Conventional fault seal analyses estimate fault zone shale content (i.e., shale/gouge ratio) which is considered to impart a first order control on fault rock capillary properties.

Yielding et al., 1997

Triassic sandstones, High Atlas, Morocco

- Normal fault with low SGR

www.dstu.univ-montp2.fr

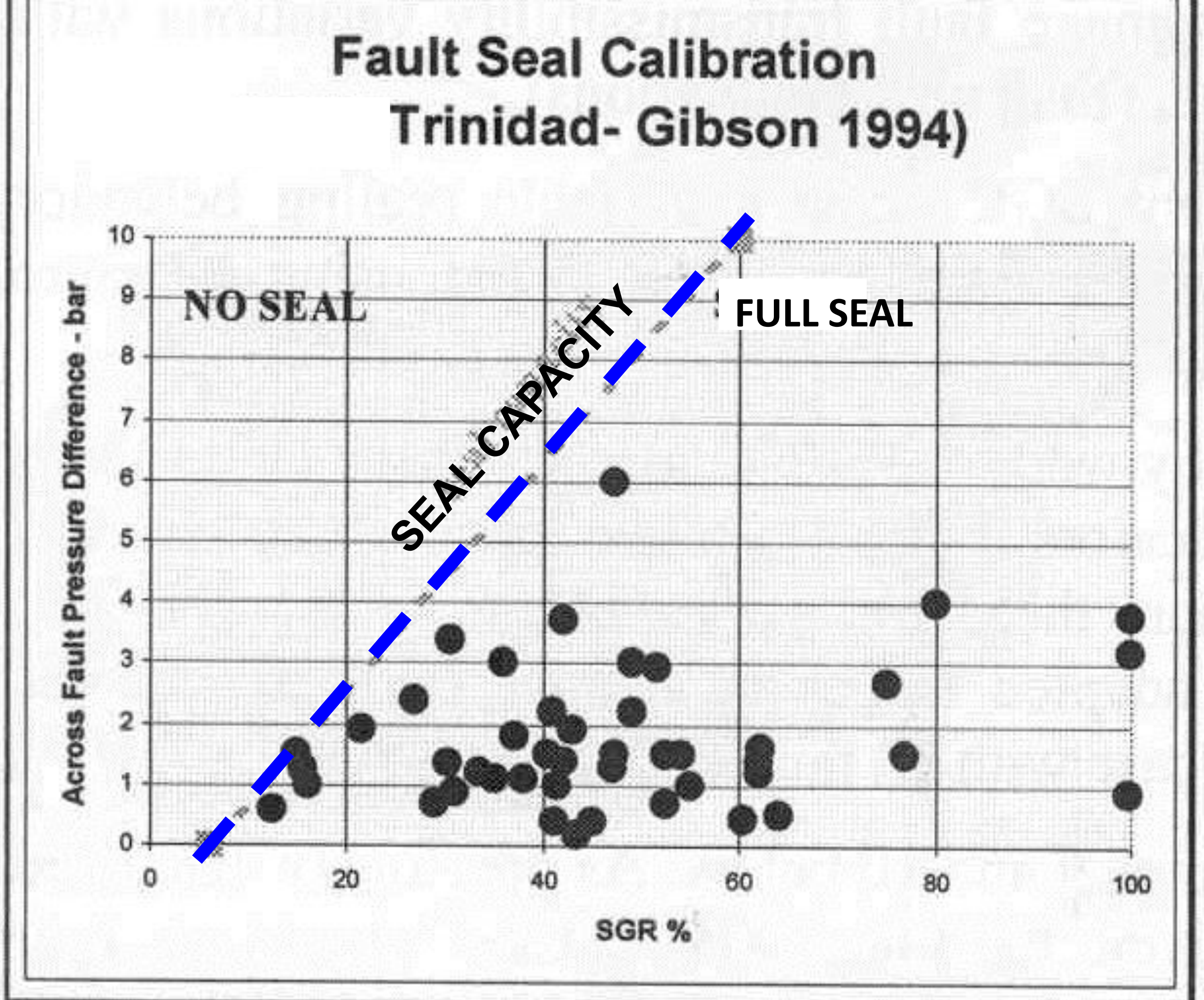

- Offshore Trinidad: Dynamic seal across siliciclastic faults as a function of shale/gouge ratio.

Gibson, 1994

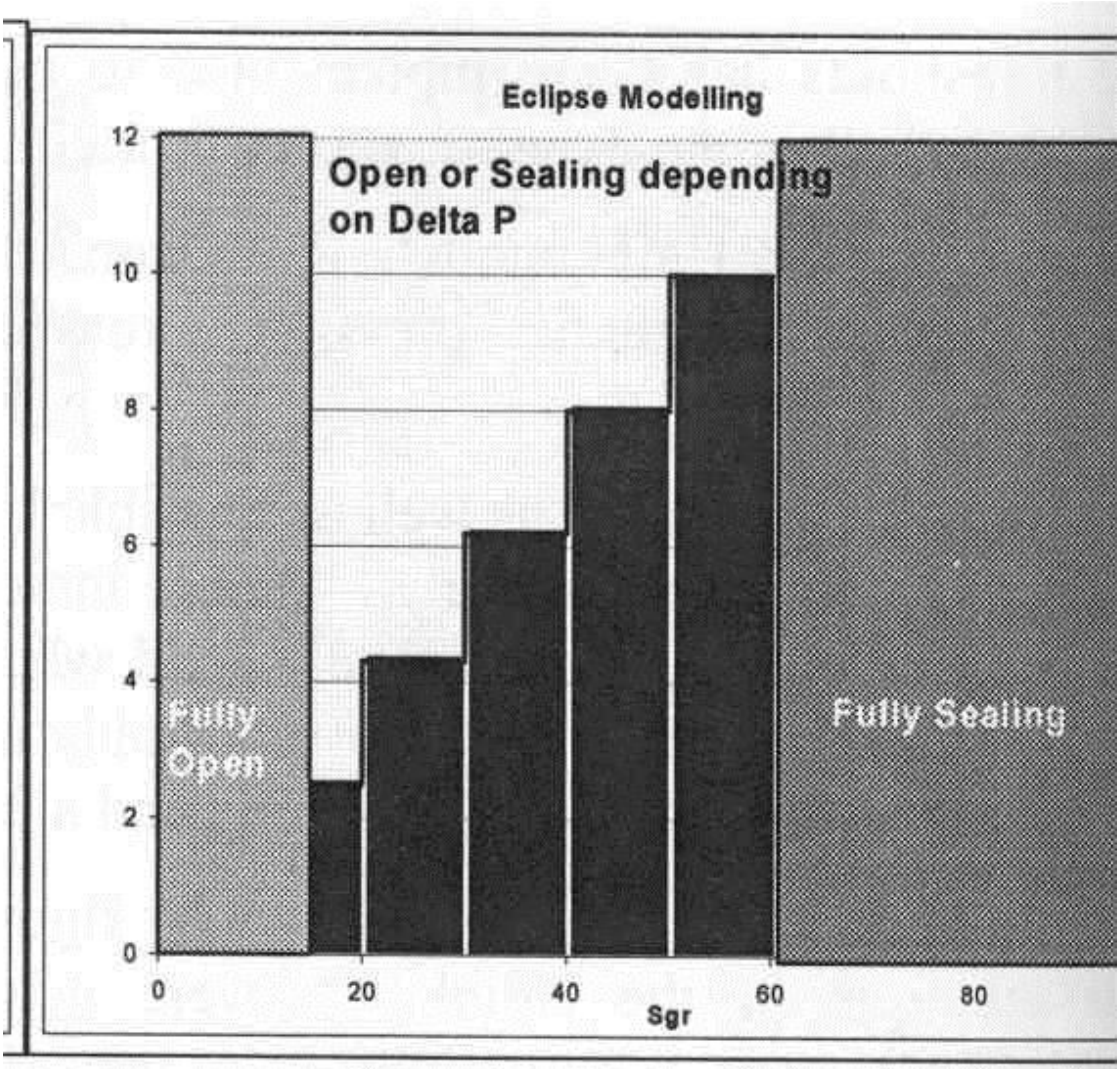

- Differential pressure across a seal as a function of SGR

Gibson, 1994

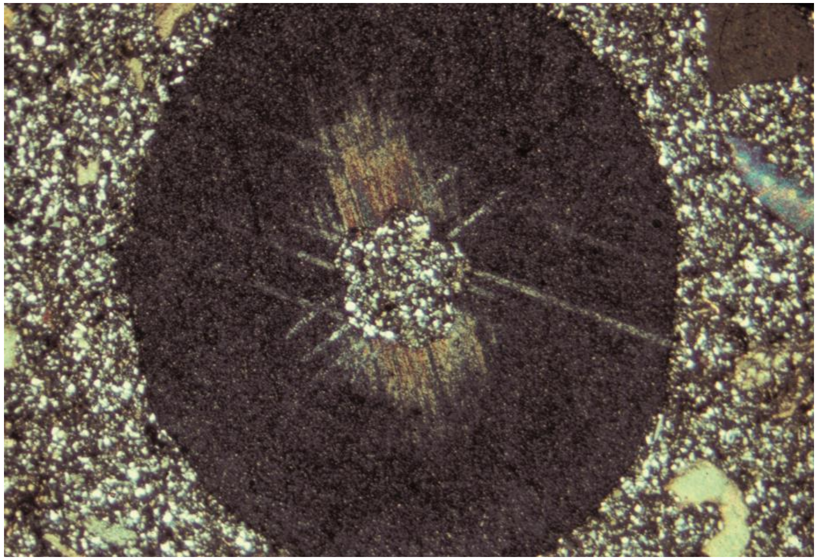

4.1.4 – Normal Fault Systems

An AAPG Short Course by
Terry Engelder
Professor of Geosciences
The Pennsylvania State University

Small Normal Fault
preCambrian Uinta Mountain Group, north flank Uinta Mountains, Utah, USA

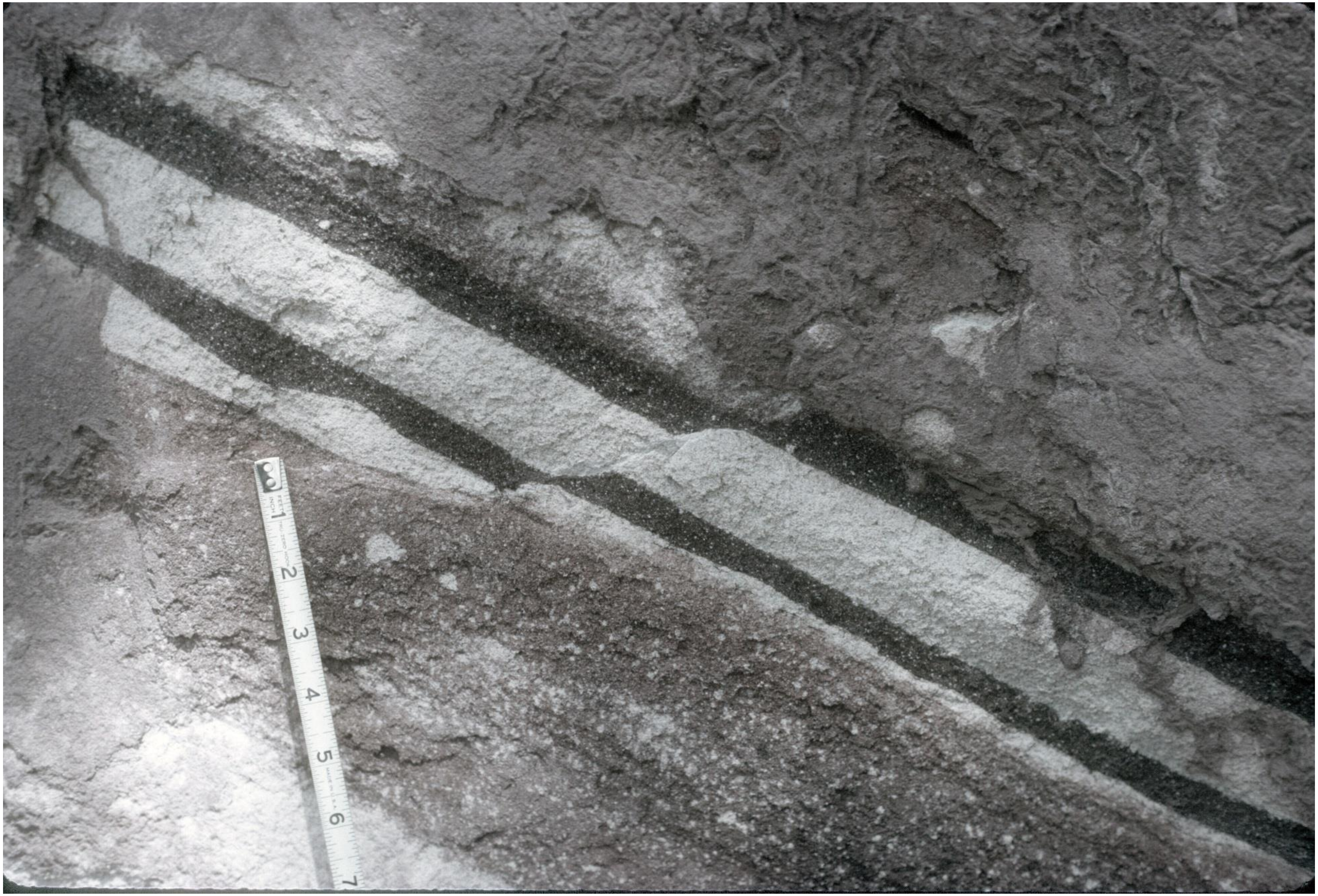

Terry Engelder

While thrust faults are characteristic of convergent margins of continental crust, normal faults are characteristic of the extension of continental crust. Normal faulting is commonly found within continental crust that has grown warm and stretched. The Basin and Range province of the western United States is finest examples in the world of crustal extension over a large region.   Central Africa is cut by extensional or rift basins and a consequence of the thermal heating of continental crust. Some rift basins eventually grow to become filled with basalts and sheeted dike complexes that are the first signs of oceanic crust. The passive margins of most continents are bounded by rift basins without extending to the point that oceanic crust has formed in the rifts.

A classic rift zone of relatively young age is the Red Sea rift. A cross section through the Red Sea rift shows a series of listric normal faults dipping toward the sea.

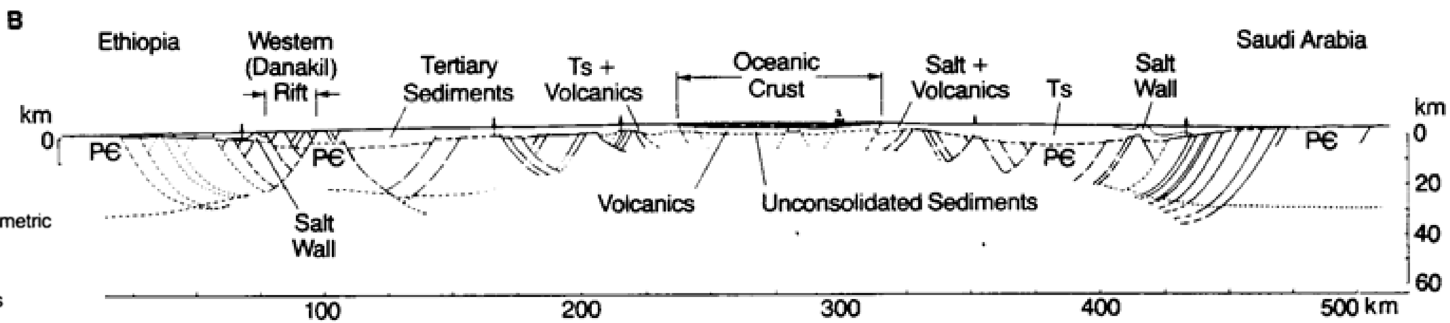

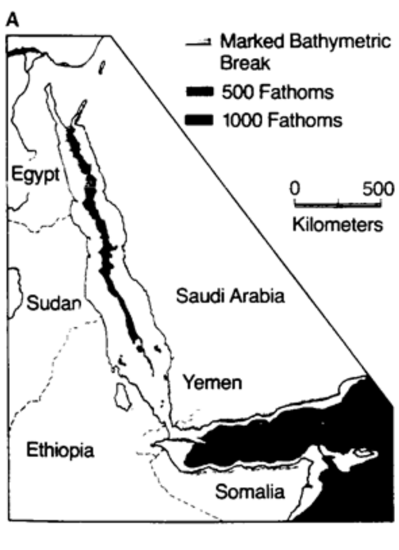

Cross section through the Red Sea (after Lowell and Genick, 1972)

Terry Engelder

African Plate Triple Junction

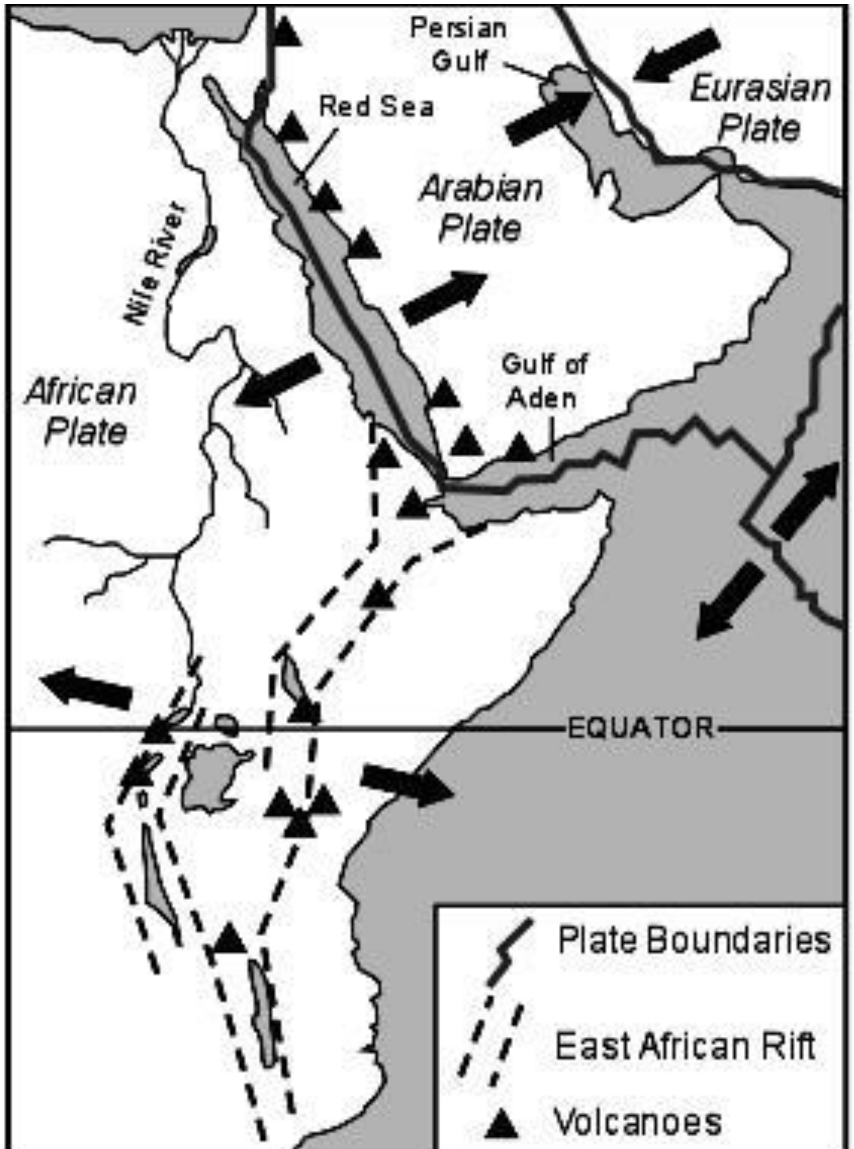

A triple junction (or triple point), where three plates are pulling away from one another: the Arabian Plate, and the two parts of the African Plate (the Nubian and the Somalian) splitting along the East African Rift Zone. In general the divergent plate margins are regions where new crustal material is formed from the mantle. As seen from the diagrams above the plumes from the mantle bring up material from the mantle to form new crust.

https://learning.uonbi.ac.ke/courses/SGL301/scormPackages/path_2/71_plate_tectonics.html

There have been a number of interesting models to explain the geometry of rifting at the edge of continents. The most difficult problem involves providing an explanation for the faulting that does not open large gaps in the crust. The listric fault geometry accomplishes this purpose. Another model that seems to work in some cases is called the domino model (Wernicke & Burchfiel, 1982).

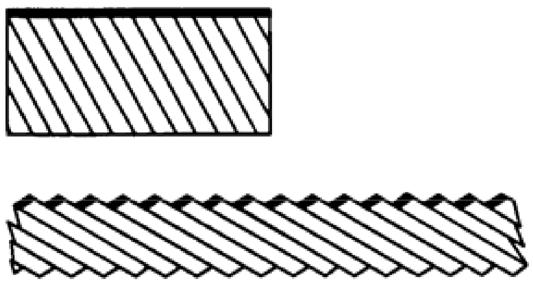

Domino-style normal faulting

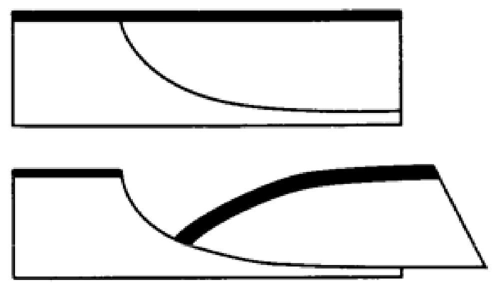

Listric normal faulting with reverse drag

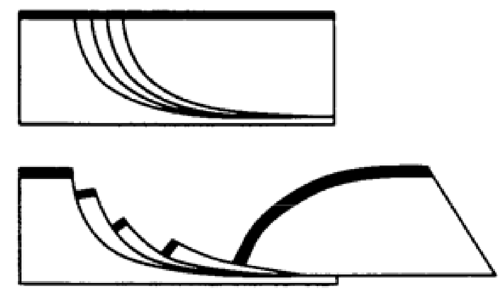

Imbricate listric normal faulting

The Basin and Range of the western United State is characterized by rift faulting with the level of erosion reaching well into basement rocks. Core complexes are believed to be a manifestation of listric faulting reaching mid- to lower crustal levels (Lister & Davis, 1989).

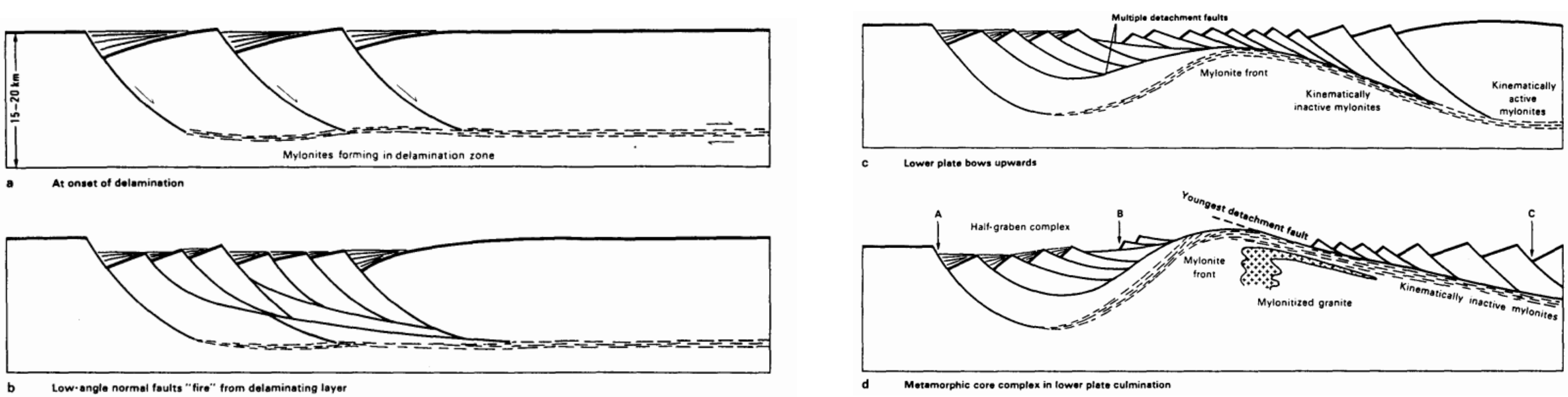

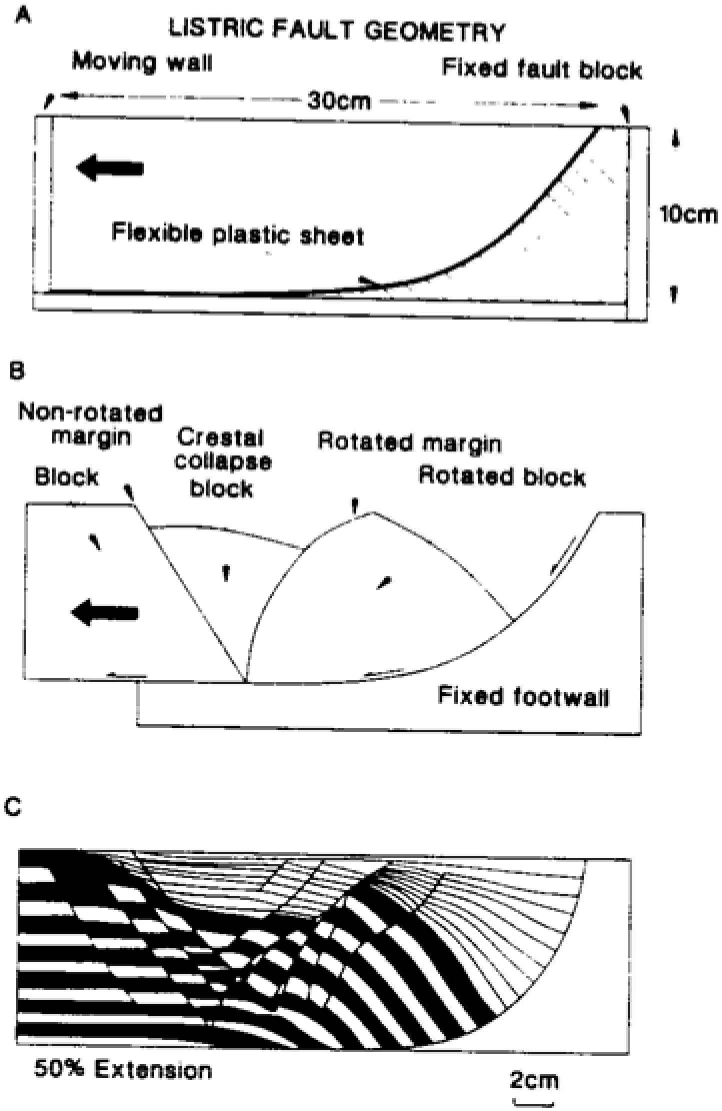

Very elegant clay models have been constructed that capture the shape of faulting at continental margins. An example from Ken McClay is shown below.

Ellis and McClay, 1988

Beatrice Field
place

Most normal faults are concave upward, or listric. This shape can be produced by geometric constraints, either because the faults reactivate curved thrusts, or because they must be curved to accommodate rotations. Another effect which will produce curved faults is the variation of rheology with depth: brittle failure at shallow depths produces less fault rotation than does distributed creep in the lower part of the crust. An important geometric feature of normal faulting is the uplift of the footwall. The amount of such uplift is related not only to the elastic properties of the lithosphere, but also to the throw and dip of the fault (Jackson & McKenzie, 1983).

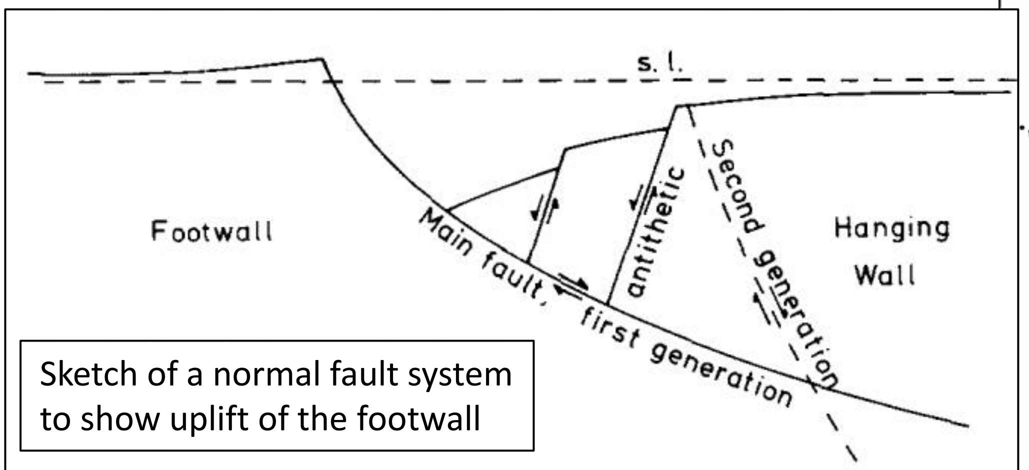

Sketch of a normal fault system to show uplift of the footwall

The uplift which forms the trap of the Beatrice oil field was produced by the unloading of a normal fault. Because the displacement on the fault has a maximum, and decreases both to the east and the west, the uplift also dies away along strike. In the southeastern direction, the structure is closed by the downthrown shales, and in the northwestern direction by the decay of the uplift with increasing distance from the fault. Hence, the uplift associated with the normal fault produces closure in all four directions to form a structural trap.

Jackson & McKenzie, 1983

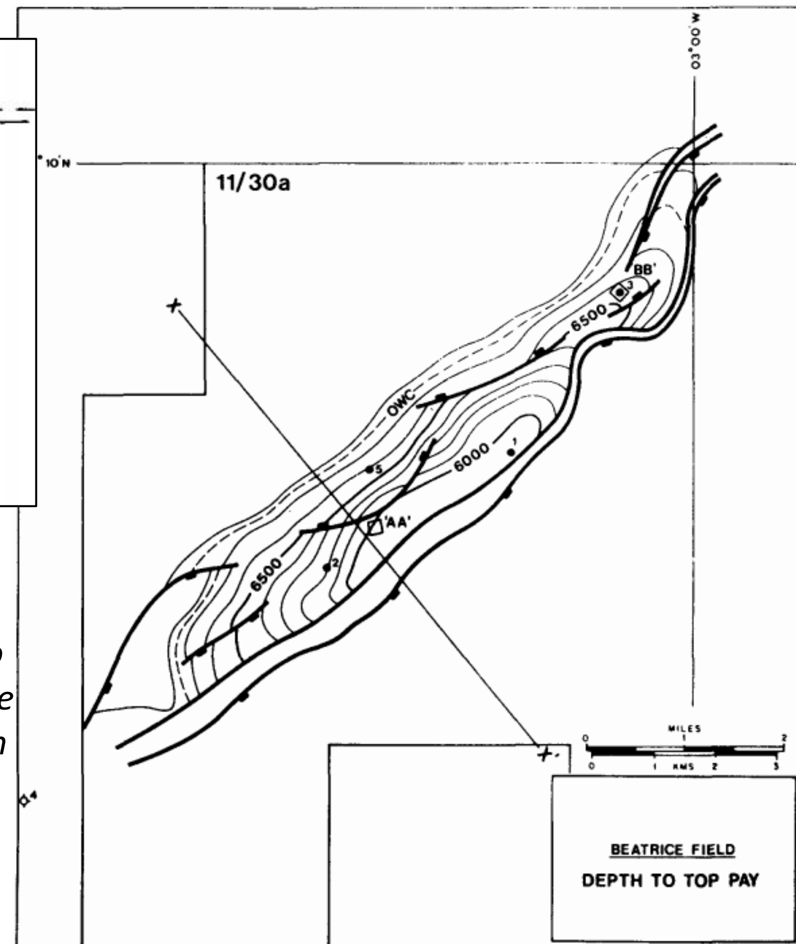

Once continents have rifted apart each continent is bounded by a series of half grabens that dip oceanward. A classic example of this is found between the Texas Gulf Coast and the Gulf of Mexico. Seismic sections show a very elaborate network of normal faults. The master faults are listric in nature but secondary faults are antithetic with dips back toward the continent. The largest listric faults on a continental margin may cut down to the Moho. In the Texas Gulf Coast many of the listric faults cut down to a detachment at the level of a salt layer in the Jurassic.

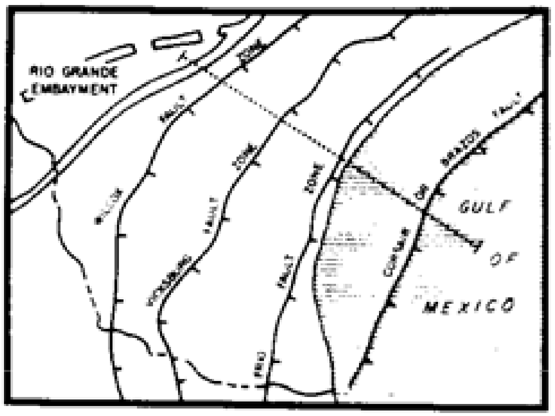

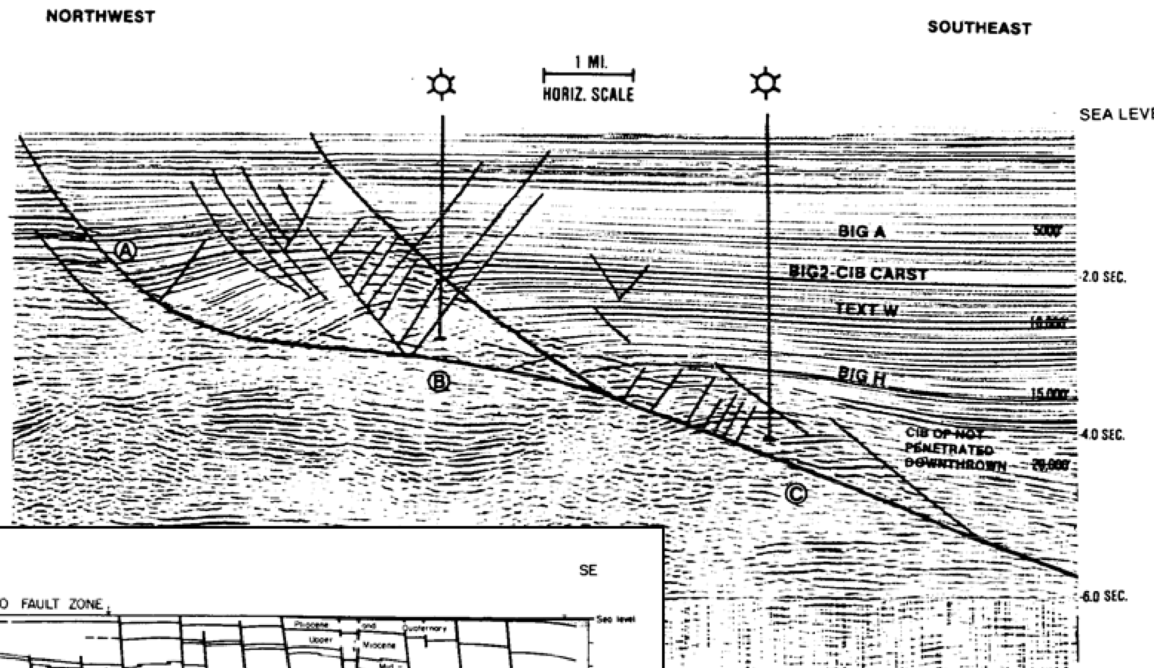

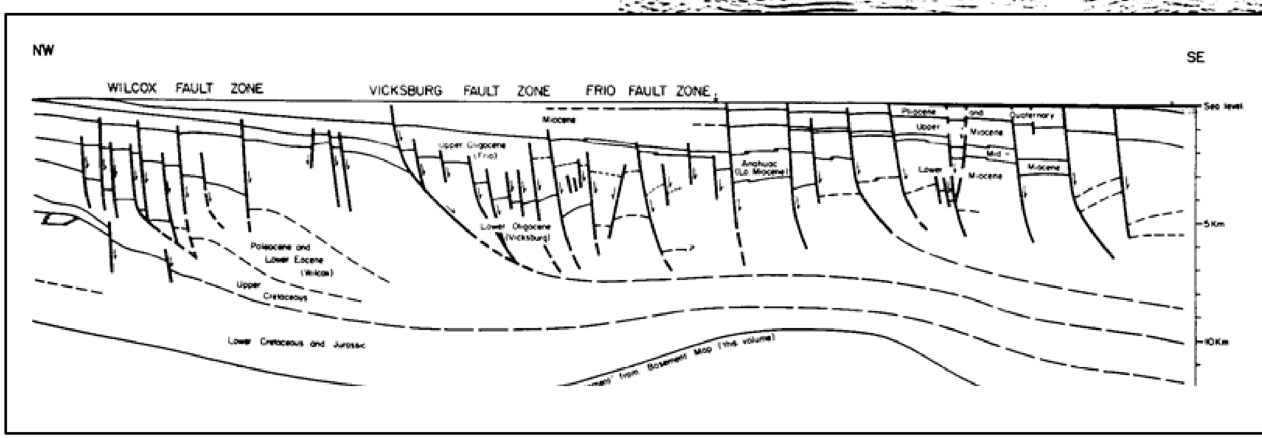

The source of these figures is unknown but Dula (1991) is offered as a reference.

Terry Engelder

Relay Ramps for Normal Faults
Blue Lias, Lilstock Beach, Bristol Channel, United Kingdom

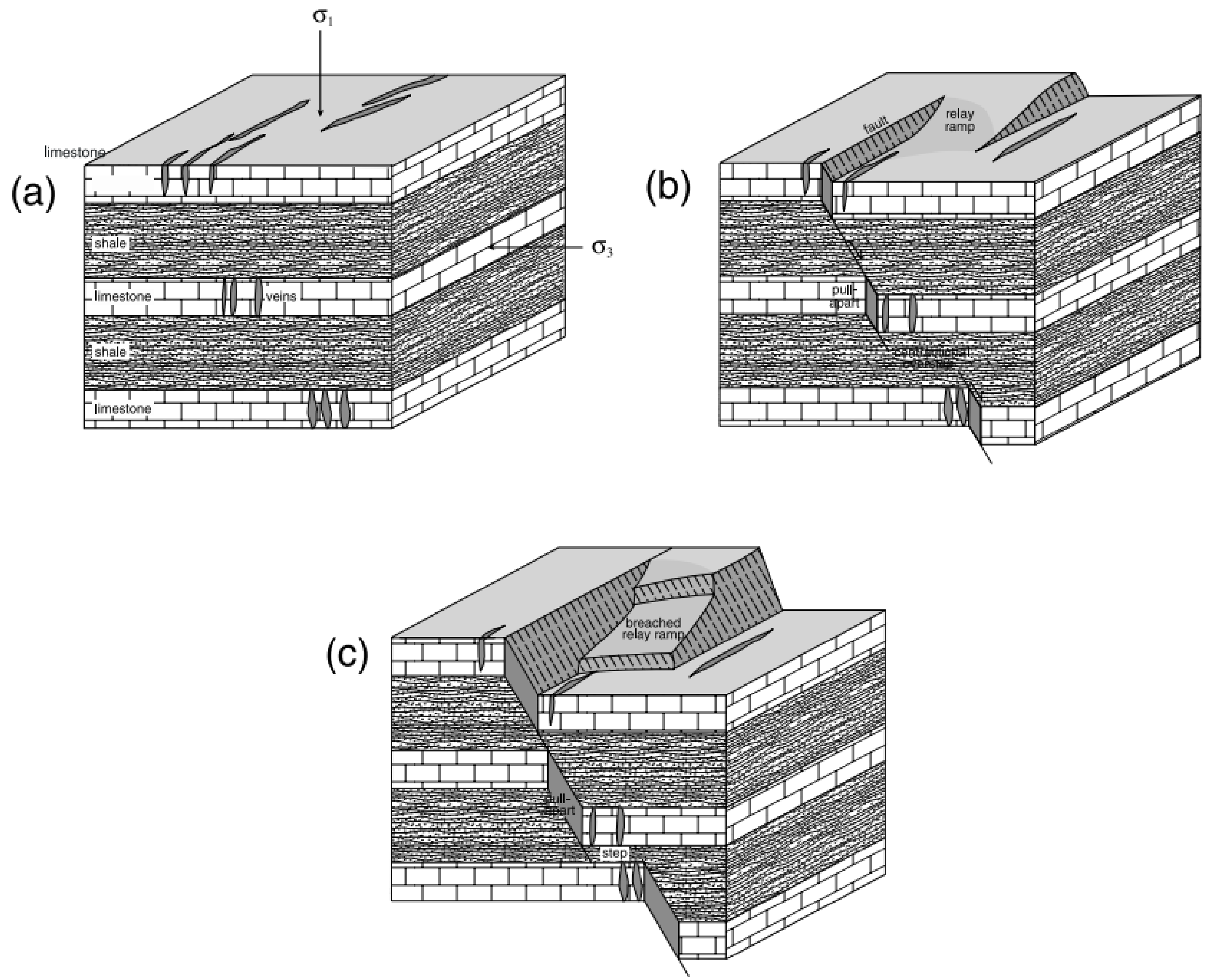

Block diagrams illustrating the development of normal faults and relay ramps in a limestone–mudrock sequence. (a) Veins initiate in the brittle limestones. (b) Extension continues, with shear across the veins and connection of veins across the mudrocks. Relay ramps develop at steps between faults in map view. Displacement minima typically occur at steps. (c) Linkage occurs between segments, with breaching of relay ramps.

Crider & Peacock, 2004

Relay Ramps for Normal Faults
Blue Lias, Lilstock Beach, Bristol Channel, United Kingdom

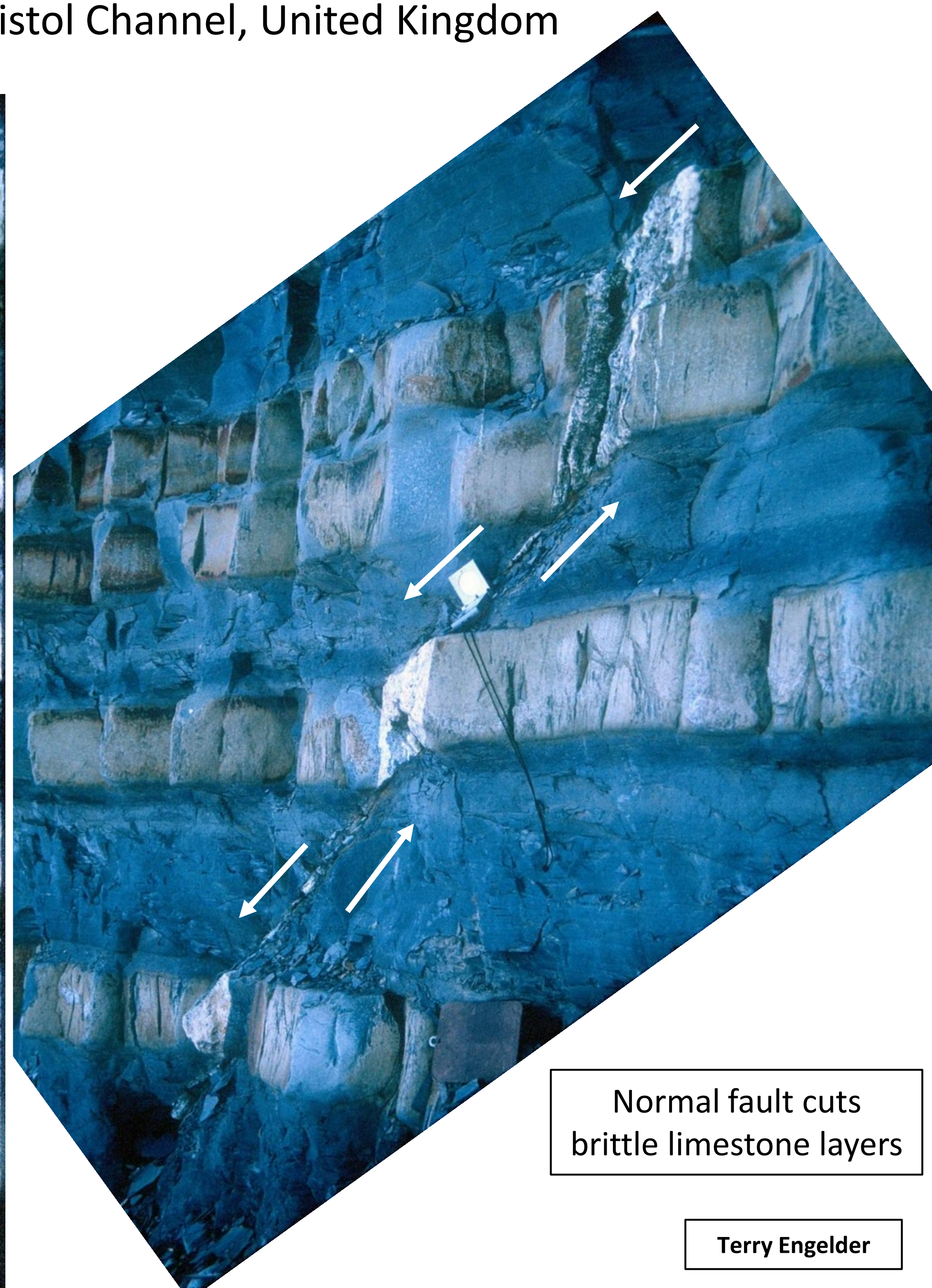

Normal fault cuts brittle limestone layers

Terry Engelder

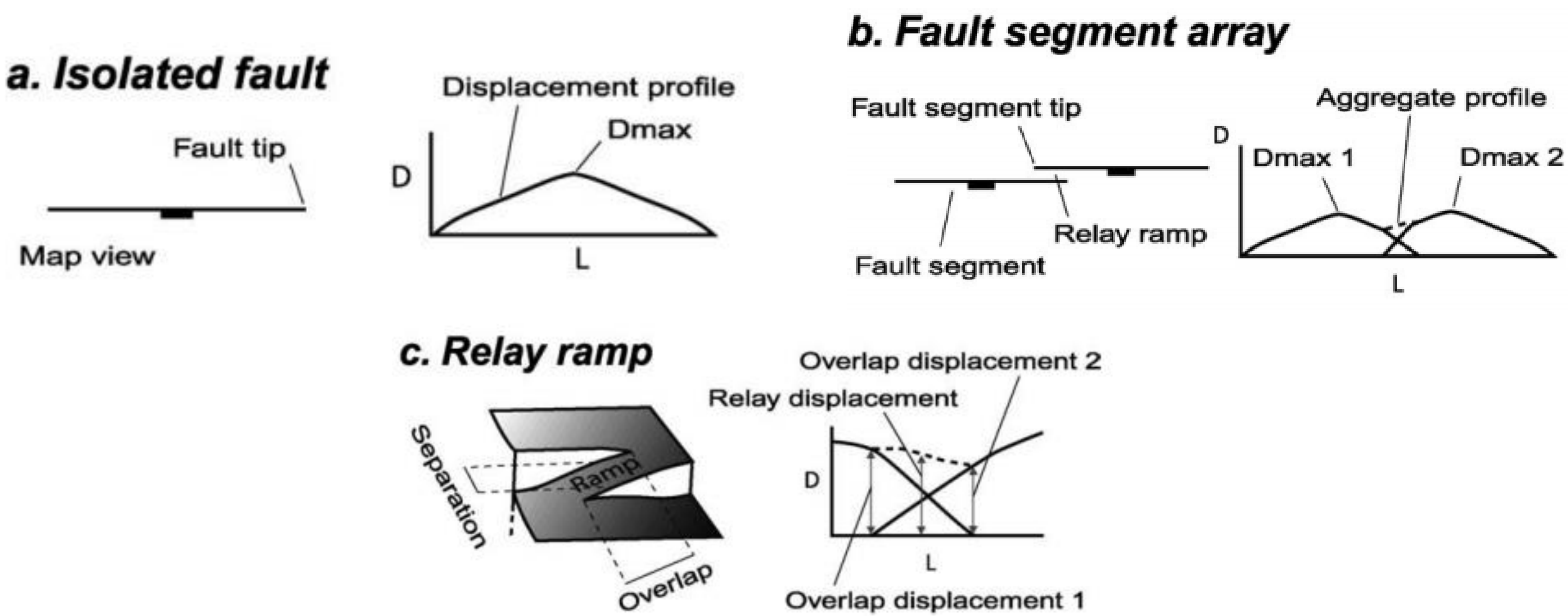

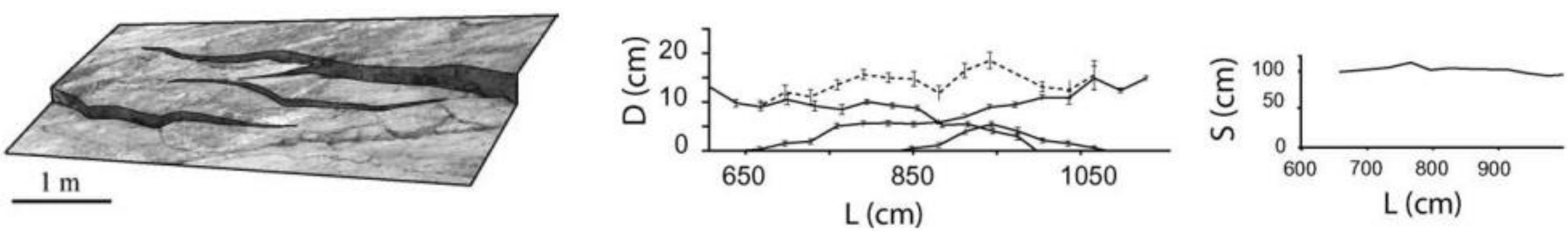

Examples of an open relays with displacement profile at relay ramps and associated separation profiles (distance between faults normal to their trace along overlap). Indisplacement profile, broken lines represent aggregate profiles at the overlap zone. Displacement profiles of each segment are projected following an axis perpendicular to fault segments. Error bars are labelled on profiles.

Soliva & Benedicto, 2004

Relay Ramp Forms and Normal Fault Linkage
Canyonlands National Park, Utah, USA

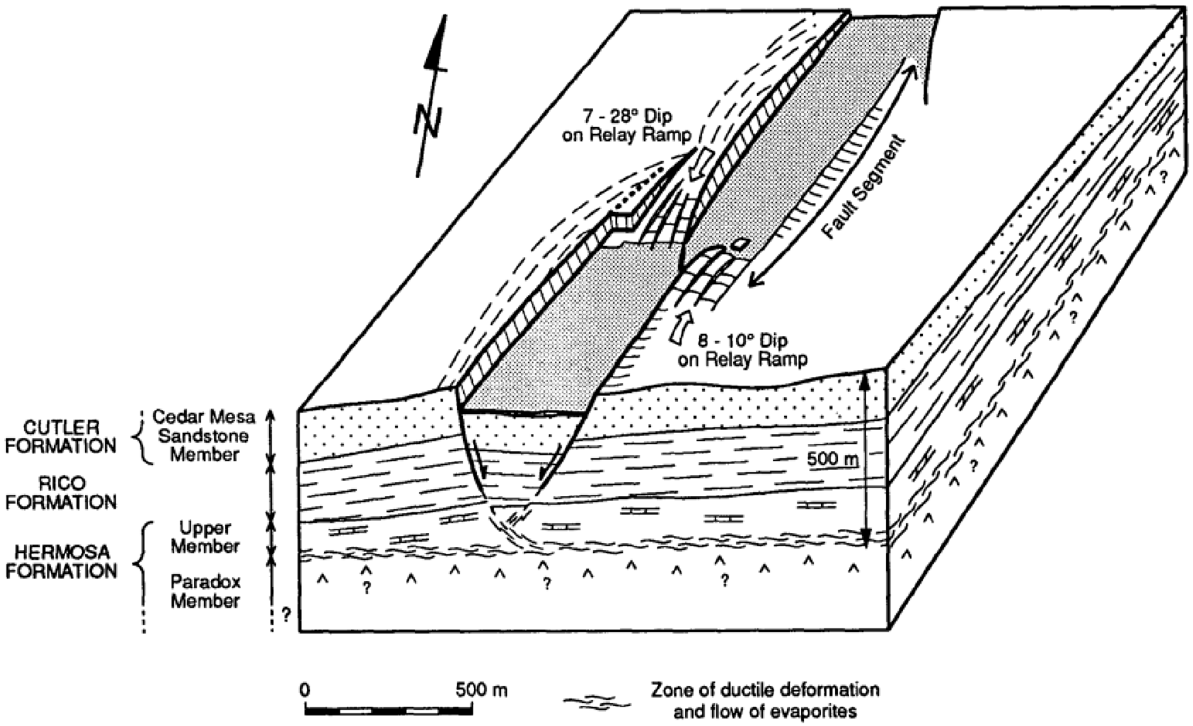

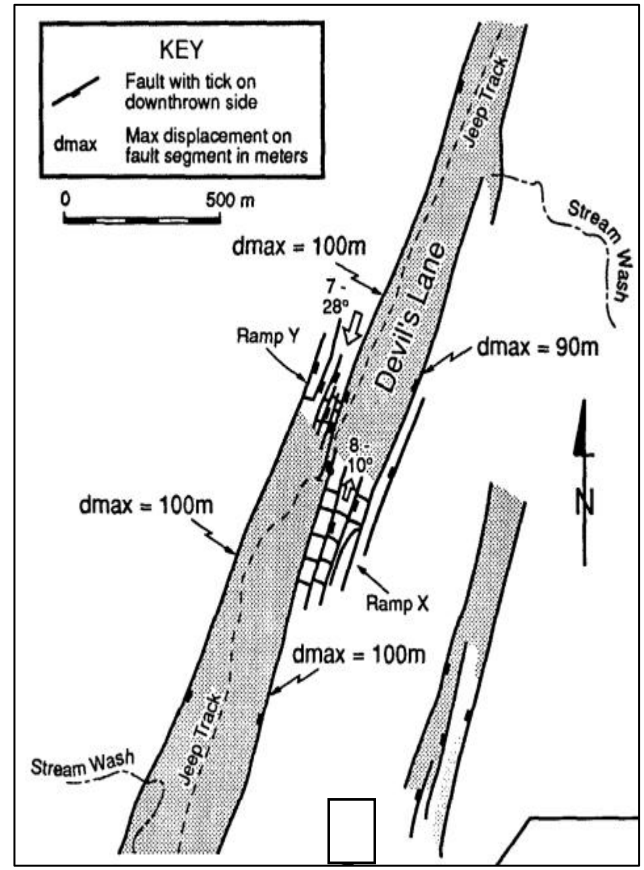

A simplified block diagram and structural map of the the Devil's Lane graben. Two major relay ramp features are present, dipping in opposing directions.

Trudgill & Cartwright, 1994

Relay Ramp Forms and Normal Fault Linkage
Canyonlands National Park, Utah, USA

Terry Engelder

The relationship between the maximum finite displacement on a fault (*D*) and its maximum dimensions (*W*) is $D = cW^n$ where *c* is a constant and *n* ranges between 1.0 and 2 (Walsh and Watterson, 1988; Gibson et al., 1989; Marrett and Allmendinger, 1991; Cowie and Scholz, 1992).

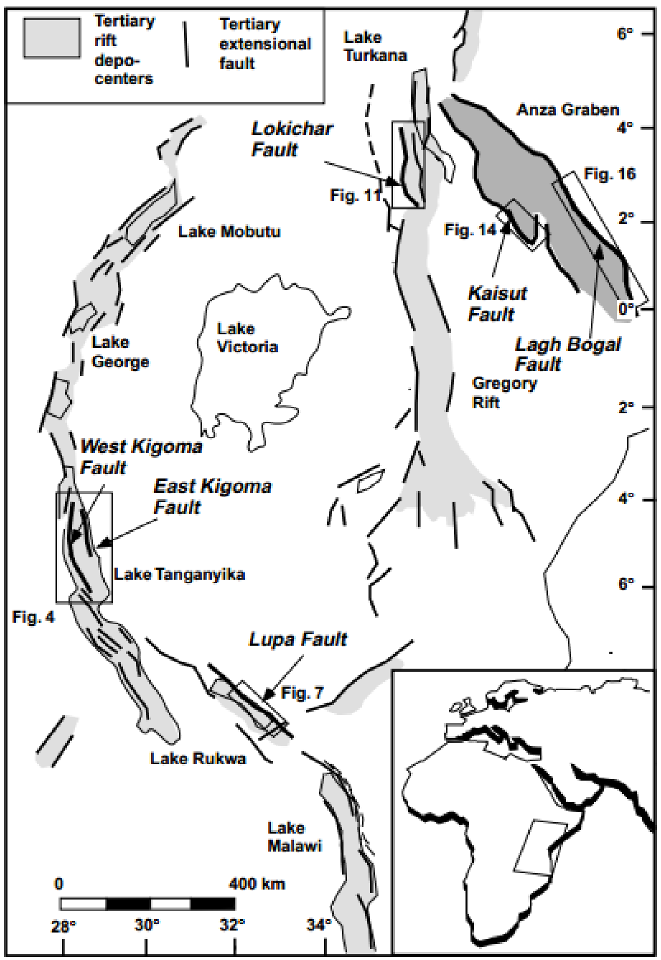

Rift boundary faults of East Africa

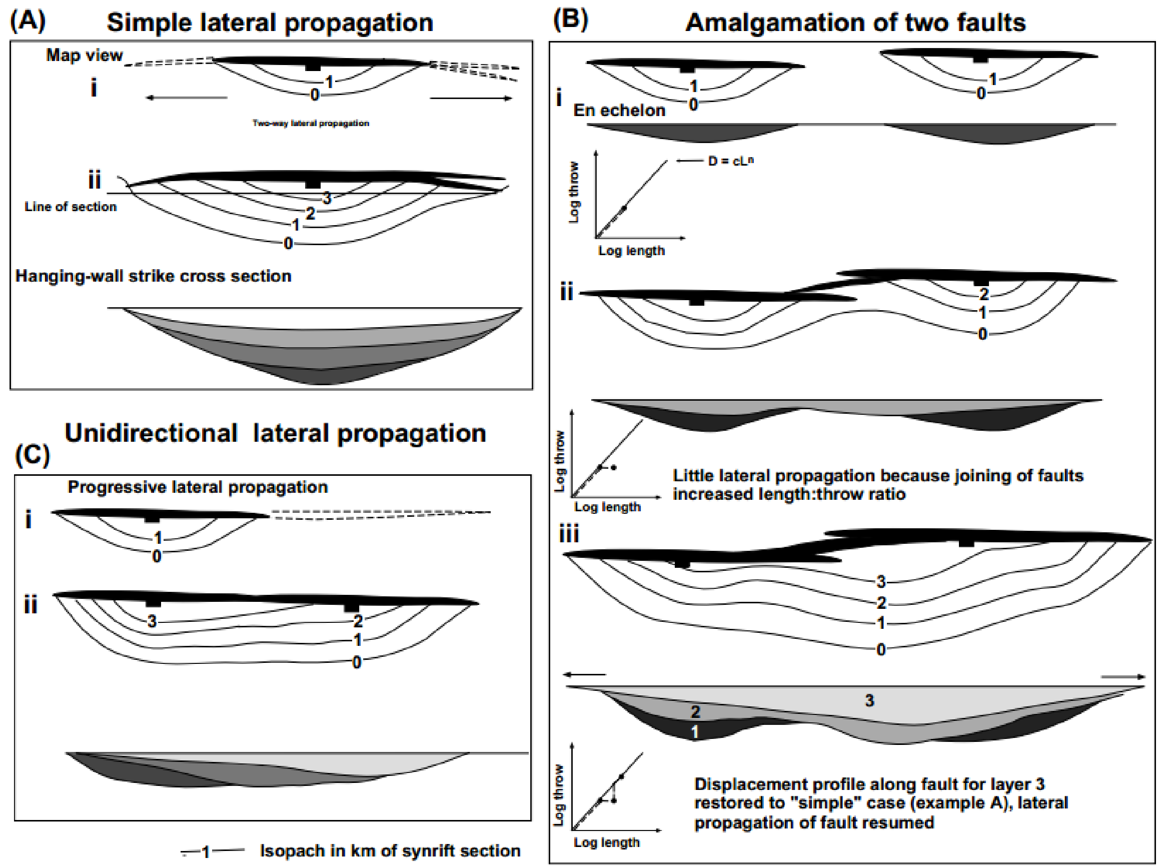

Examples of basin geometries assuming boundary fault propagation occurs during basin formation; based on a model by Schlische and Anders (1996). L = fault length; other letters are the same as equation 1.

Morley, 1999

Growth of normal faults
738 ka Bishop Tuff, Basin and Range, California, USA

Watterson (1986) and Walsh and Watterson (1989) proposed an empirical growth model based on combined data that they interpreted as $D \propto L^2$ Their model assumes that brittle faults grow in elliptical slip events in which the fault length (which they call width) increases by a constant increment. Marrett and Allmendinger (1991) interpreted a similar combined data set as $D \propto L^{1.5}$. Dawers et al., (1993) find that the ratio D_{avg}/L for the Volcanic Tableland faults is 10^{-2}.

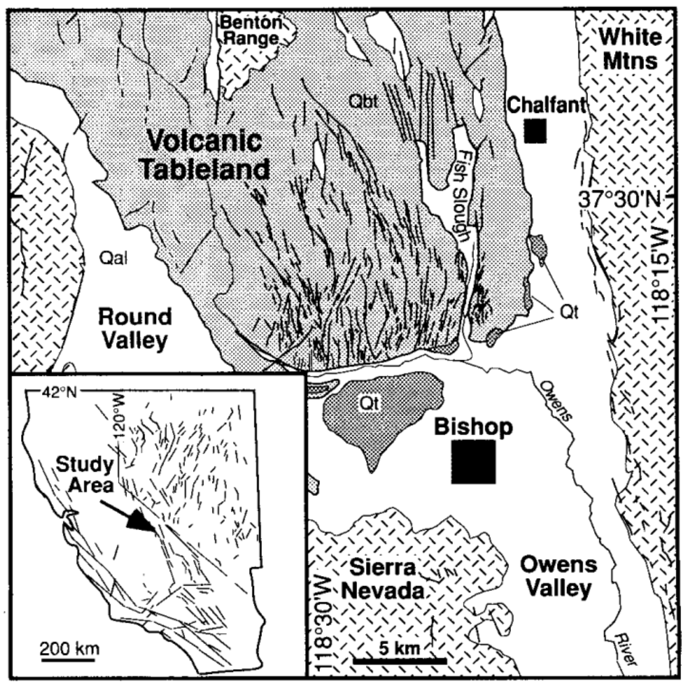

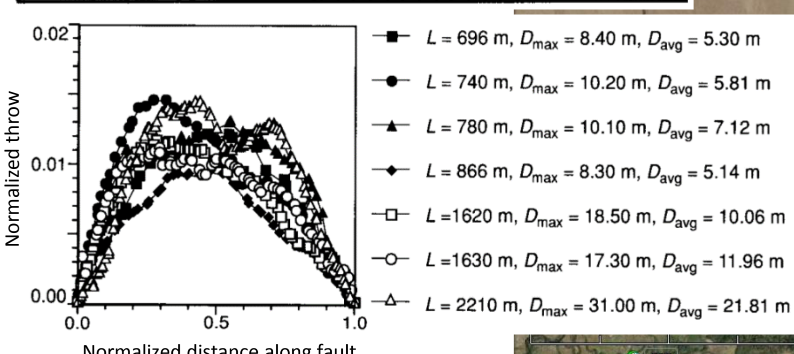

Dawers et al., 1993

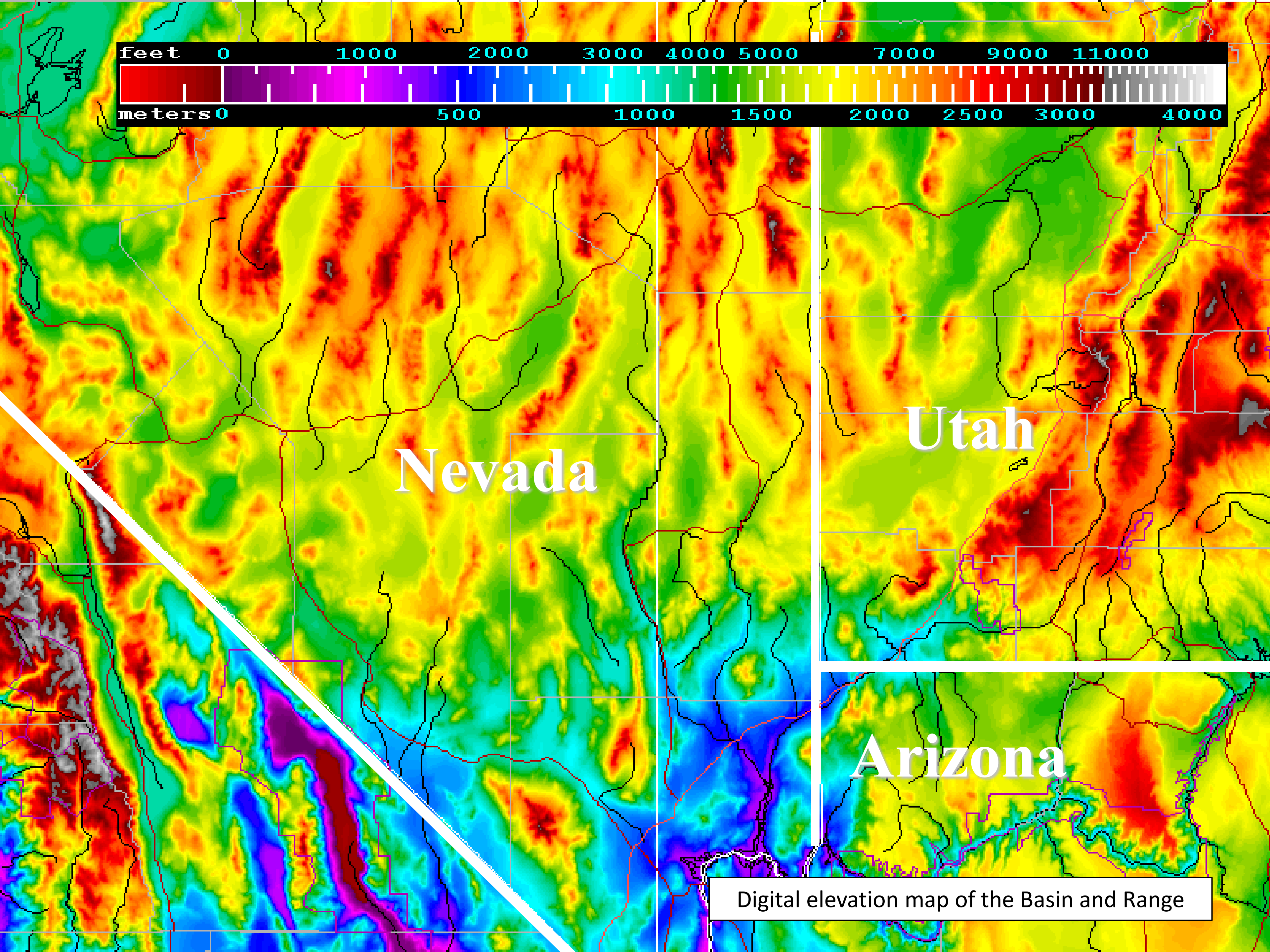

Digital elevation map of the Basin and Range

Domino normal faults in the Newfoundland Mountains, northwest Utah. These faults offset a Pennsylvanian-Devonian unconformity in a top to the east (left) sense of shear. Note that the faults , although presently nearly horizontal, cut the steeply dipping bedding at high angles.

From Rick Allmendinger, Cornell

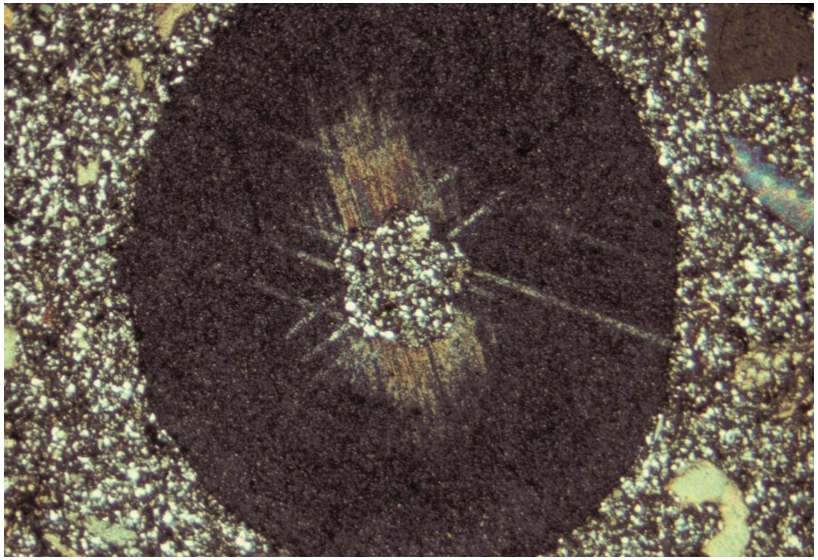

4.2.1 - The Overthrust Problem

The Hubbert-Rubey (1959) solution to Escher's "colossal over-shove" problem

An AAPG Short Course by
Terry Engelder
Professor of Geosciences
The Pennsylvania State University

Fold nappes represent behavior in the middle crust where ductile deformation enables for most of the tectonic displacement. In the upper crust brittle behavior mainly through frictional slip enable most of the tectonics behavior. Even in the brittle crust pressure solution is a ductile mechanism that accompanies frictional slip. Overthrust terrains, which operate in the brittle crust, can be divided into two general classes: 1.) Those where the decollement surface is parallel to bedding within the sedimentary section. The central Appalachian Valley and Ridge and the Canadian Rockies are representative examples. 2.) Those terrains where a horizontal thrust sheet develops in crystalline basement and breaks upward through the sedimentary overburden. The Wyoming Province of the U.S. Rockies is a type example of structures in sedimentary rocks developing over crystalline upthrusts. The outer crystalline thrusts of the Blue Ridge in the southern Appalachians are believed to be other examples.

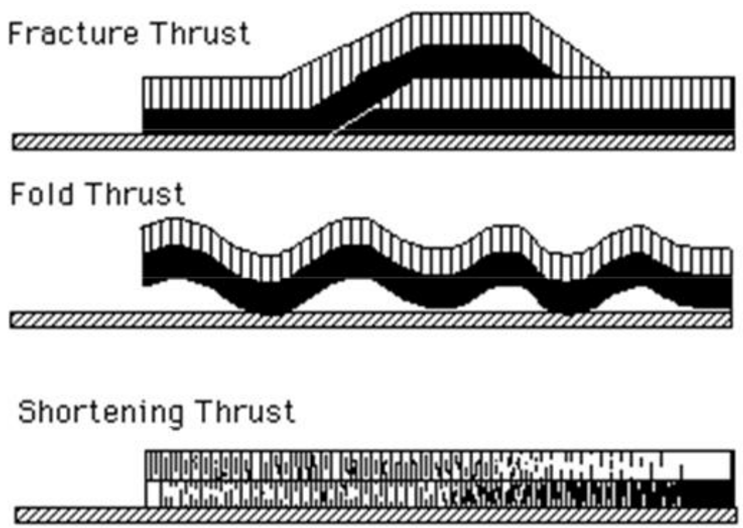

Three general classes of thrust faults develop within thrust sheets whose decollement is within the sedimentary section. Geiser (198) identified these structures as: Break Thrusts, Fold Thrusts, and Shortening Thrusts. Each of the three has a different mechanical behavior as explained below.

Break thrusts develop where the Coulomb-Mohr failure criterion is favored over folding and shortening. Fold-thrust belts developed in a thick but reasonably homogeneous stratigraphic section seem to favor the break thrust style. The southern Appalachians is one example of the break thrust style. This style seems to be the most common throughout the upper crust.

Fold thrusts develop where the viscosity contrast between a sheet of sediments (η_1) and the underlying rock (η) is large.

$$\eta > \eta_1$$

In this case the Euler Buckling Force is relatively low compared with the Coulomb-Mohr failure criterion.

$$\pi EI/L^2 < S_0 + \mu_i \sigma_n$$

A fine example of fold thrusts may be found in the Swiss Jura where thin box folds form over a Mesozoic salt.

Shortening thrusts develop in association with volume loss strain. An example is the Appalachian Plateau where the plateau is folded slightly over blind thrusts but the dominant mechanism for absorbing the decollement slip layer parallel shortening. The mechanism for shortening is the development of solution cleavage where the dissolved rock is carried out of the section in circulating water. Shortening occurs because the yield stress for pressure solution cleavage is less than the Euler Buckling Force and the Coulomb-Mohr failure criterion

Escher (1841) identified the Glarus thrust as, “Folge einer kolossalen Ueberschiebung oder eines Umbiegens der Schichten” (an episode of colossal over-shove or over-fold).

Bailey (1935) says of Escher’s interpretation, “he admits that this interpretation lands one into <u>great difficulties</u>”

View of Glarus Thrust from the south side of Segnes Pass, Swiss Alps

Glarus Thrust
Alps, Switzerland

Terry Engelder

Glarus Thrust
Alps, Switzerland

Terry Engelder

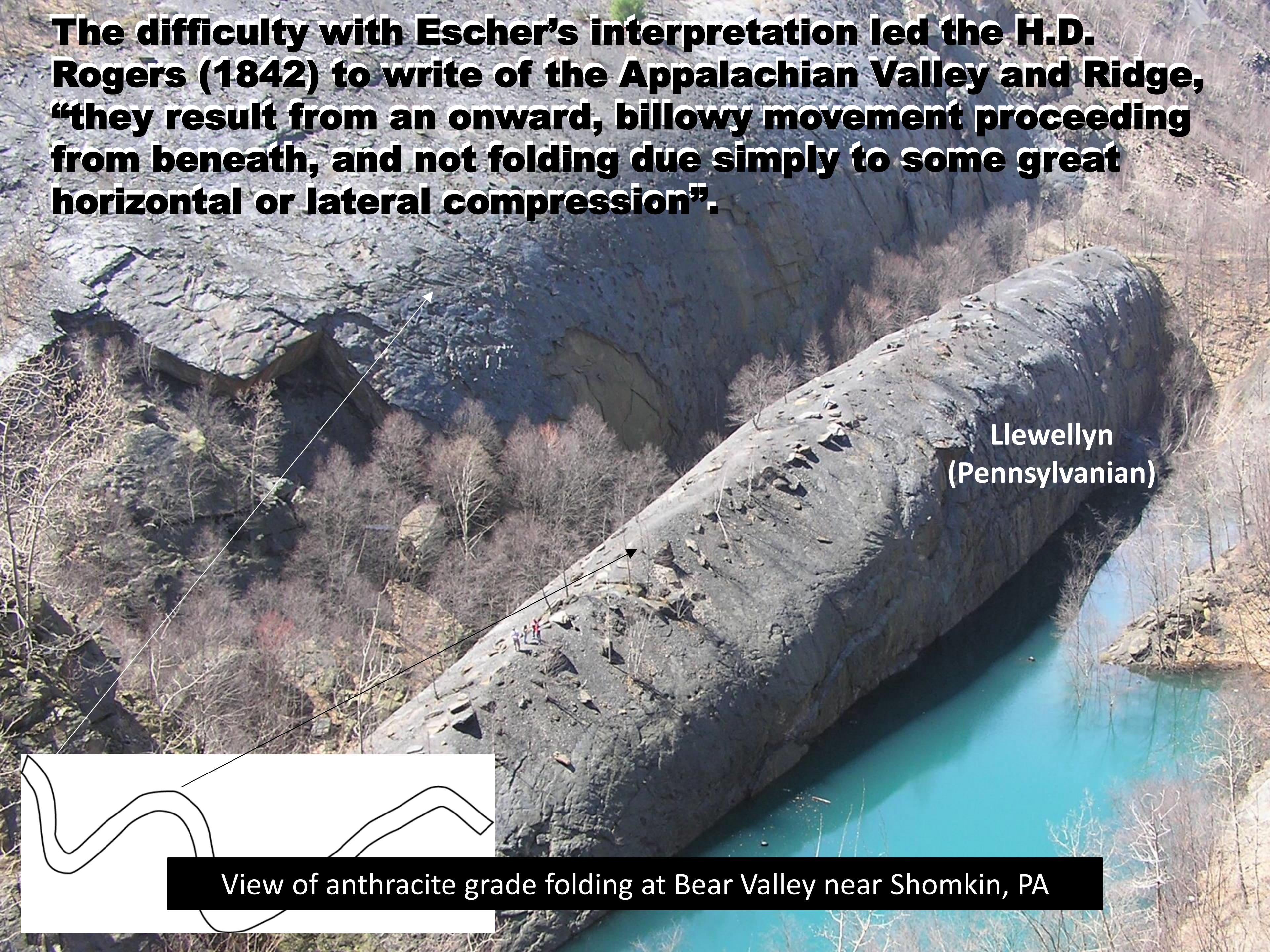
The difficulty with Escher's interpretation led the H.D. Rogers (1842) to write of the Appalachian Valley and Ridge, "they result from an onward, billowy movement proceeding from beneath, and not folding due simply to some great horizontal or lateral compression".
Llewellyn
(Pennsylvanian)
View of anthracite grade folding at Bear Valley near Shomkin, PA

Observations of the "colossal over-shove" by lateral compression lasted almost 70 years before Escher's (1841) great difficulty was understood in terms of mechanics.

Moine – Scotland: Nicol (1861)
Scandinavia – Norway: Tornebohm (1883)
Rocky Mountains – Canada: McConnell (1887)
Himalayans – India: Oldam (1893)

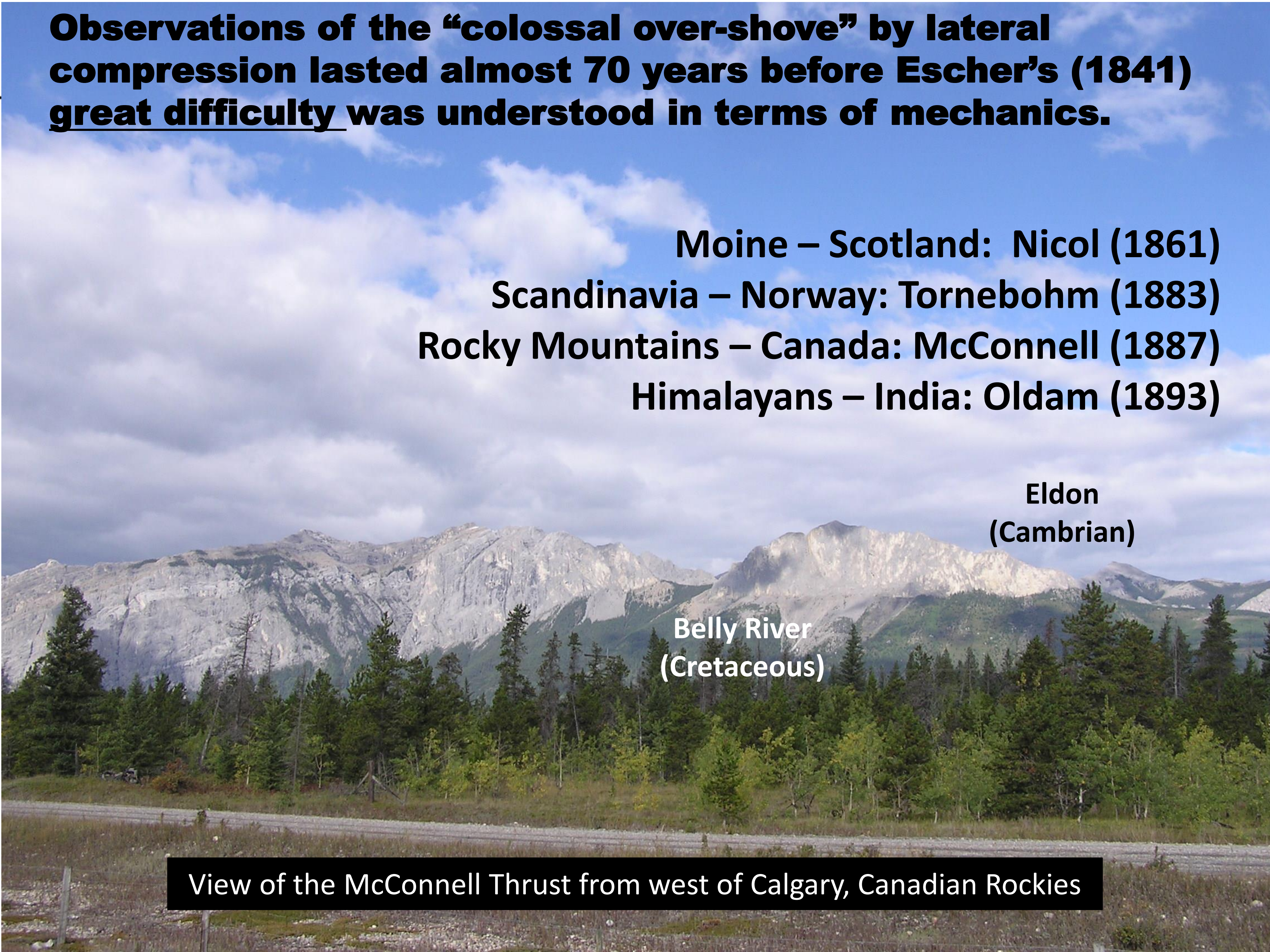

View of the McConnell Thrust from west of Calgary, Canadian Rockies

Smoluchowski' (1909) Dilemma:

Granite has the strength to support a column 3 km high. Thus, sliding on a fault with a friction of ≈ 0.6, granite has the strength support the stress necessary to slide a block ≈ 5 km long.

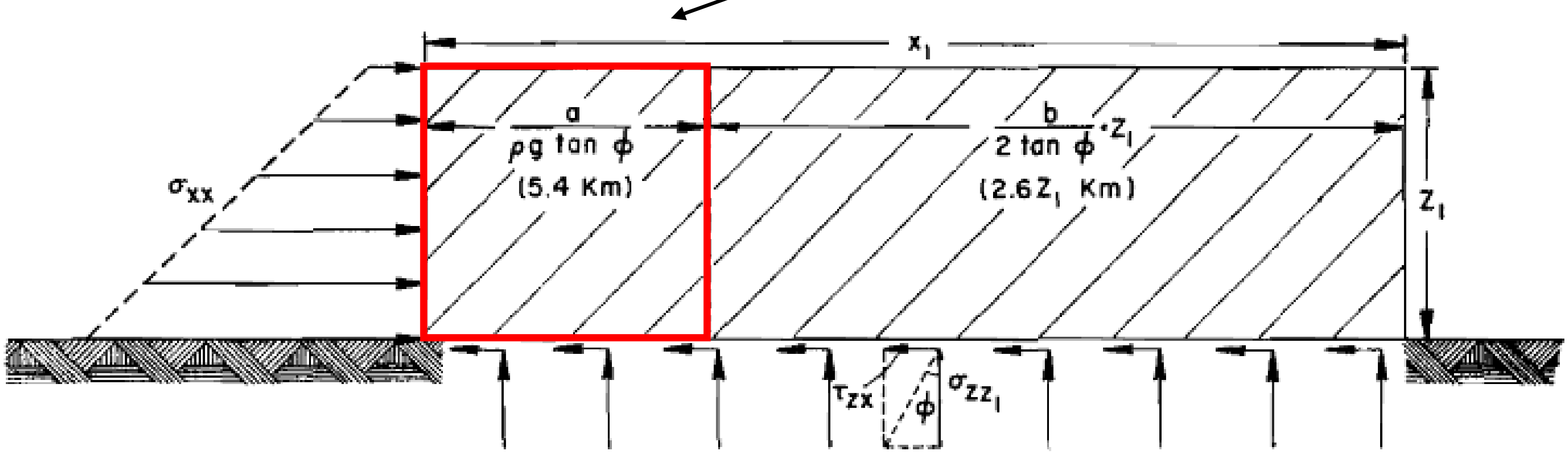

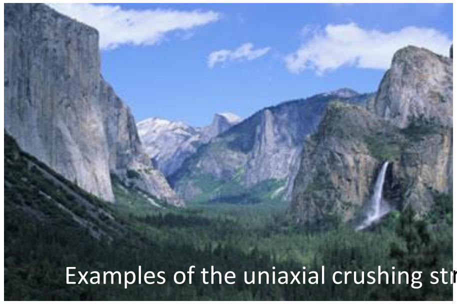

Examples of the uniaxial crushing strength of rock

Drawing from Hubbert and Rubey (1959)

The density hoops supporting a silo is an analog for stress in the earth and depth-related increase in rock strength

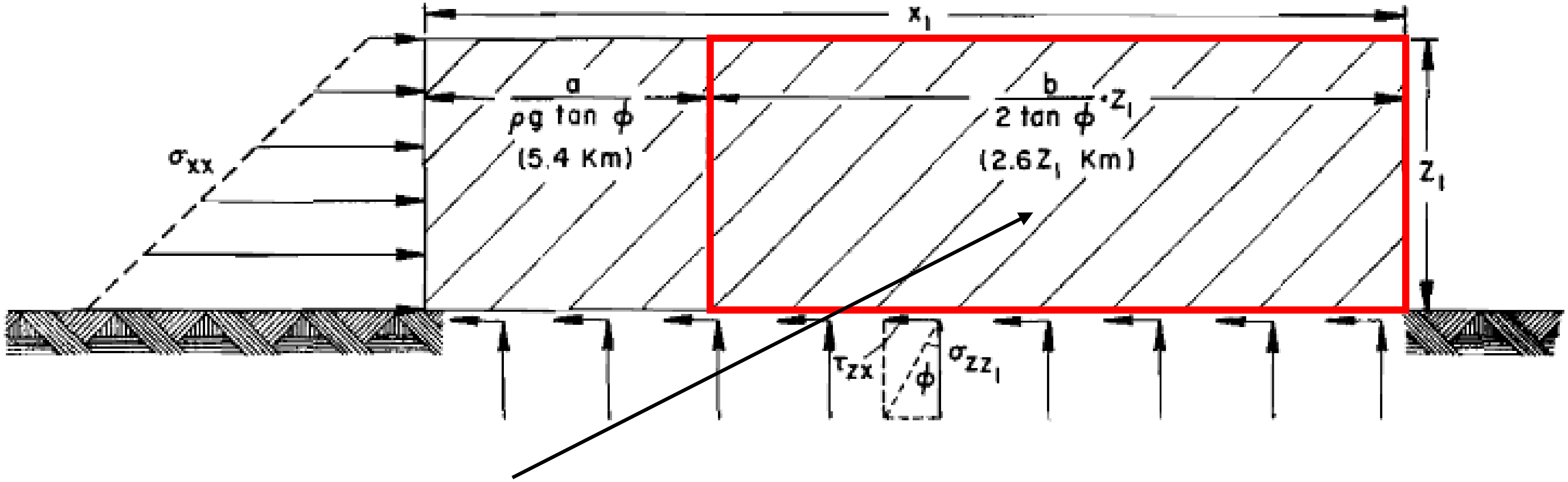

Hubbert and Rubey (1959) point out that thickness of the block adds strength so that blocks may get longer by 2.6 km per km of thickness.

Reasonable crustal thicknesses can account for up to 10 to 15 km of over-shove on a detachment of normal friction!

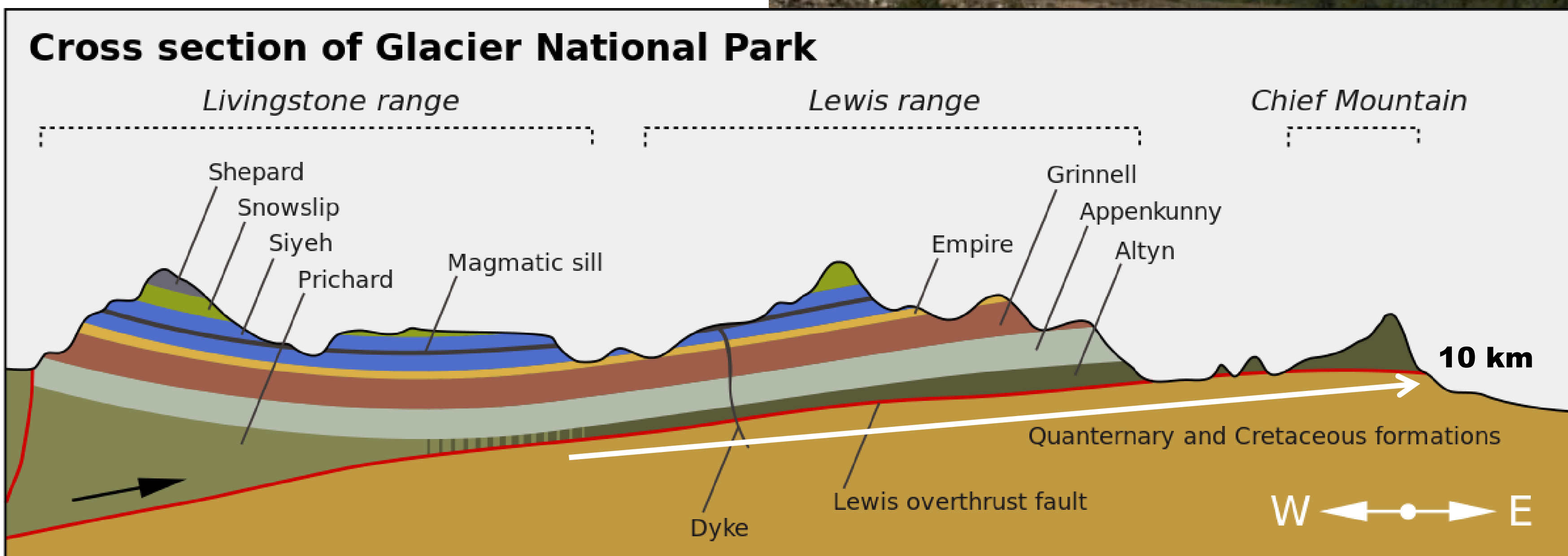

http://www.nps.gov/history/history/online_books/glac/3/images/fig3.jpg

The Glarus thrust has a minimum displacement of 40 km and the Scandinavian over thrusts have a displacement of 130 km.

View of Glarus Thrust from the south side of Segnes Pass, Swiss Alps

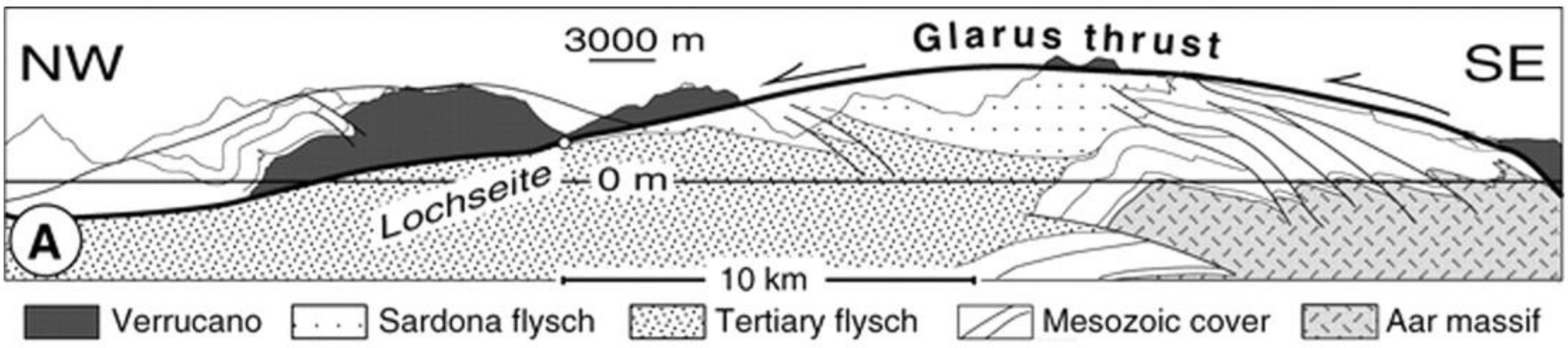

Three solutions to Escher's colossal over-shove

1. A high temperature detachment
2. A strong tectonic wedge
3. A low-strength detachment

Under the heading of "Swiss Tectonic Arena Sardona", Switzerland asks UNESCO support for the "Glarus overthrust" World Heritage site.

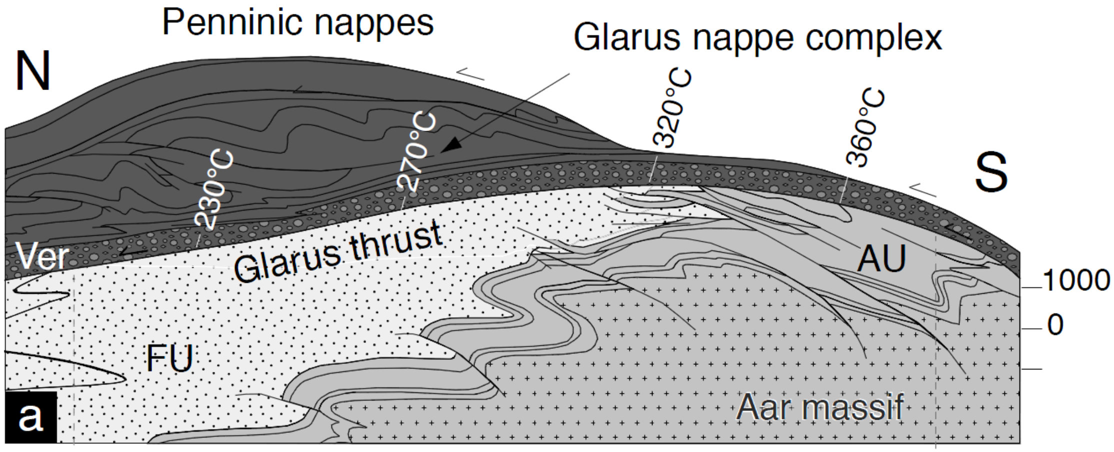

High Temperature Detachment

Herwegh et al., (2008)

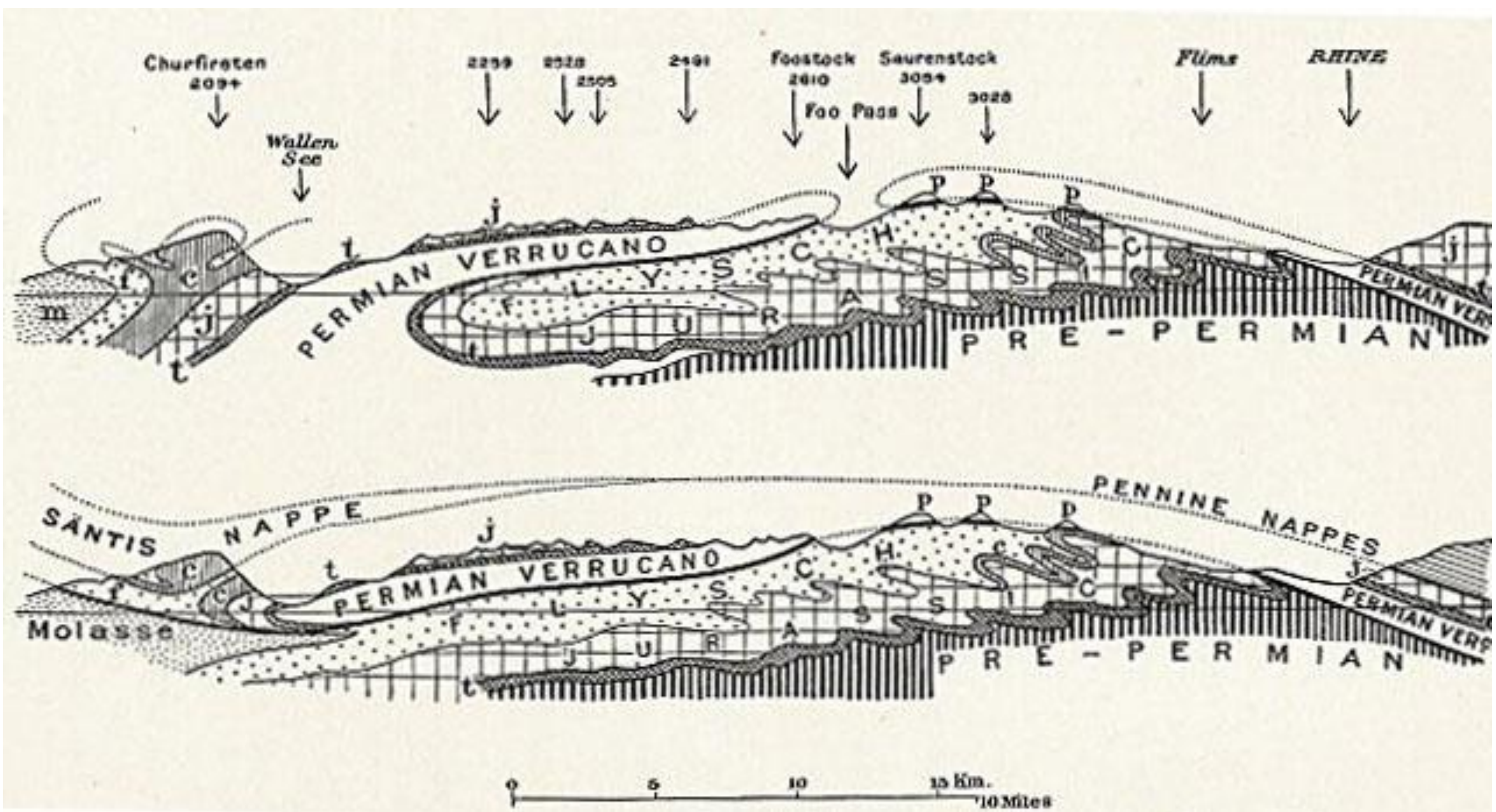

The contrasting "double-fold" of Escher and Heim with the single Glarus thrust sheet proposed by Bertrand (E.B. Bailey, 1935).

Strong Tectonic Wedge

Davis et al, 1985

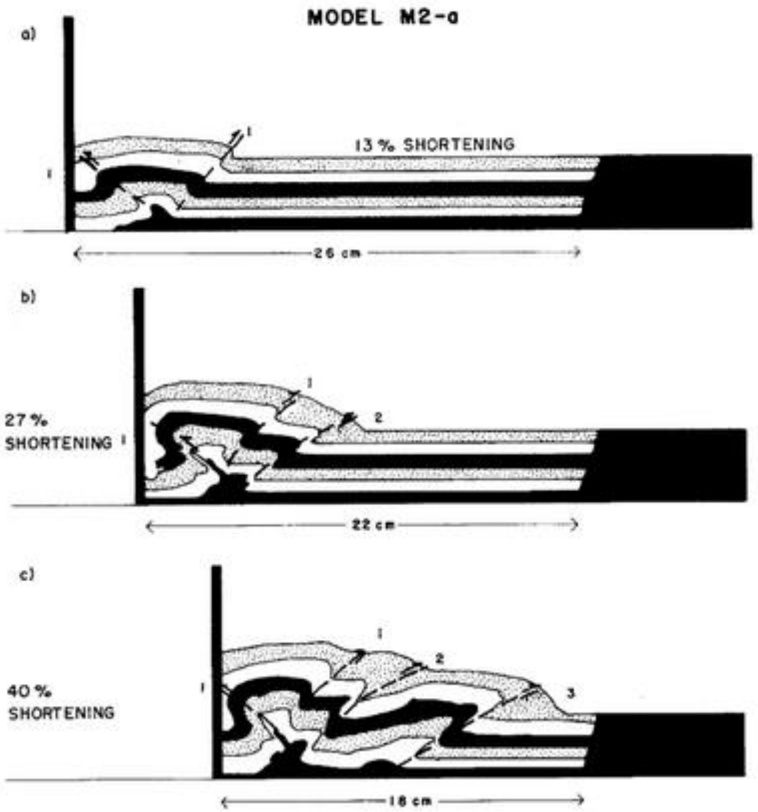

Rockies, Montana to Canada

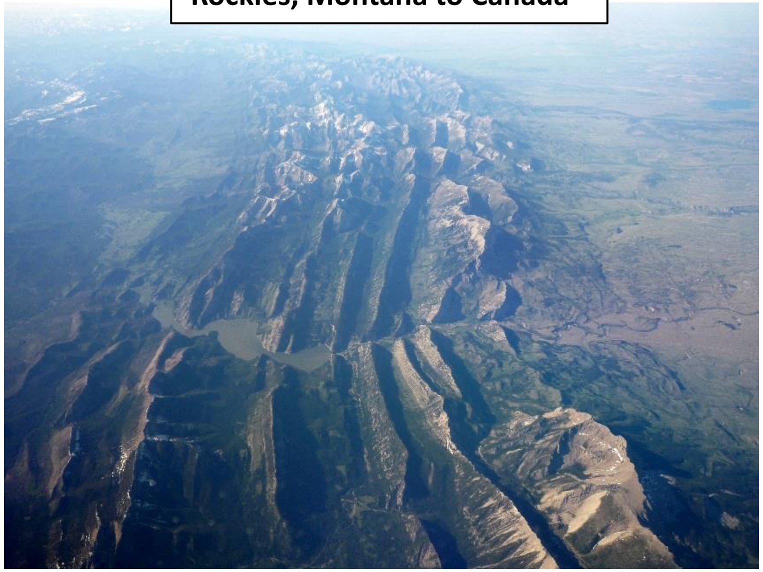

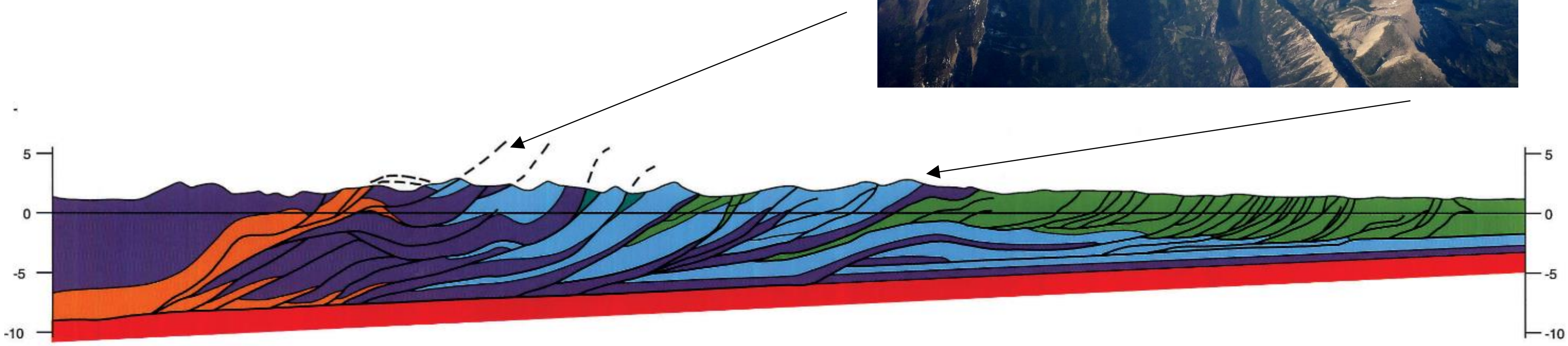

Low Strength Detachment

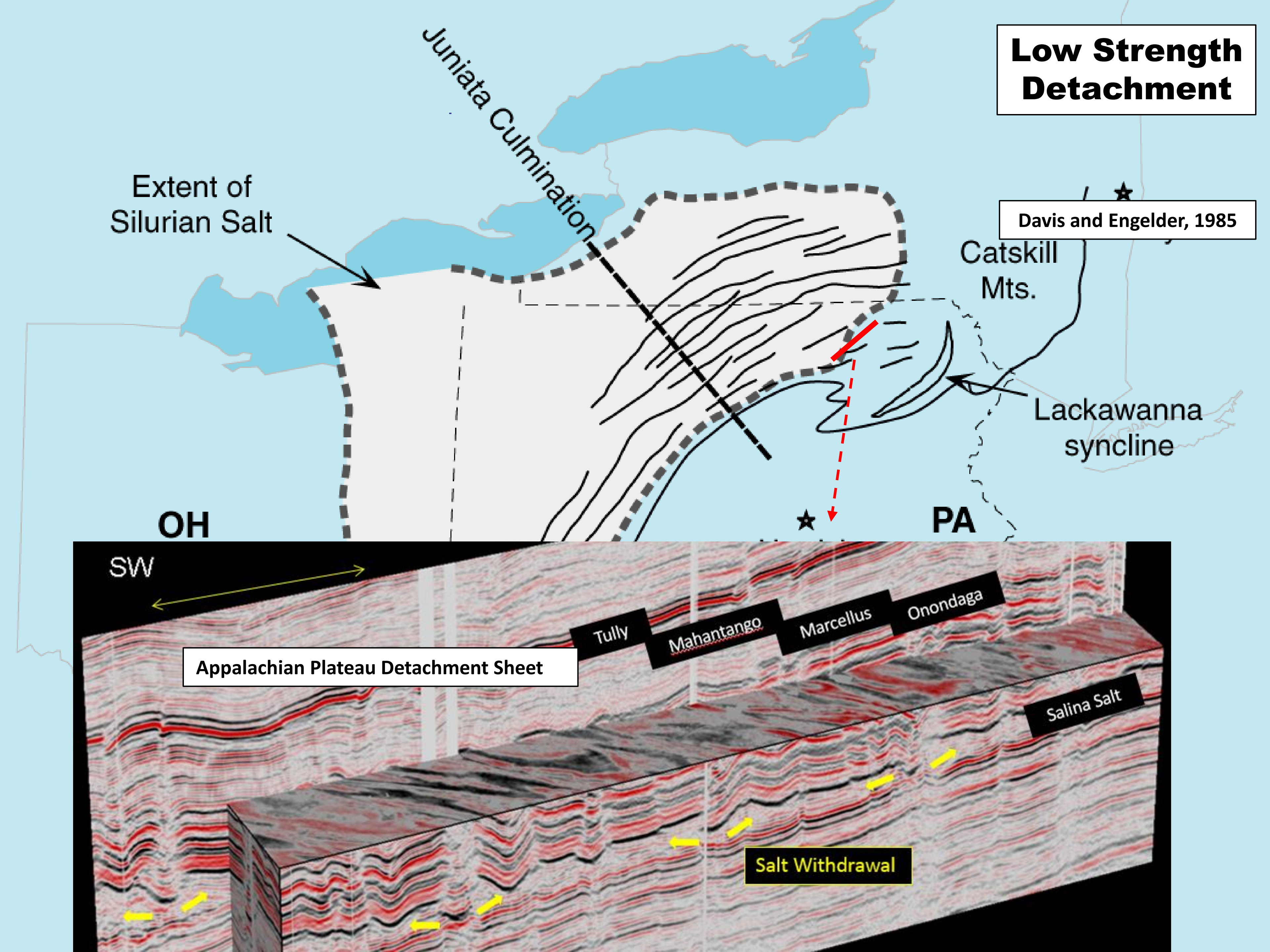

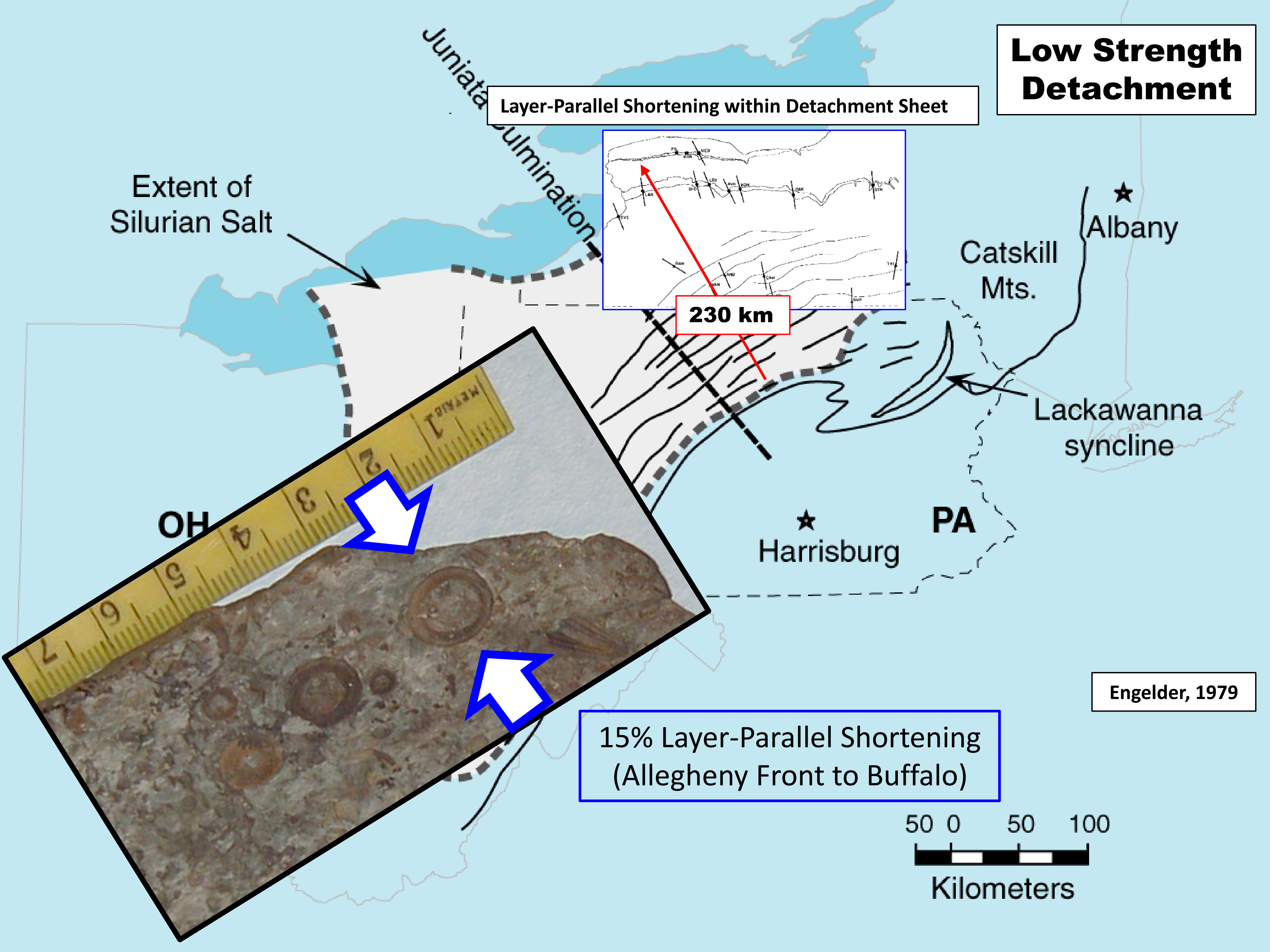

Low Strength Detachment
Layer-Parallel Shortening within Detachment Sheet
Juniata Culmination
Extent of Silurian Salt
230 km
Catskill Mts.
Albany
Lackawanna syncline
OH
Harrisburg
PA
Engelder, 1979
15% Layer-Parallel Shortening (Allegheny Front to Buffalo)
50 0 50 100
Kilometers

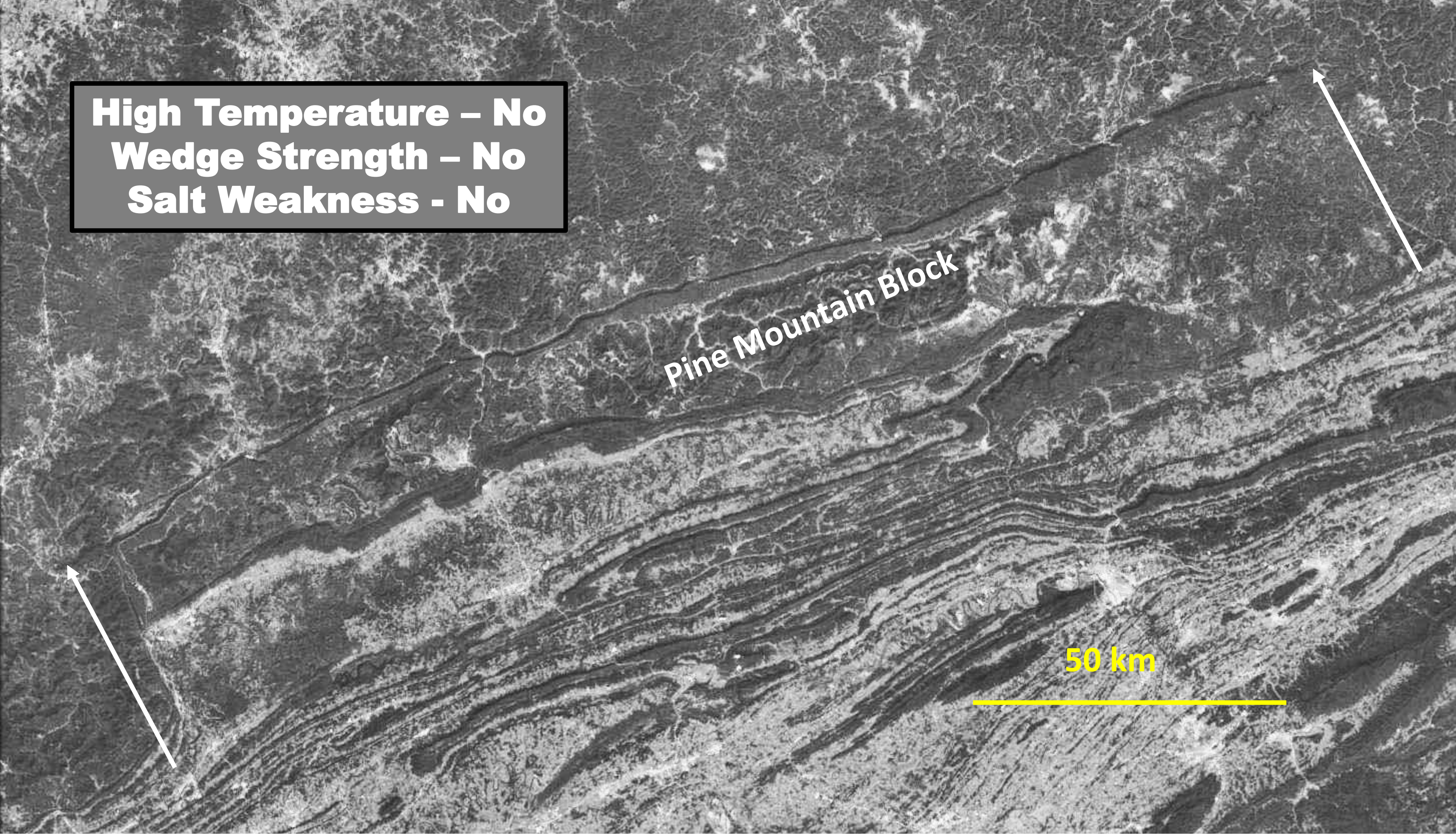
High Temperature – No
Wedge Strength – No
Salt Weakness - No
Pine Mountain Block
50 km

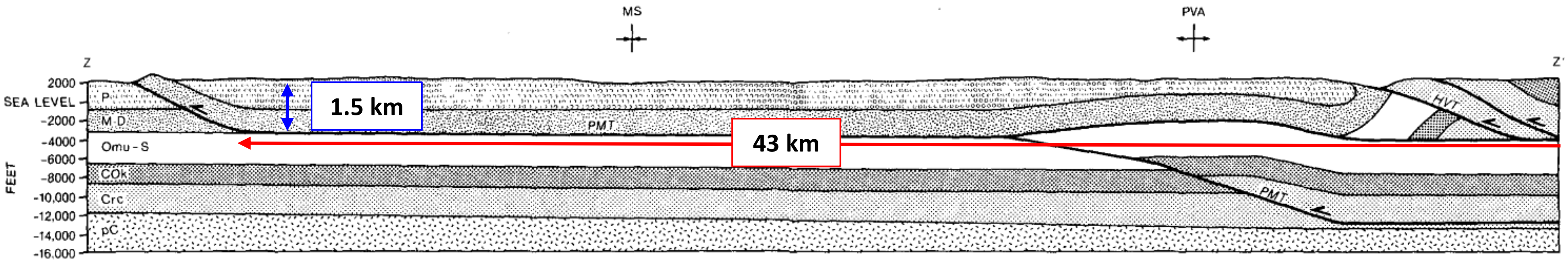
MS
PVA
Z
Z'
2000
SEA LEVEL
-2000
-4000
-6000
-8000
-10,000
-12,000
-14,000
-16,000
FEET
P
M-D
Omu-S
COk
Crc
pC
PMT
HVT
1.5 km
43 km

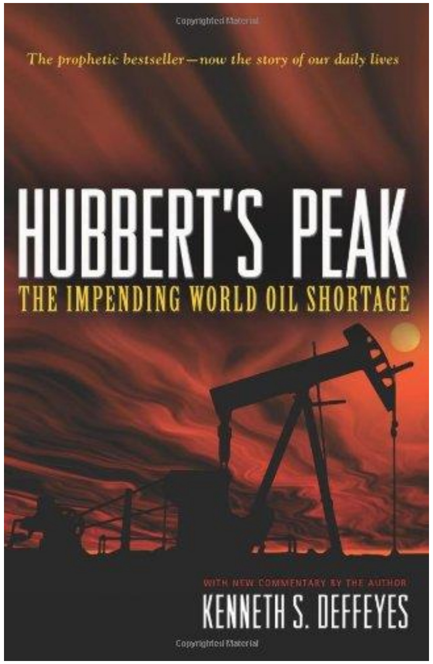

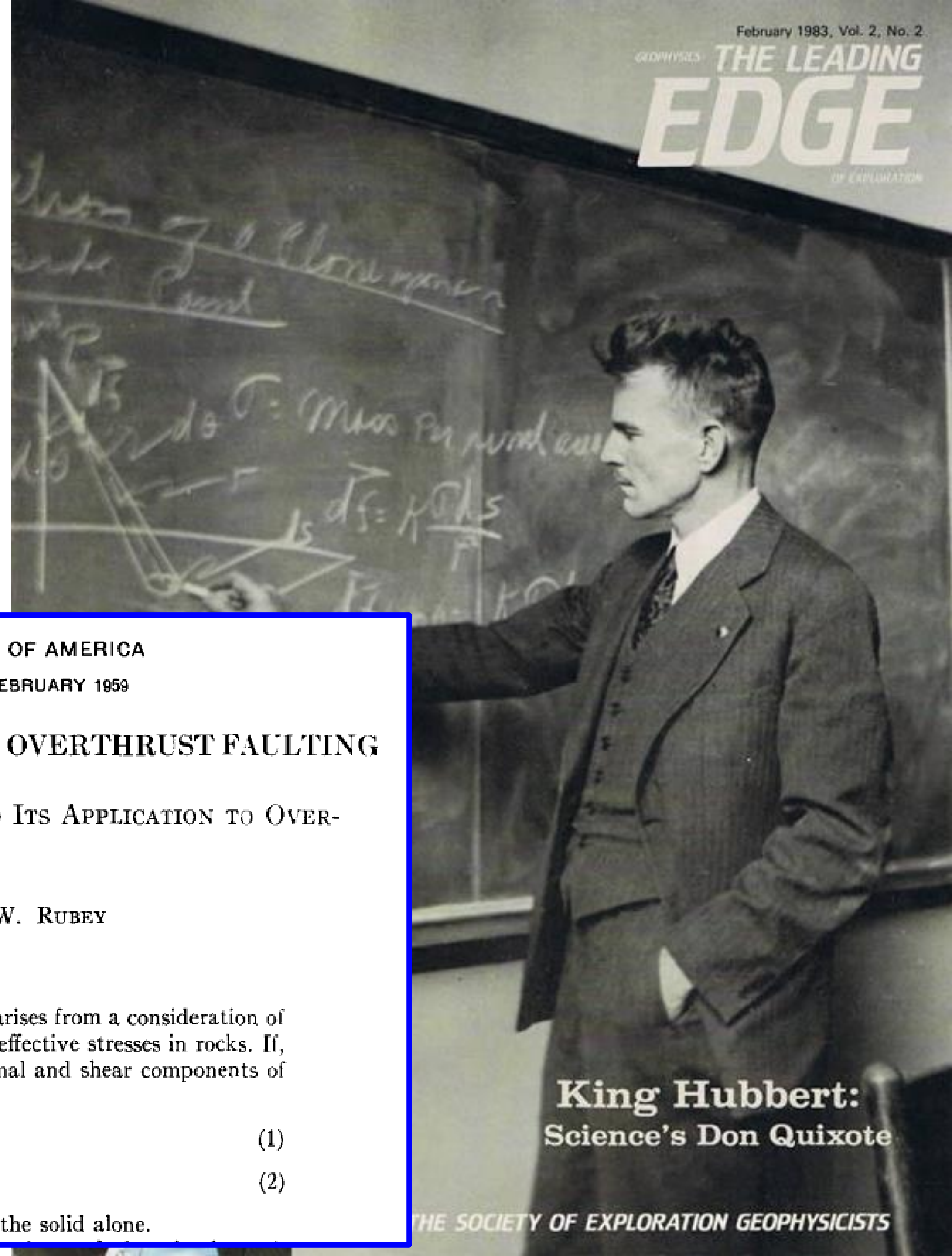

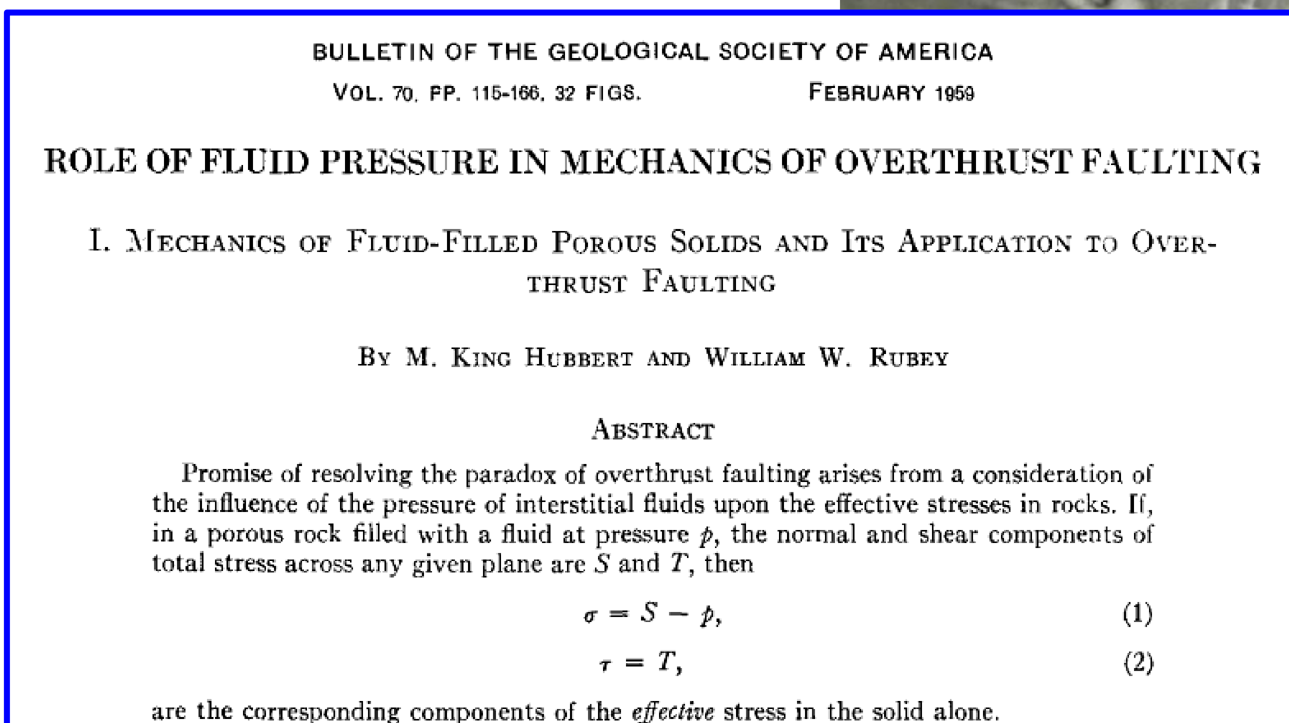

BULLETIN OF THE GEOLOGICAL SOCIETY OF AMERICA
VOL. 70, PP. 115-166, 32 FIGS. FEBRUARY 1959

ROLE OF FLUID PRESSURE IN MECHANICS OF OVERTHRUST FAULTING

I. Mechanics of Fluid-Filled Porous Solids and Its Application to Overthrust Faulting

By M. King Hubbert and William W. Rubey

Abstract

Promise of resolving the paradox of overthrust faulting arises from a consideration of the influence of the pressure of interstitial fluids upon the effective stresses in rocks. If, in a porous rock filled with a fluid at pressure p, the normal and shear components of total stress across any given plane are S and T, then

$$\sigma = S - p, \quad (1)$$

$$\tau = T, \quad (2)$$

are the corresponding components of the *effective* stress in the solid alone.

Three necessary geological conditions for the Hubbert-Rubey mechanism for overthrust faulting:

Biot actually suggested this experiment to Hubbert

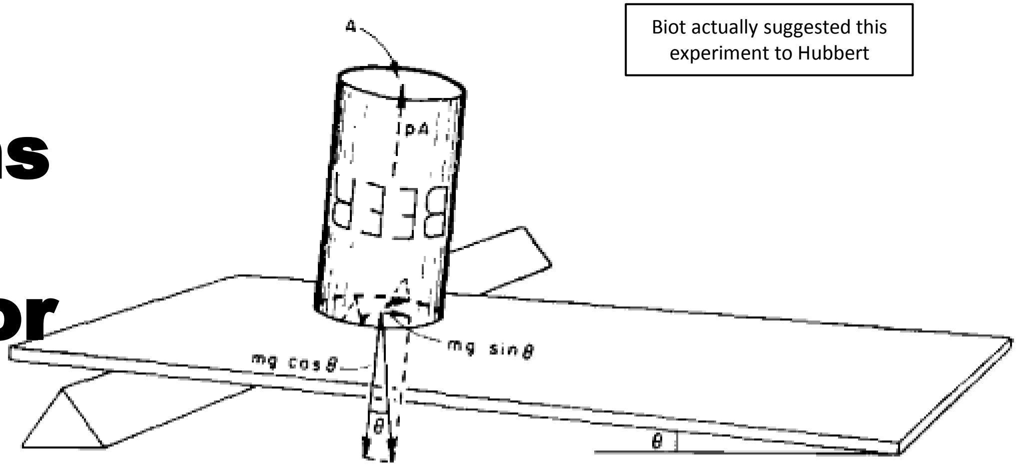

FIGURE 32.—BEER-CAN EXPERIMENT

1. Requires a mechanism(s) for generating abnormal pore pressure.

   Expansion of cold air

2. Requires a mechanism(s) for delivering abnormal pressure to the slip surface.
   1. High permeability rock

   The popped top

3. Requires a mechanism(s) for maintaining pressure even when leakage occurs.
   1. Low permeability rock

   Time-dependent expansion

Mechanisms for Generating Overpressure

Most effective generation mechanisms

- Stress-Related Mechanisms ★
  - Disequilibrium Compaction
  - Tectonic Compaction
- Fluid Volume Increase Mechanisms
  - Aquathermal Expansion
  - Water release during mineral diagenesis
  - Hydrocarbon generation ⇦
- Fluid Dynamic Mechanisms ★ ⇦
  - Potentiometric head
  - Hydrocarbon buoyancy

★ Hubbert-Rubey focus
⇦ Engelder focus

Swarbrick & Osborne, 1998

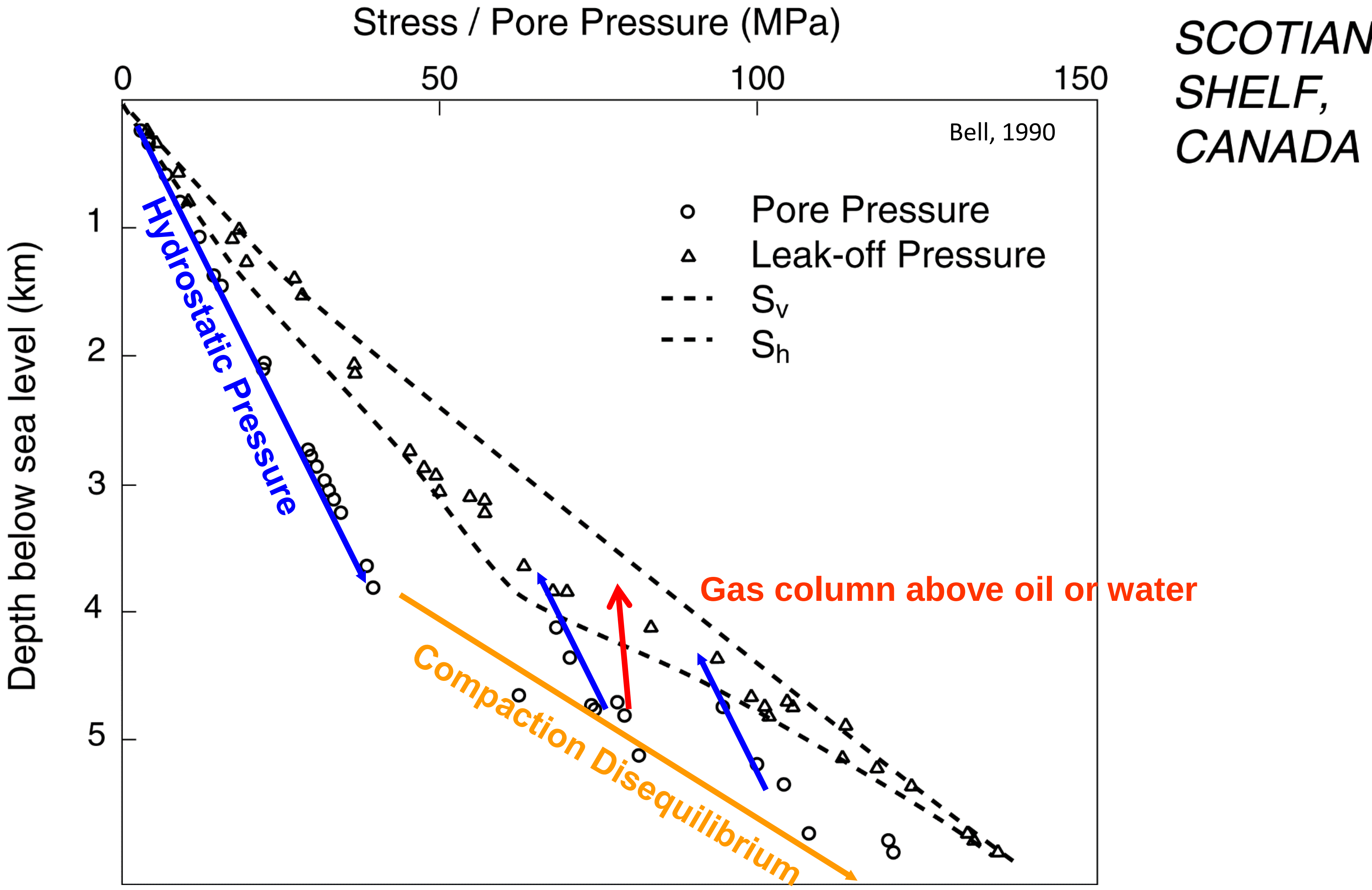

Two (2) Hubbert-Rubey (1959) mechanisms for abnormal pore pressure (mechanical compaction = stress mechanism - Orange) and (buoyancy = fluid dynamic mechanism - Red)

M King Hubbert (1903-1989)

Signed at a 1980 AAPG Hedberg Conference when Hubbert was 77 years old.

With appreciation to Terry Engelder for working on such an important problem

M. King Hubbert

Deformation associated with the movement of the Muddy Mountain overthrust in the Buffington window, southeastern Nevada

WILLIAM G. BROCK *AMOCO Production Company, Security Life Building, Denver, Colorado 80202*
TERRY ENGELDER *Lamont-Doherty Geological Observatory, Palisades, New York 10964*

ABSTRACT

The Muddy Mountain overthrust, exposed in the Buffington window, southeastern Nevada, consists of a Paleozoic carbonate sheet thrust over Mesozoic Aztec Sandstone, with a molasse filling topographic lows. Evidence suggests that the thrust sheet moved across an erosional surface and that the molasse may have been a

on a fault when the shear stress on this plane exceeds the sum of the cohesive strength and the product of the coefficient of friction and the effective normal stress. The Hubbert-Rubey hypothesis suggests a mechanism for reducing the effective normal stress, whereas the Wilson hypothesis suggests a way to reduce the coefficient of friction.

We wished to study deformation associated with overthrust

Brock and Engelder (1977) Geological Society of America Bulletin

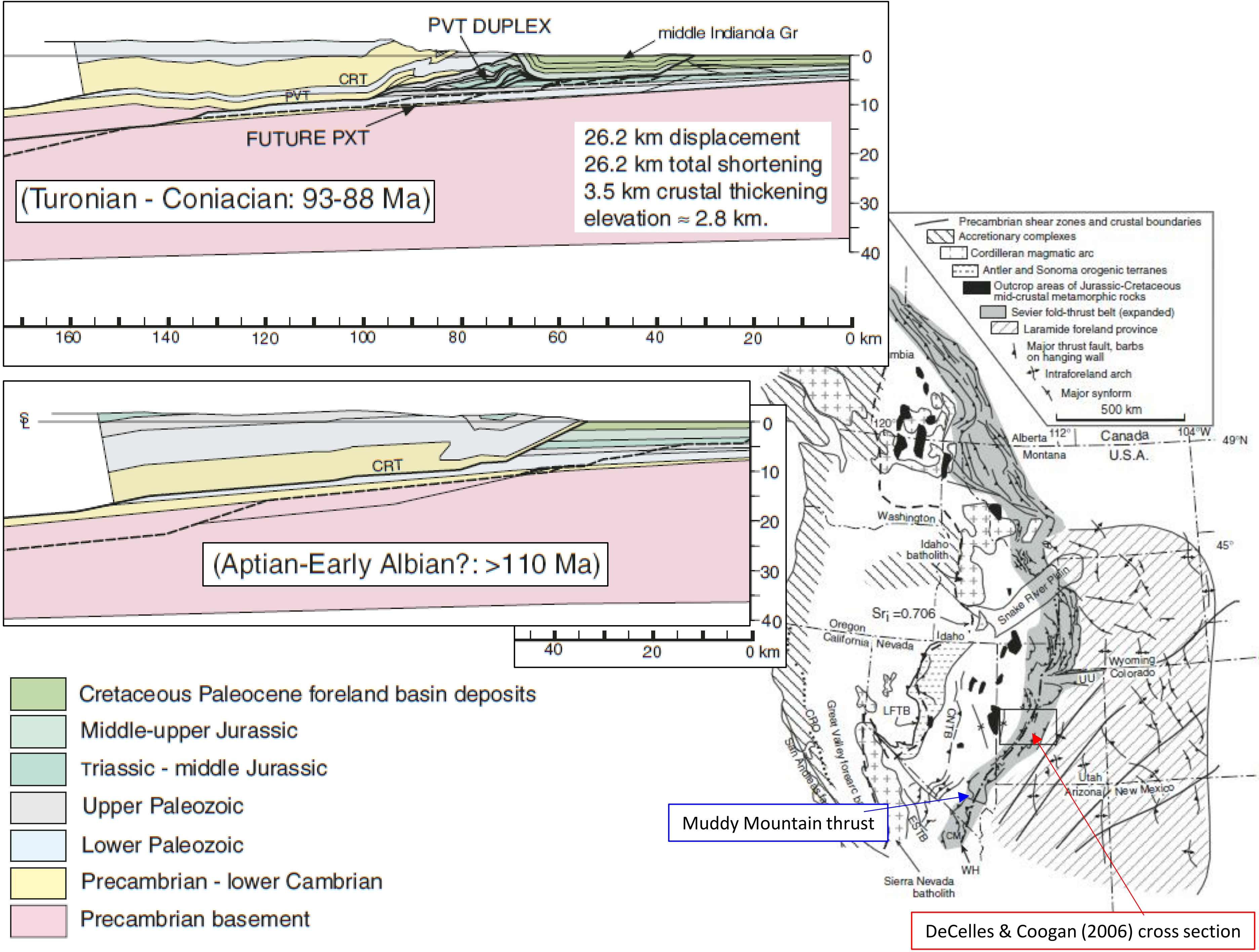
PVT DUPLEX
middle Indianola Gr
CRT
PVT
FUTURE PXT
26.2 km displacement
26.2 km total shortening
3.5 km crustal thickening
elevation ≈ 2.8 km.
(Turonian - Coniacian: 93-88 Ma)
0
10
20
30
40
160 140 120 100 80 60 40 20 0 km
SL
CRT
(Aptian-Early Albian?: >110 Ma)
40 20 0 km
Cretaceous Paleocene foreland basin deposits
Middle-upper Jurassic
Triassic - middle Jurassic
Upper Paleozoic
Lower Paleozoic
Precambrian - lower Cambrian
Precambrian basement
Precambrian shear zones and crustal boundaries
Accretionary complexes
Cordilleran magmatic arc
Antler and Sonoma orogenic terranes
Outcrop areas of Jurassic-Cretaceous mid-crustal metamorphic rocks
Sevier fold-thrust belt (expanded)
Laramide foreland province
Major thrust fault, barbs on hanging wall
Intraforeland arch
Major synform
500 km
Alberta
Montana
Canada
U.S.A.
49°N
45°
Washington
Idaho batholith
Snake River Plain
Sri =0.706
Oregon
California
Nevada
Idaho
Wyoming
Colorado
UU
LFTB
CNTB
Great Valley forearc
San Andreas
Utah
Arizona
New Mexico
ESTB
CM
WH
Sierra Nevada batholith
Muddy Mountain thrust
DeCelles & Coogan (2006) cross section

The Muddy Mountain Thrust

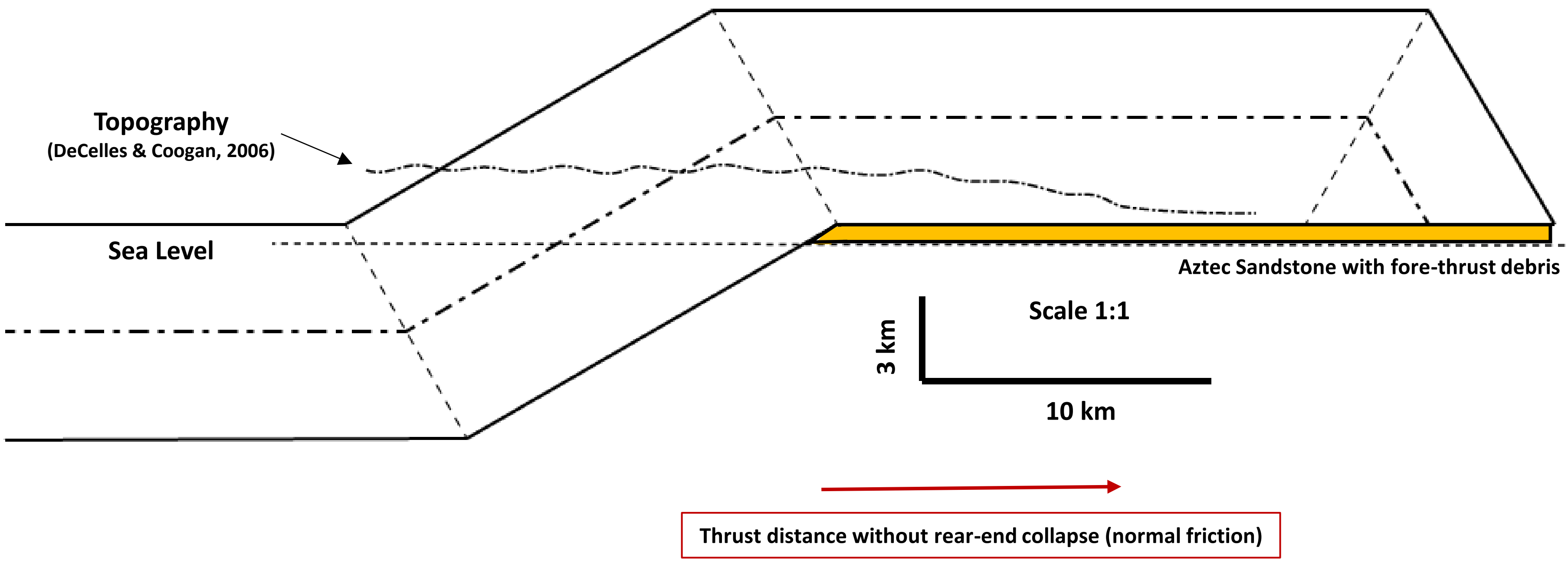

Longwell (1922) discovered the Muddy Mountain overthrust in southeastern Nevada, in which a block of Paleozoic strata with a stratigraphic thickness of about 25,000 feet had overridden the same section for about 15 miles.

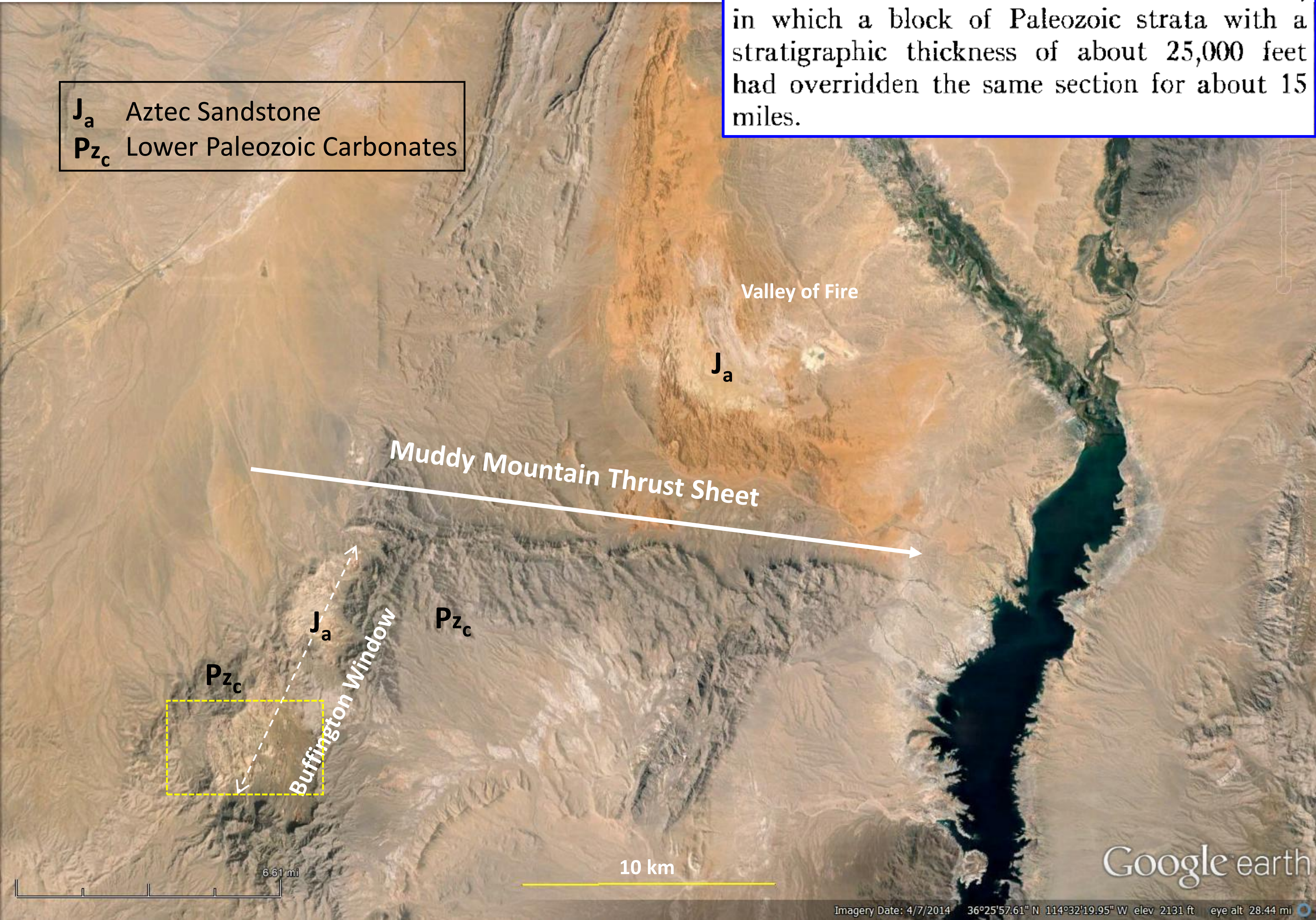


Engelder – Kodachrome Slide
Buffington Window
Looking west (1971)
Pz_c
J_a

Muddy Mountain Thrust
J$_a$
Pz$_c$
K$_m$
99 Ma fore-thrust debris (Fleck and Carr, 1990)
3144 ft
1990
Imagery Date: 3/24/2014 36°19'22.65" N 114°43'12.42" W elev 3580 ft eye alt 17278 ft
Google earth

How can a pore pressure be maintained when the detachment rides over the land surface?

"It can't!" (Brock and Engelder, 1977)

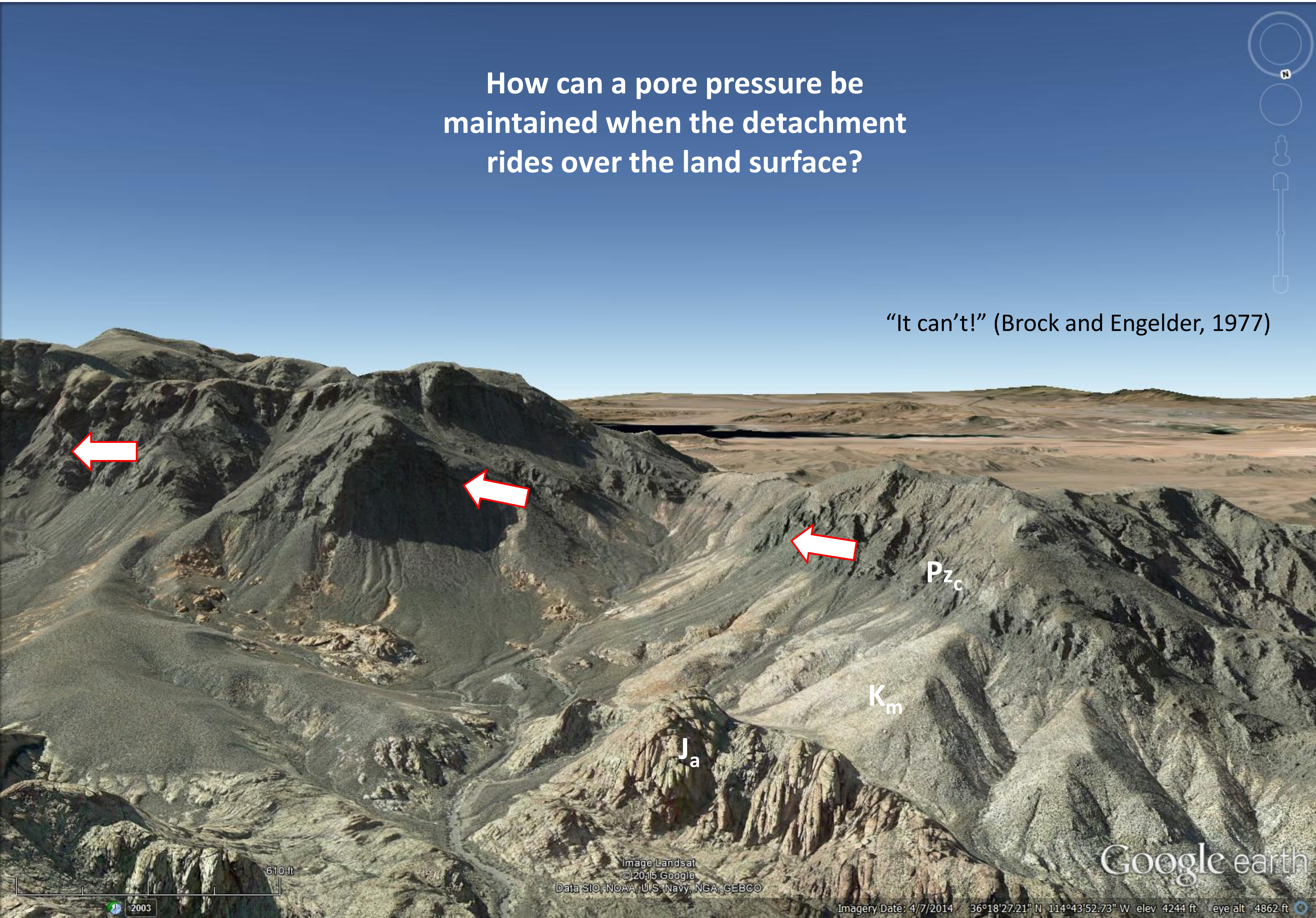

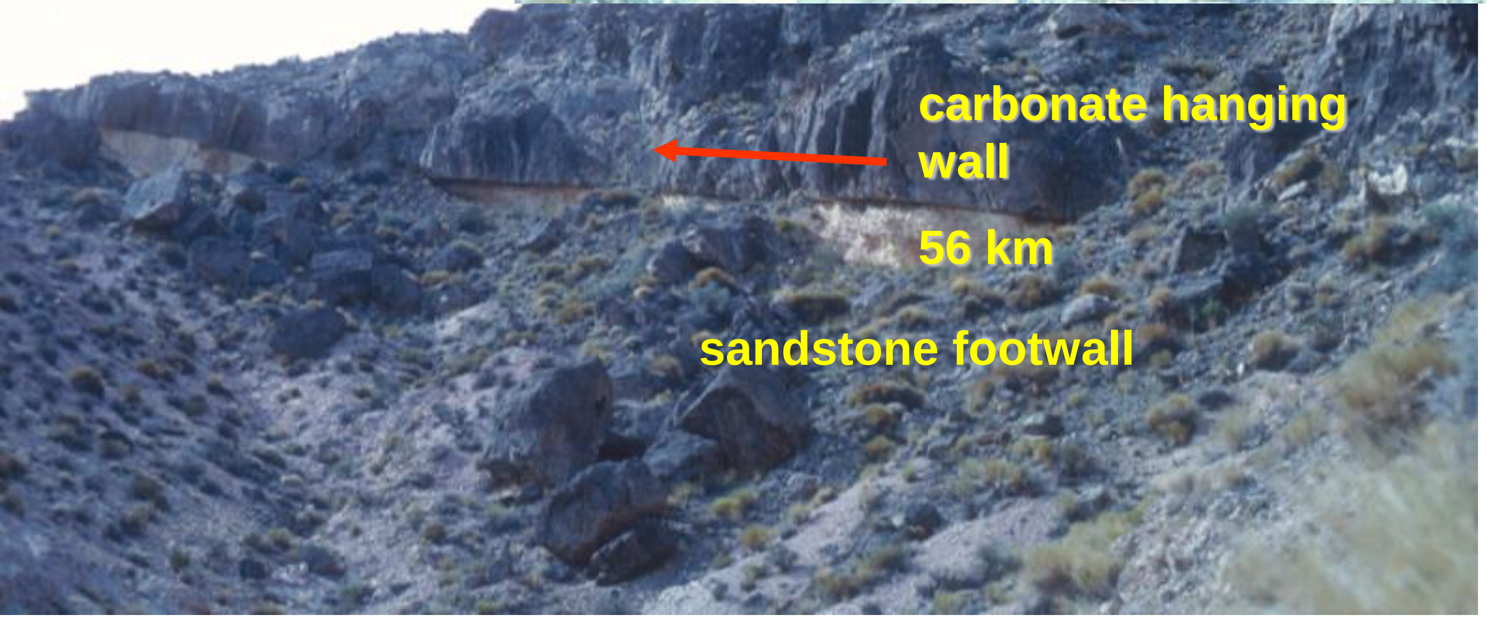

What does rock look like at the sliding surface when slip = 56 km??

BULLETIN OF THE GEOLOGICAL SOCIETY OF AMERICA
VOL. 60, PP. 923-968, 14 FIGS, 11 PLS. MAY 1949

STRUCTURE OF THE NORTHERN MUDDY MOUNTAIN AREA, NEVADA

BY CHESTER R. LONGWELL

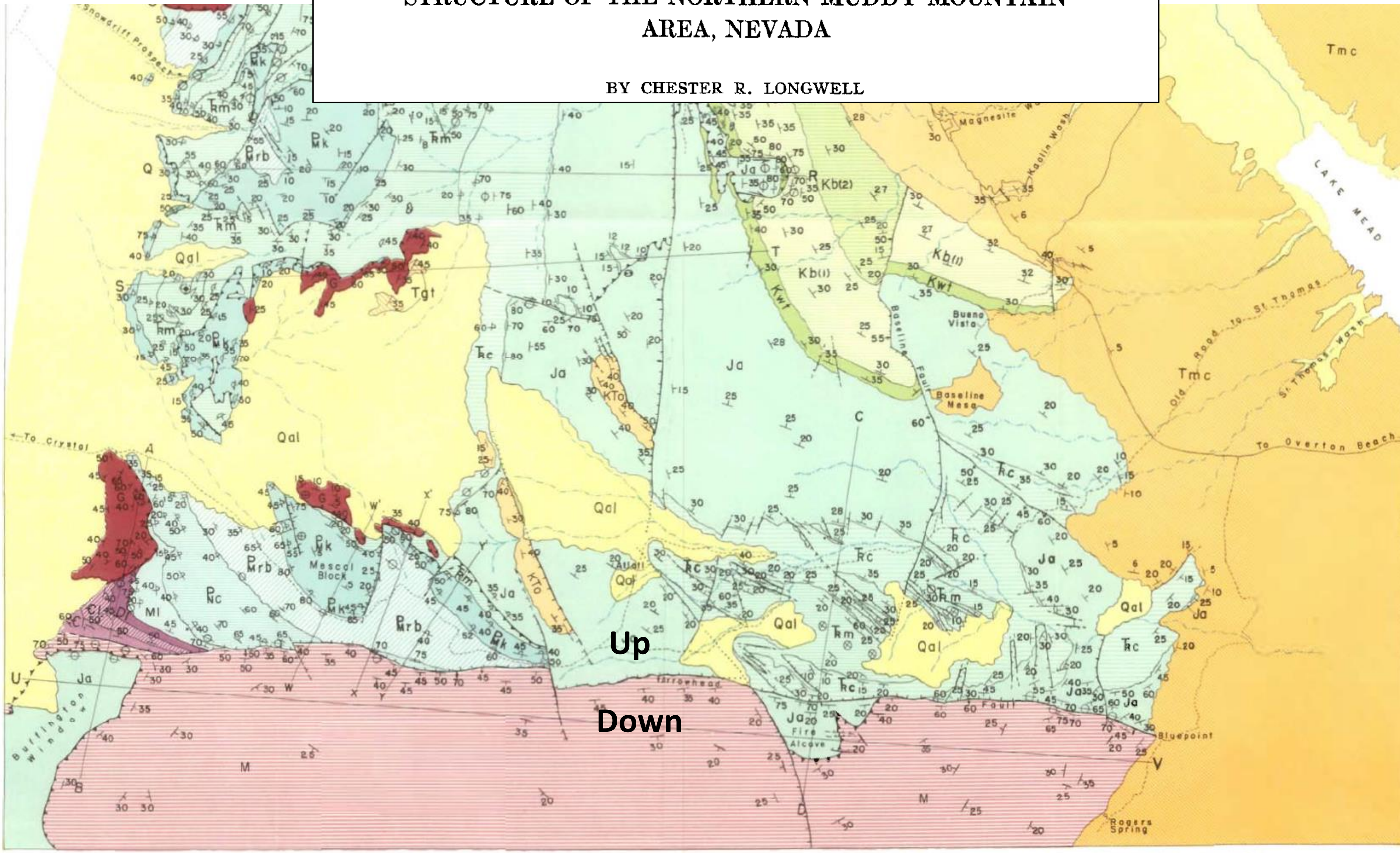

GEOLOGIC AND TECTONIC MAP OF THE NORTHERN MUDDY MOUNTAIN AREA

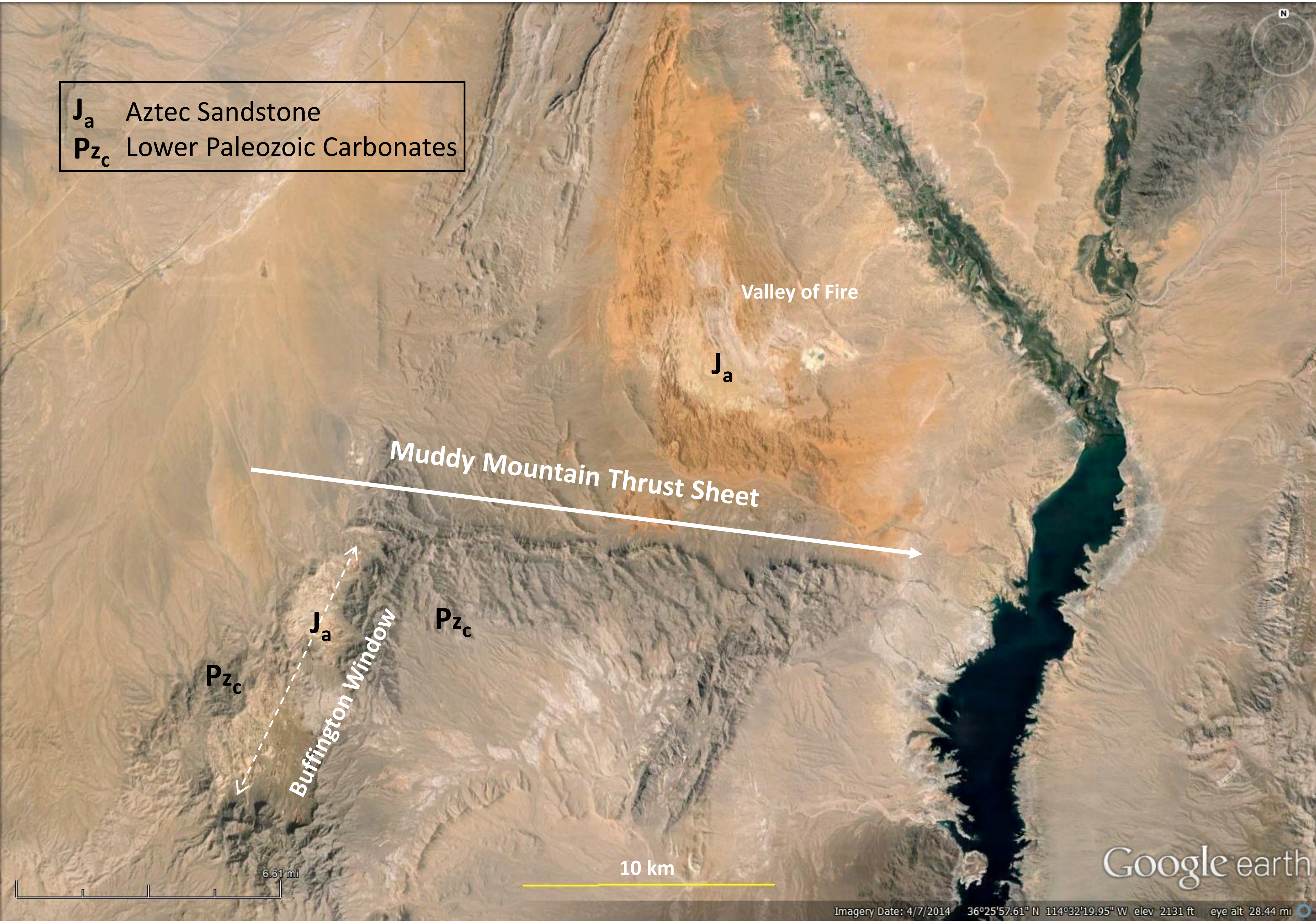

J_a Aztec Sandstone
Pz_c Lower Paleozoic Carbonates
Valley of Fire
J_a
Muddy Mountain Thrust Sheet
J_a
Pz_c
Pz_c
Buffington Window
10 km
6.61 mi
Google earth
Imagery Date: 4/7/2014 36°25'57.61" N 114°32'19.95" W elev 2131 ft eye alt 28.44 mi


Beitler et al., 2003
Zion National Park from Checkerboard Mesa
Dune cross-strata: High permeability
No Hematite
Hematite
Oil-Water Contact?
Horizontal bedding: Low permeability zones that restrict fluid flow
Navajo Sandstone
© Photography by Tanya

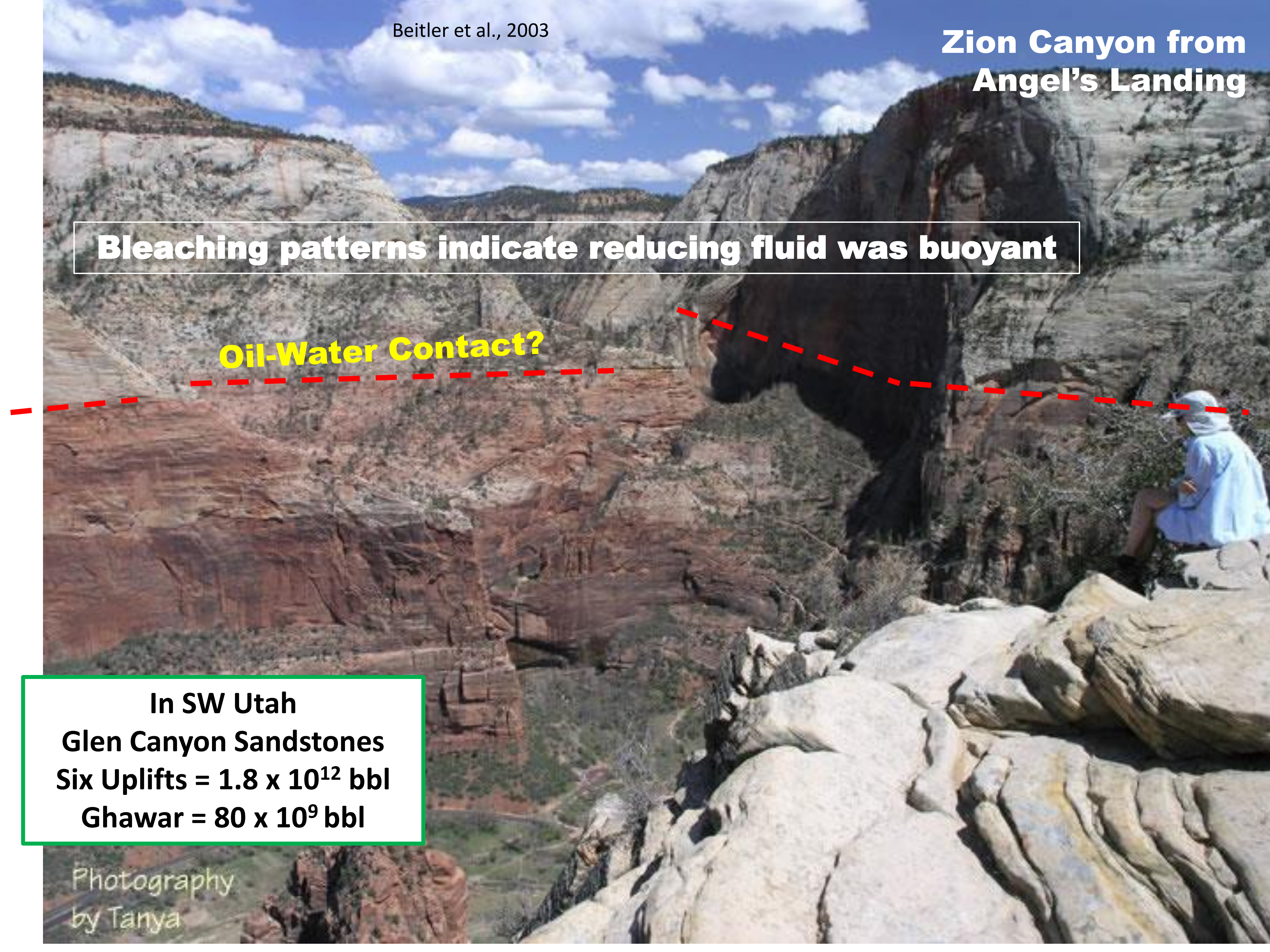
Beitler et al., 2003
Zion Canyon from Angel's Landing
Bleaching patterns indicate reducing fluid was buoyant
Oil-Water Contact?
In SW Utah
Glen Canyon Sandstones
Six Uplifts = 1.8 x 10^12 bbl
Ghawar = 80 x 10^9 bbl
Photography by Tanya

5 km
Angel's Landing
Checkerboard Mesa
9
Oil-water contact
© 2015 Google
2.44 mi
Imagery Date: 4/22/2013 37°13'29.71" N 112°53'26.25" W elev 5533 ft

Valley of Fire

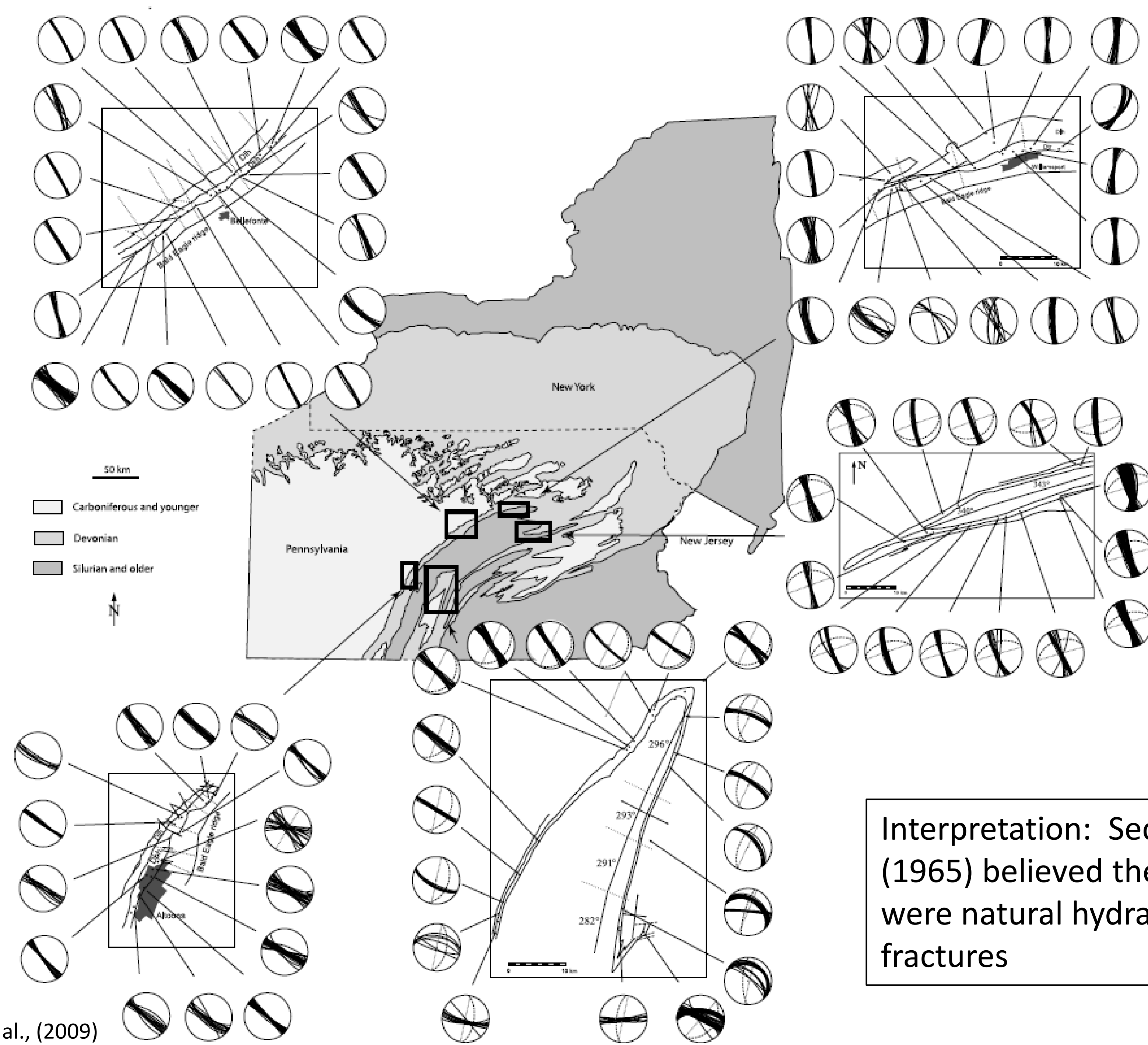

Interpretation: Secor (1965) believed these were natural hydraulic fractures

Engelder et al., (2009)

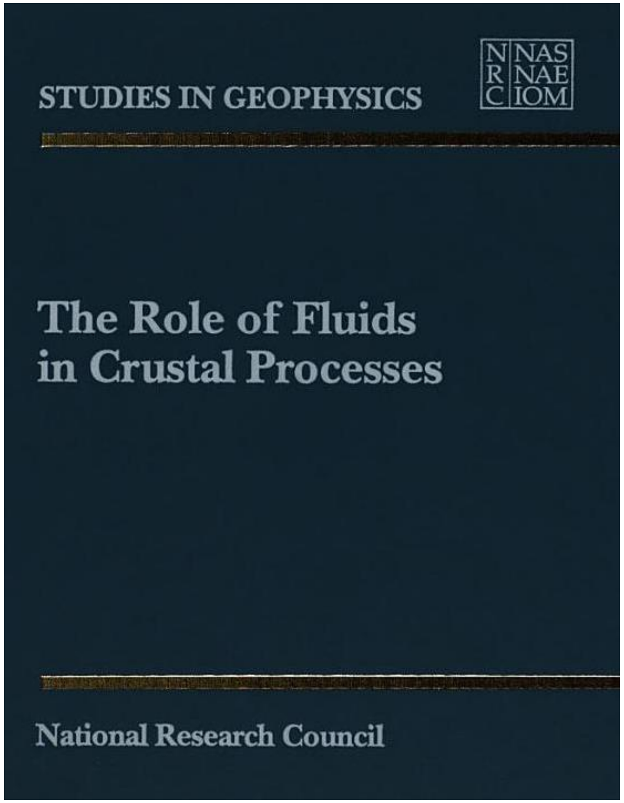

Smoluchowski's Dilemma Revisited: A Note on the Fluid Pressure History of the Central Appalachian Fold-Thrust Belt

9

TERRY ENGELDER
The Pennsylvania State University

Smoluchowski's Dilemma Revisited: A Note on the Fluid Pressure History of the Central Appalachian Fold-Thrust Belt
T ENGELDER - The Role of Fluids in Crustal Processes, 1990 - books.google.com
ABSTRACT Cross-fold joints in the Central Appalachian fold-thrust belt propagated during periods of abnormally high fluid pressure prior to tectonic compaction and the development of first-order Alleghanian structures in the valley and ridge. These early joints, found in ...
Cited by 2 Related articles All 2 versions Cite Save

Not every scientific paper is a smash hit!

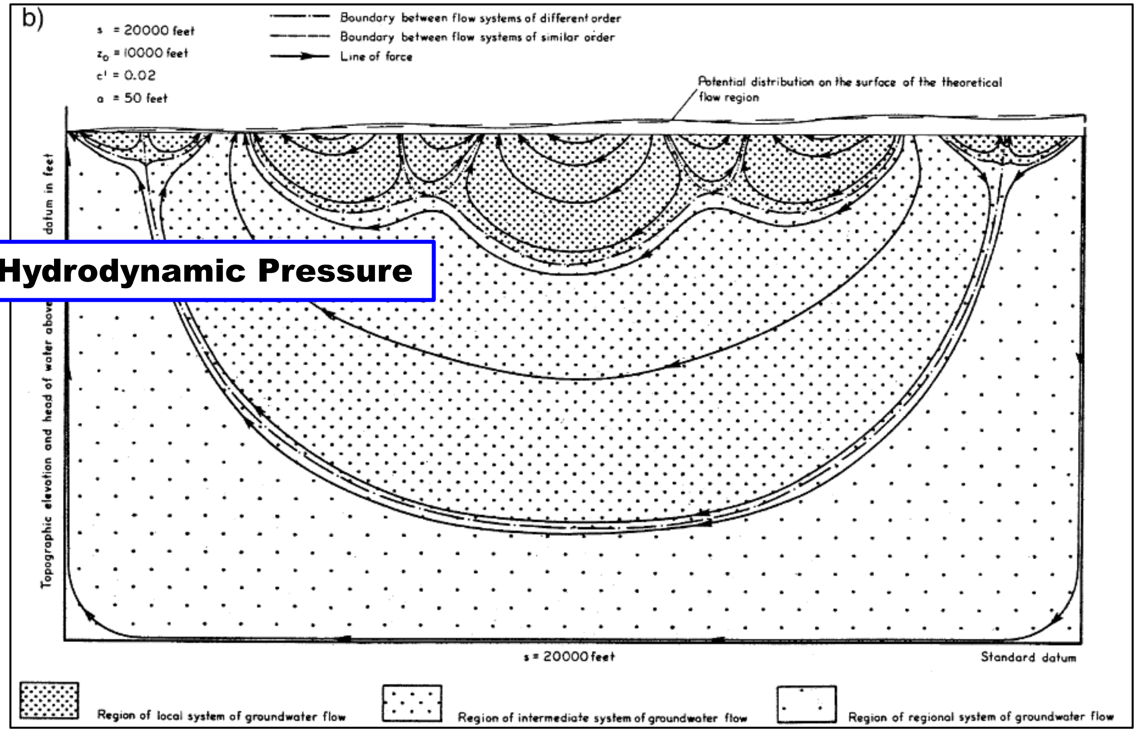

Toth, 1962

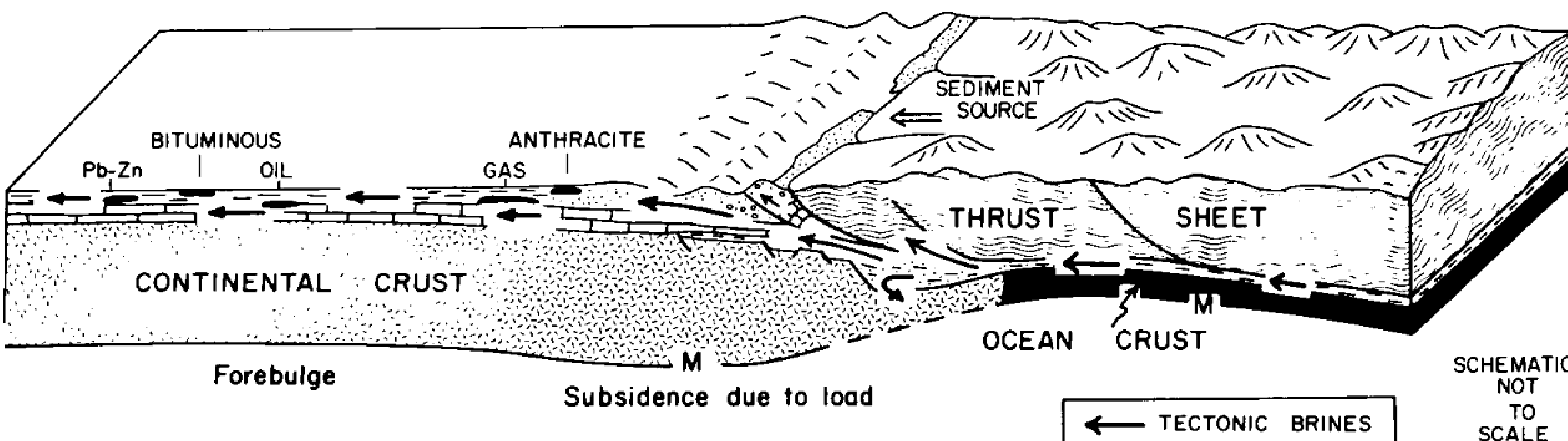

Oliver, 1986

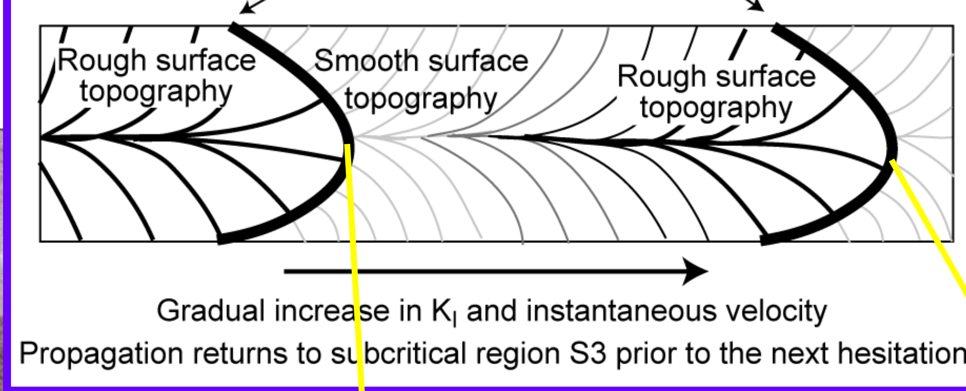

Savalli & Engelder, 2005

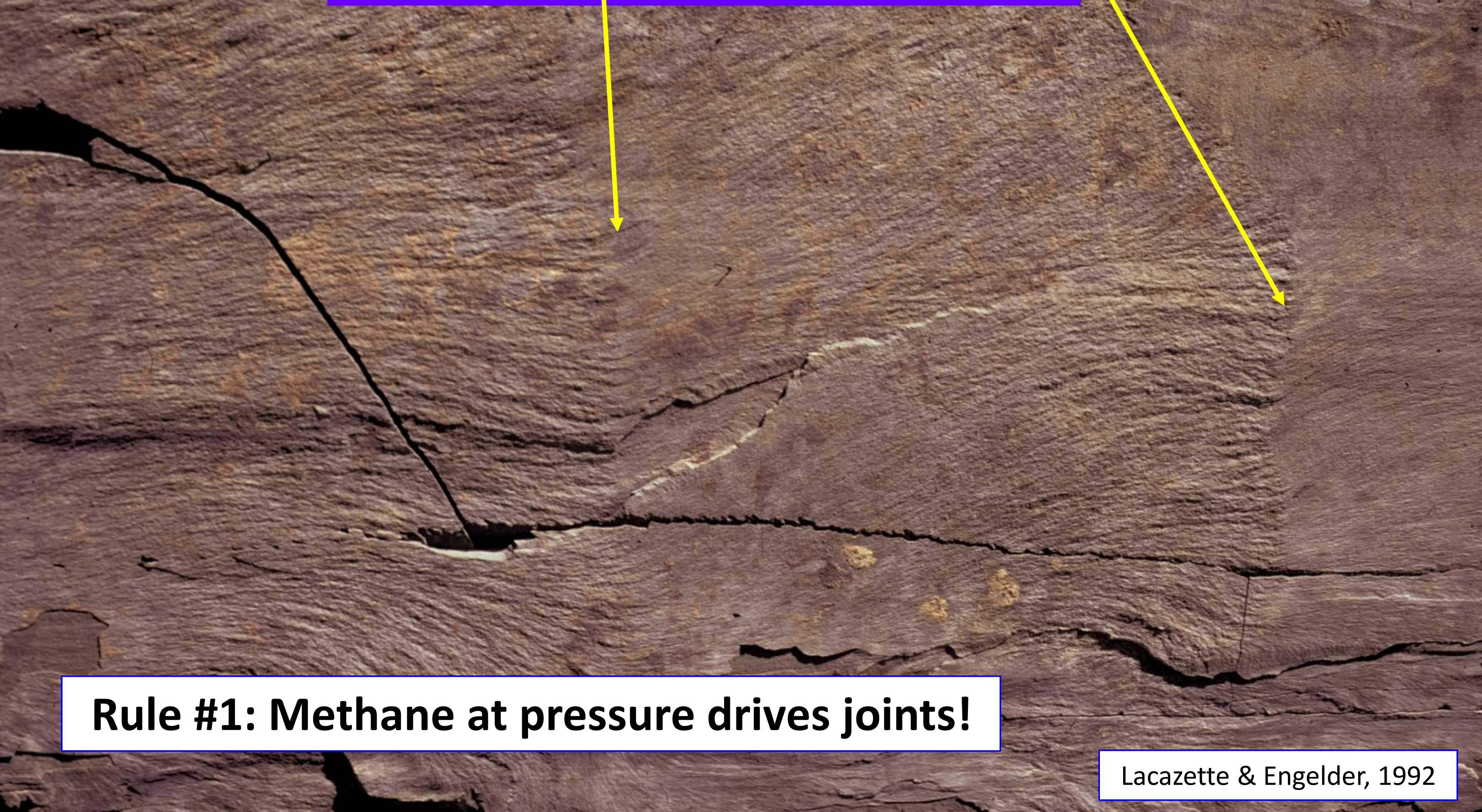

Rule #1: Methane at pressure drives joints!

Lacazette & Engelder, 1992

Rule #2: Orientation of NHF controlled by superposition of gravity-related stress and tectonic stress yoked to pore pressure!

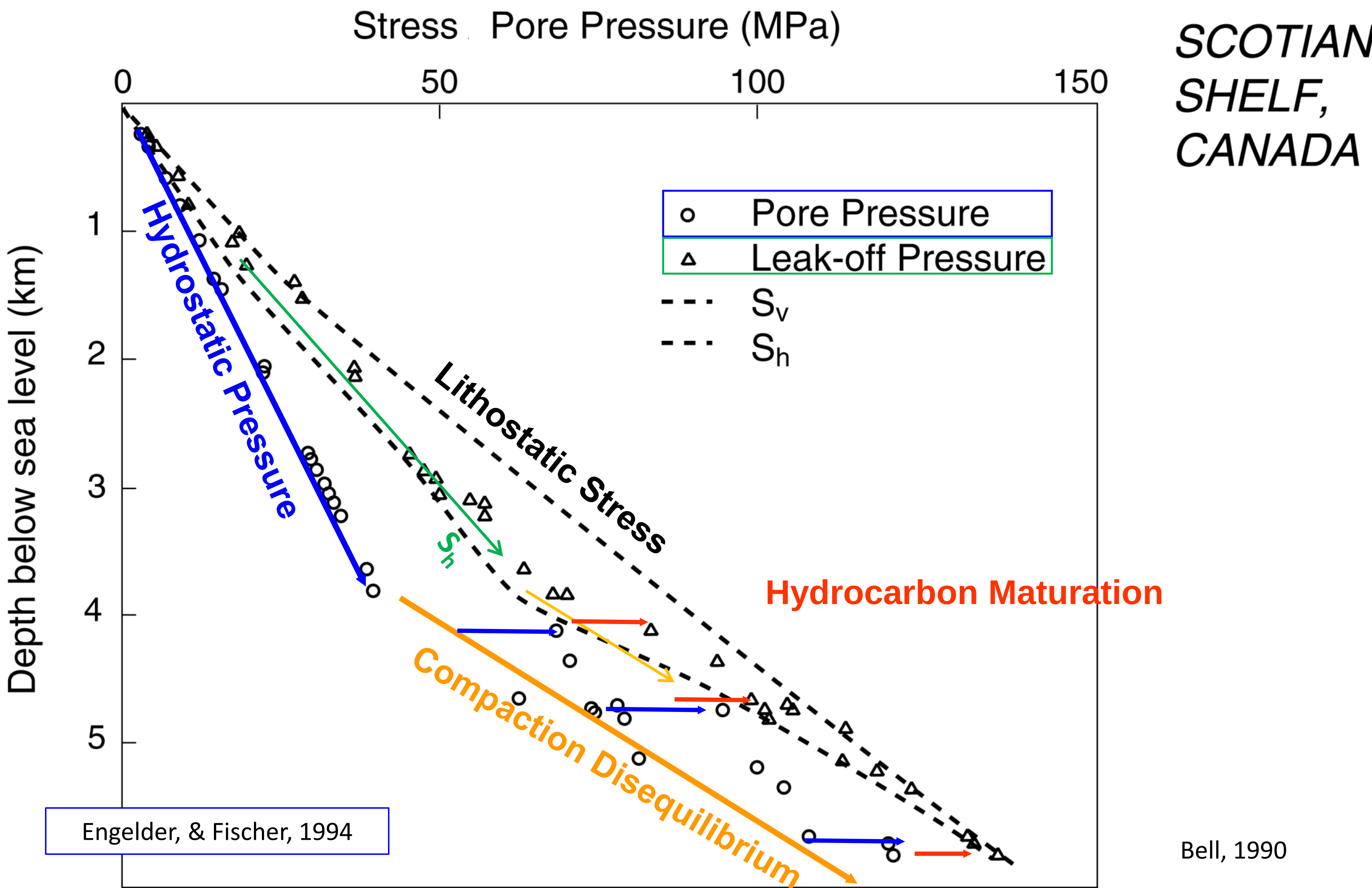

Engelder, & Fischer, 1994

Rule #2: Orientation of NHF controlled by superposition of gravity-related stress and tectonic stress yoked to pore pressure!

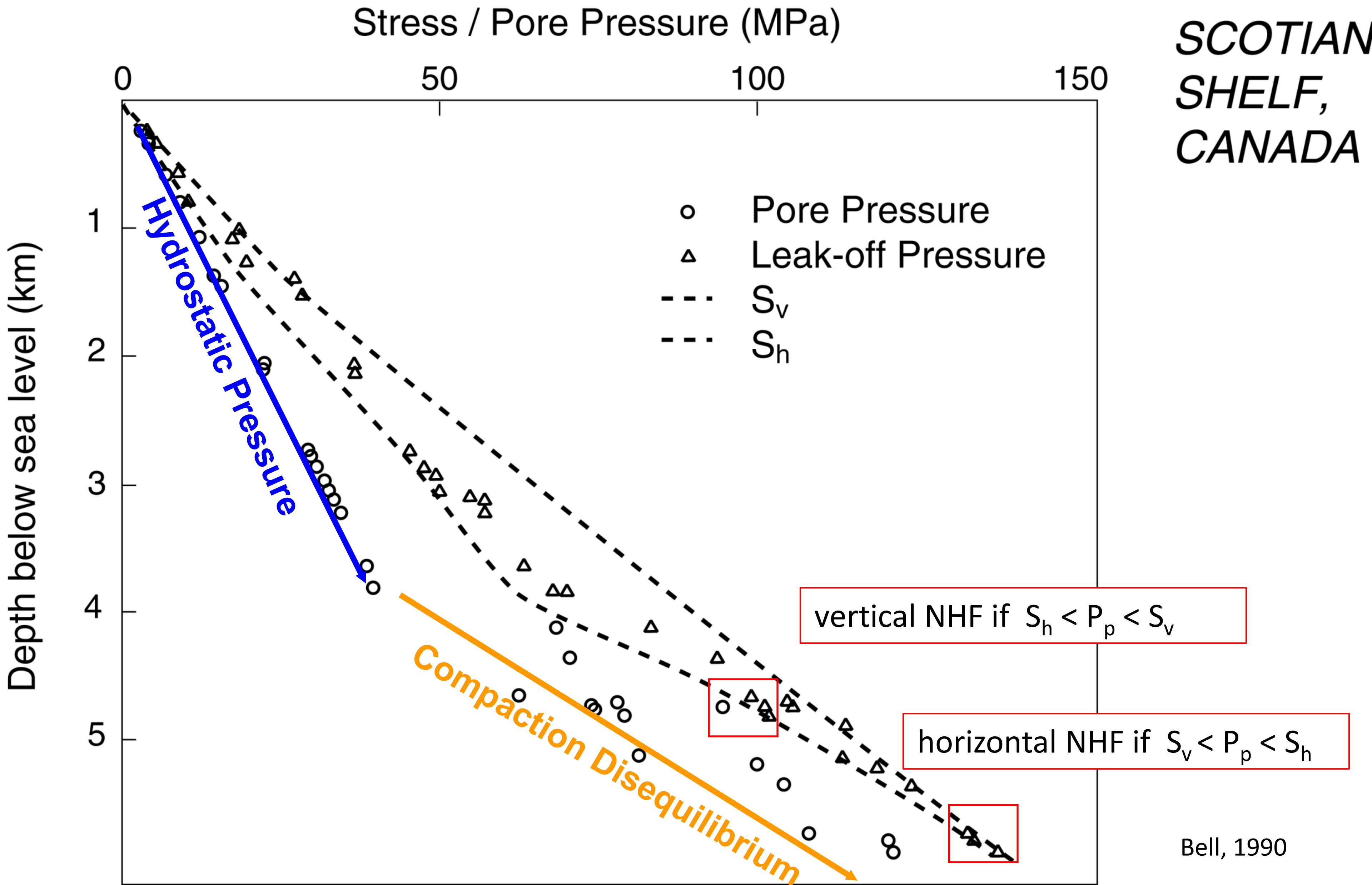

BULLETIN OF THE GEOLOGICAL SOCIETY OF AMERICA
VOL. 70, PP. 115-166, 32 FIGS. FEBRUARY 1959

ROLE OF FLUID PRESSURE IN MECHANICS OF OVERTHRUST FAULTING

I. MECHANICS OF FLUID-FILLED POROUS SOLIDS AND ITS APPLICATION TO OVERTHRUST FAULTING

BY M. KING HUBBERT AND WILLIAM W. RUBEY

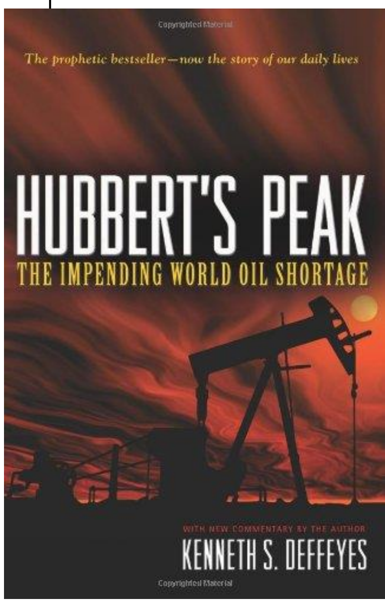

Journal of Structural Geology 69 (2014) 519–537
Journal of Structural Geology
journal homepage: www.elsevier.com/locate/jsg

Revisiting the Hubbert–Rubey pore pressure model for overthrust faulting: Inferences from bedding-parallel detachment surfaces within Middle Devonian gas shale, the Appalachian Basin, USA

Murat G. Aydin [1], Terry Engelder*
Department of Geosciences, The Pennsylvania State University, University Park, PA 16802, USA

- Marcellus not created equal
  - Gas in place
  - Reservoir quality
  - Completions quality
- Engineering practices
  - Drilling
  - Completions

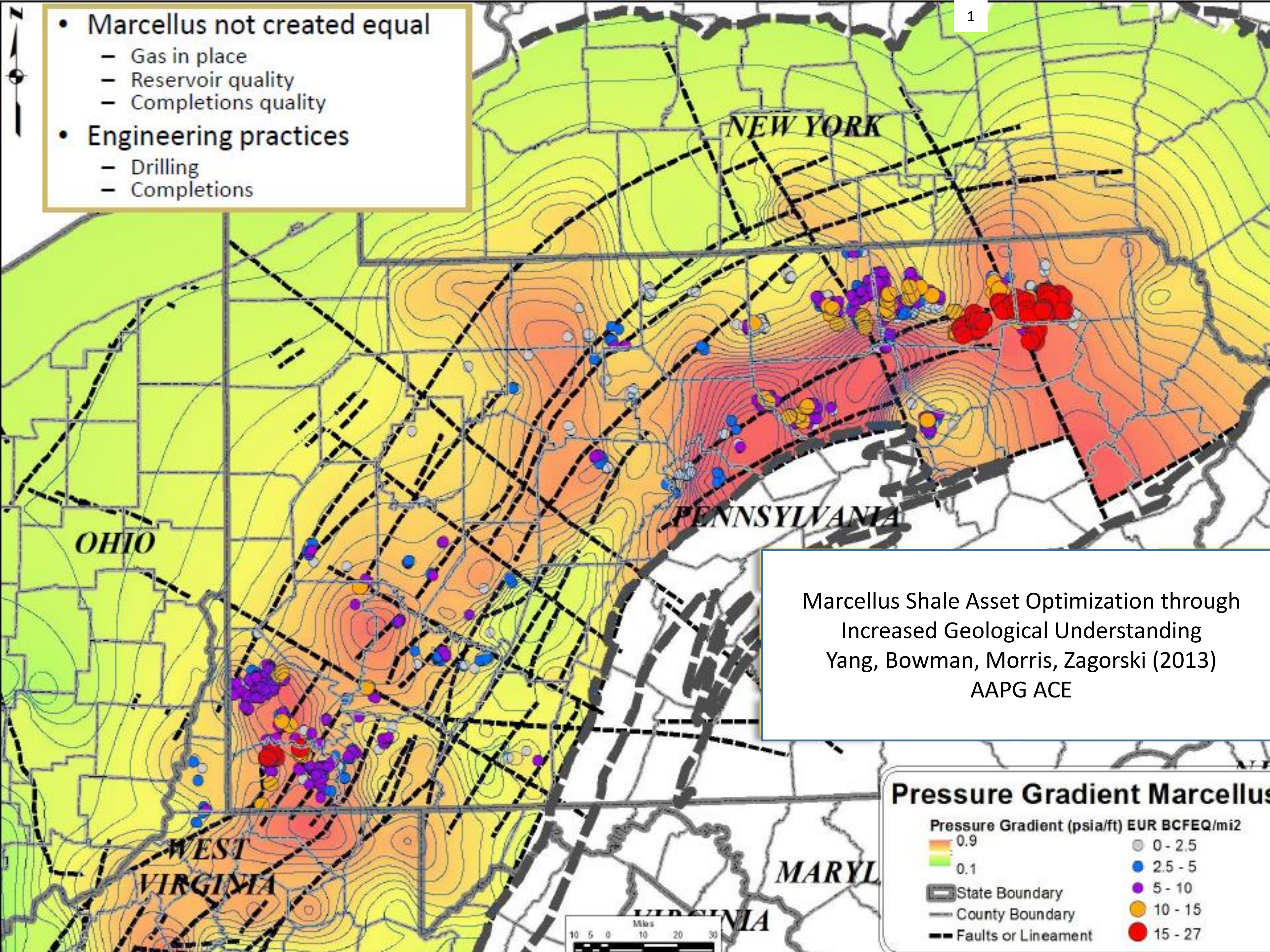

Marcellus Shale Asset Optimization through Increased Geological Understanding
Yang, Bowman, Morris, Zagorski (2013)
AAPG ACE

Another major Appalachian overthrust is the Pine Mountain overthrust and the Cumberland thrust block first described by Wentworth (1921a; 1921b) and subsequently studied in more detail by Butts (1927), Rich (1934), and

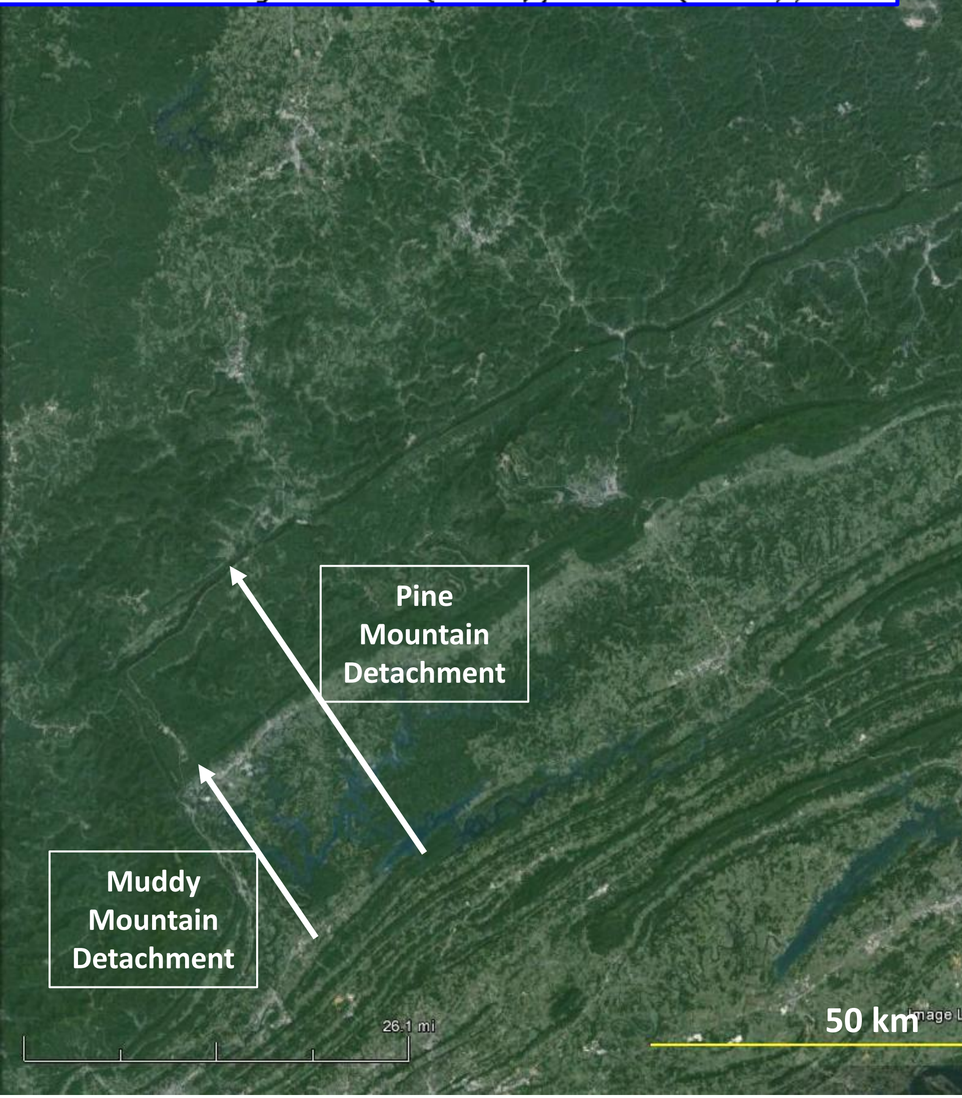

Hubbert and Rubey (1959) said:

According to Young (1957), the fault surface has been intersected by numerous gas wells which show that it occurs near the base of a Devonian shale at an average depth of about 5500 feet, or a little more than a mile. It is also of interest that high pressures encountered in the fault zone cause troublesome blowouts while drilling. No pressure measurements were given, but since the drilling was with cable tools this does not necessarily imply that the pressure was abnormally high.

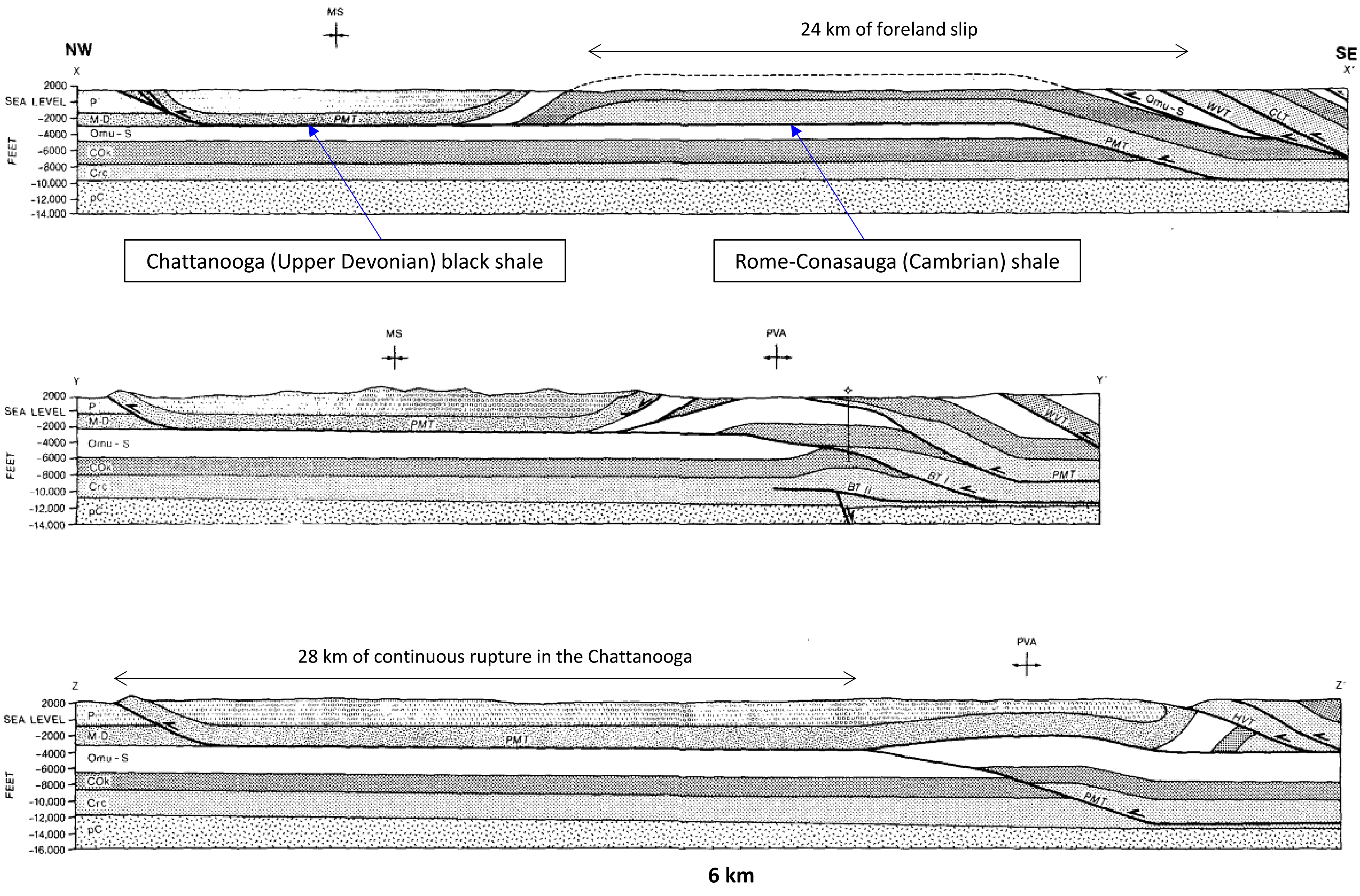

Mitra, 1988, GSAB

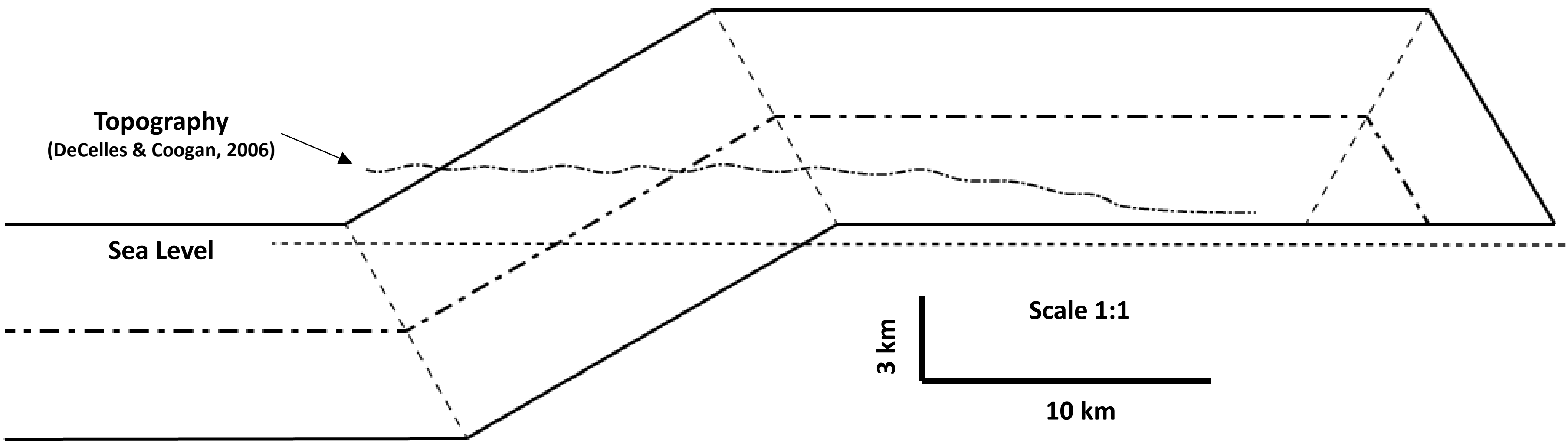

Topography
(DeCelles & Coogan, 2006)
Sea Level
Scale 1:1
3 km
10 km

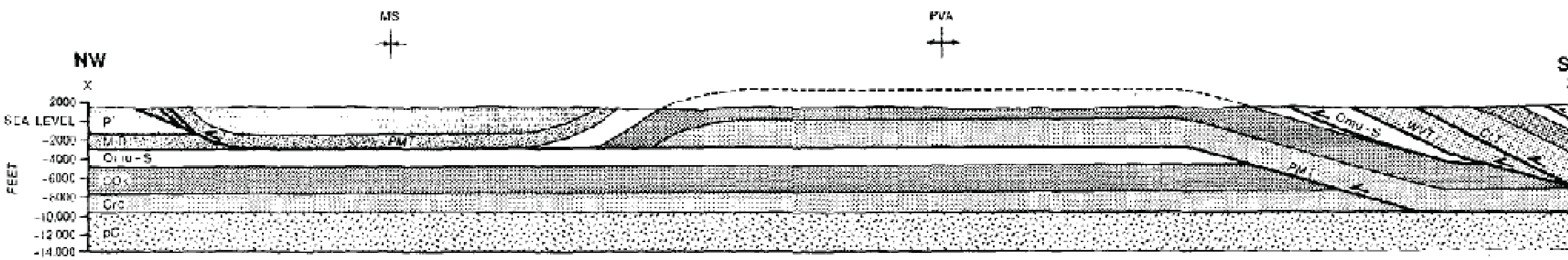

MS
PVA
NW
X
SE
X'
2000
SEA LEVEL
-2000
-4000
-6000
-8000
-10,000
-12,000
-14,000
FEET
PMT
Omu - S

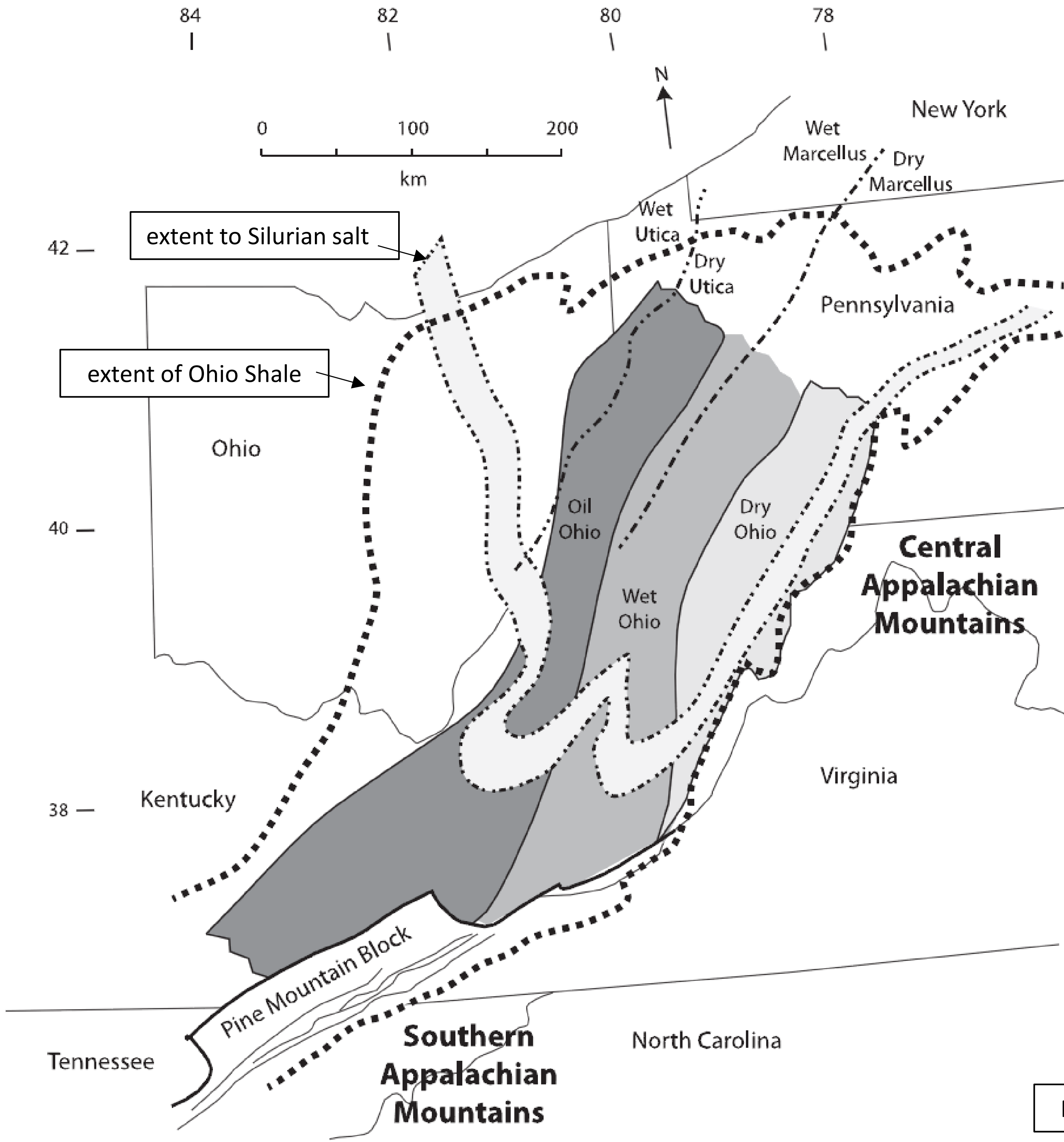

Rimmer et al., 1993

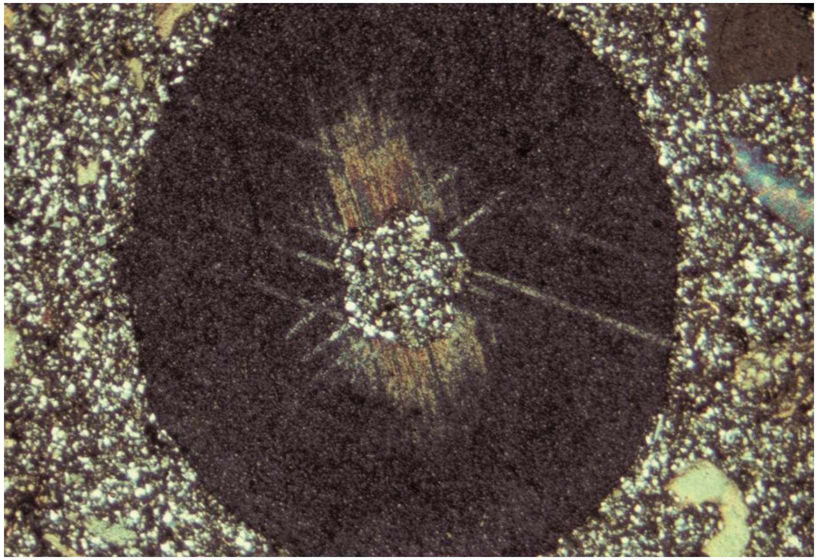

4.2.2 – Fault Bend Folding

An AAPG Short Course by
Terry Engelder
Professor of Geosciences
The Pennsylvania State University

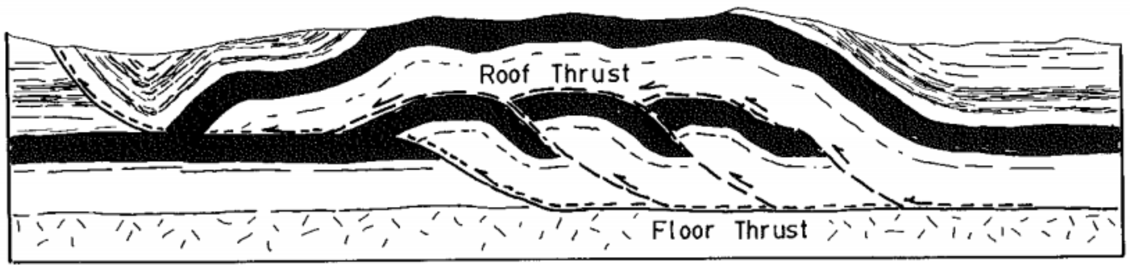

After Boyer & Elliott, 1982

BLIND AUTOCTHONOUS ROOF DUPLEX

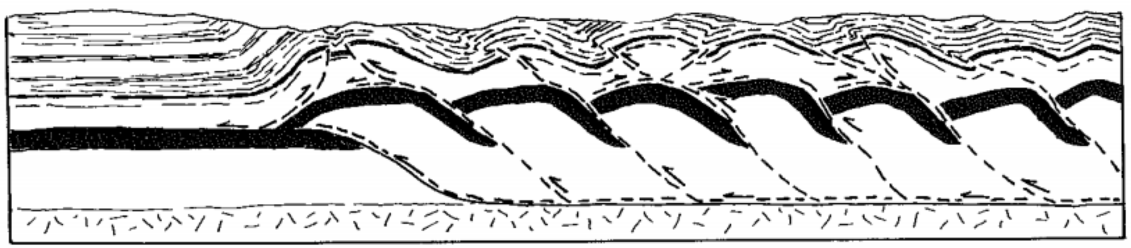

EMERGENT AUTOCTHONOUS ROOF DUPLEX

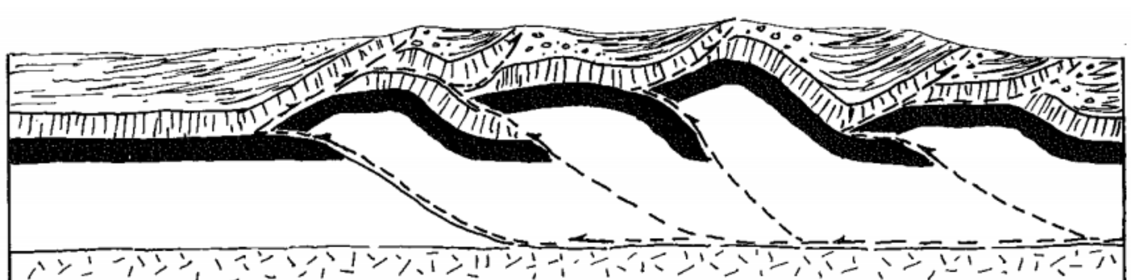

After Banks & Warburton, 1985

Geiser, 1988

Kink Band Structures in the Appalachian Valley and Ridge

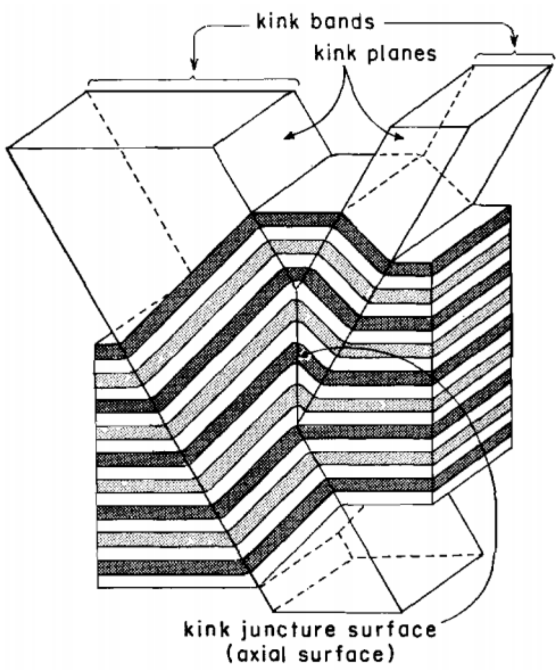

Faill, 1969

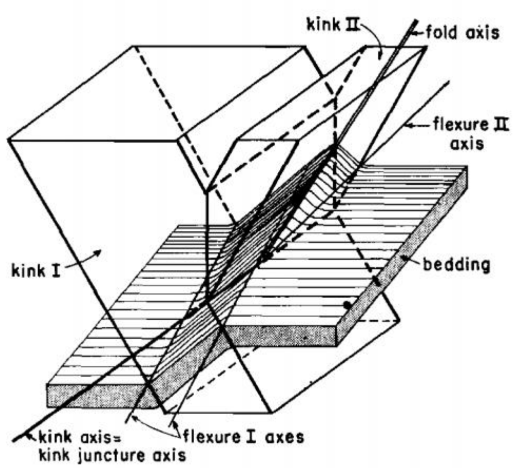

These are the types of structures that gave rise to the fault-bend fold model of Suppe (1983). The fault-bend fold model was greatly simplified by cutting some of the section out with a hanging wall ramp.

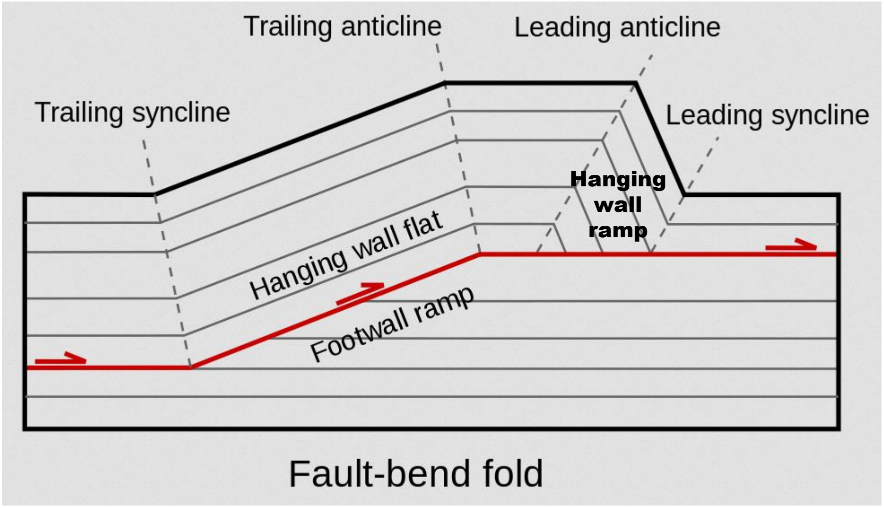

The effect of the hanging wall ramp was to over steepen the beds of the lending syncline so that the fault-bend fold became asymmetrical with the nose of the fold dipping on the order of 65^{o} while the trailing hanging wall flat dips toward the hinterland at about 25^{o}.

Terry Engelder

Dip Domains
Appalachian Valley and Ridge

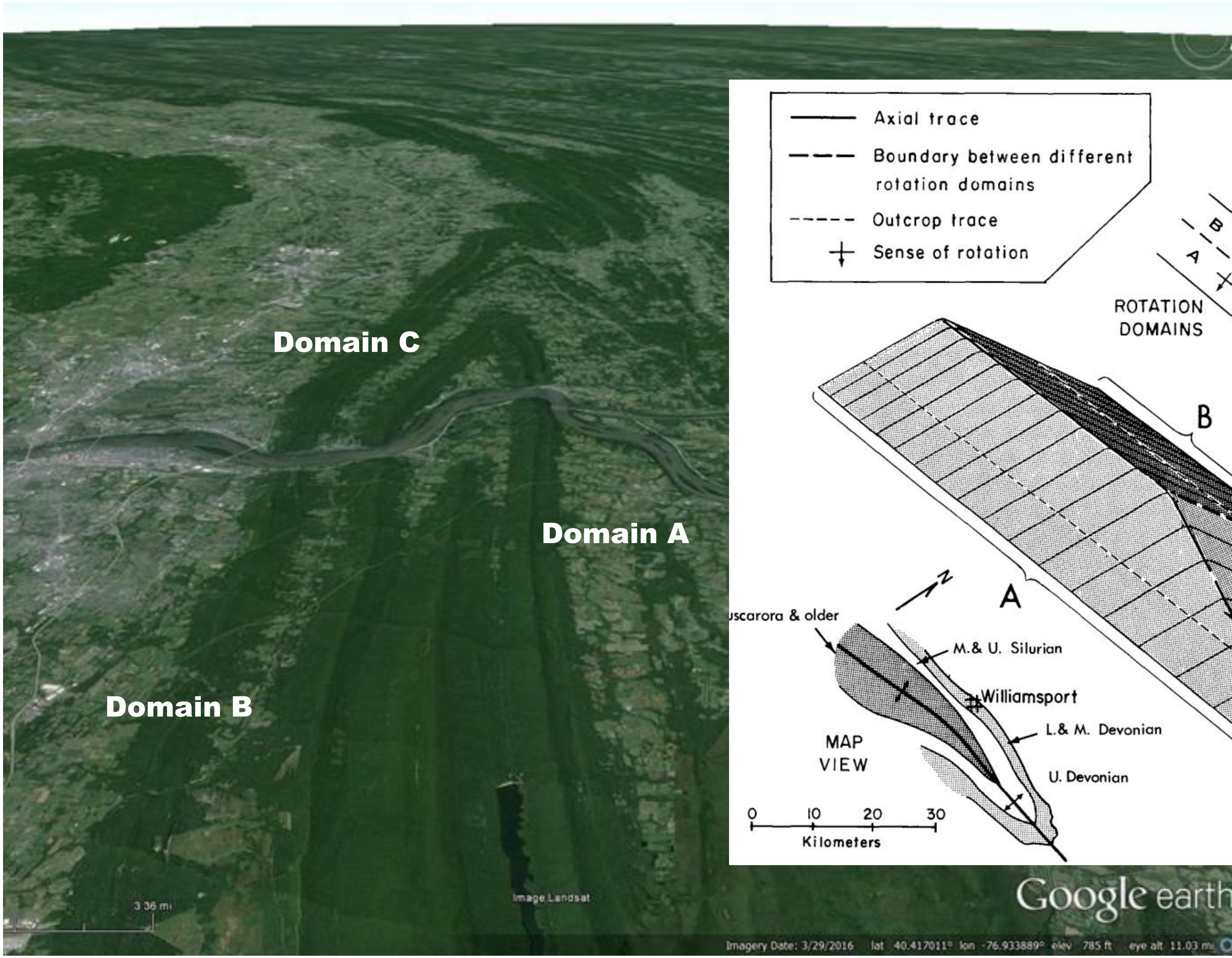

Faill, 1973

Dip Domains
Appalachian Valley and Ridge

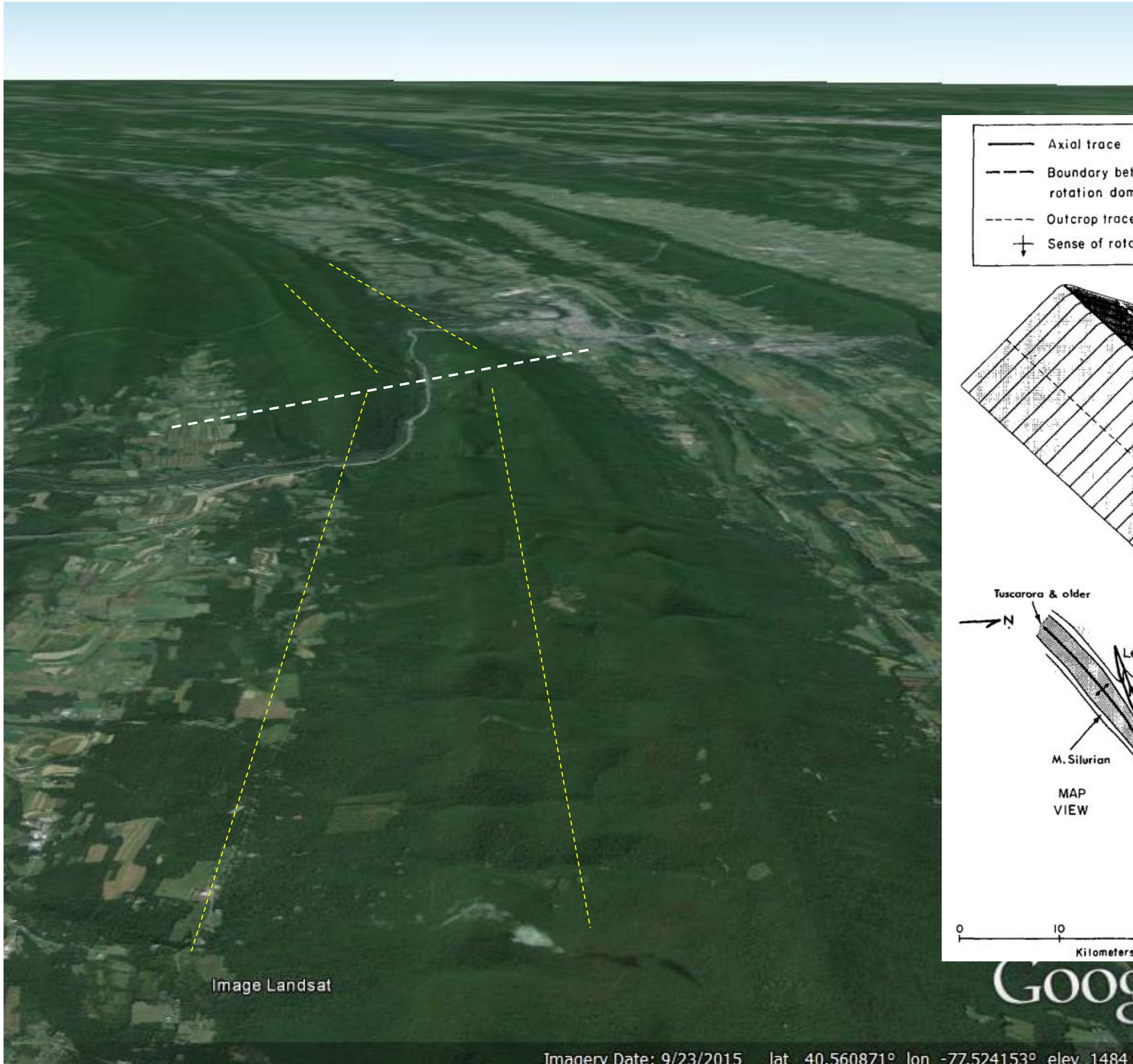

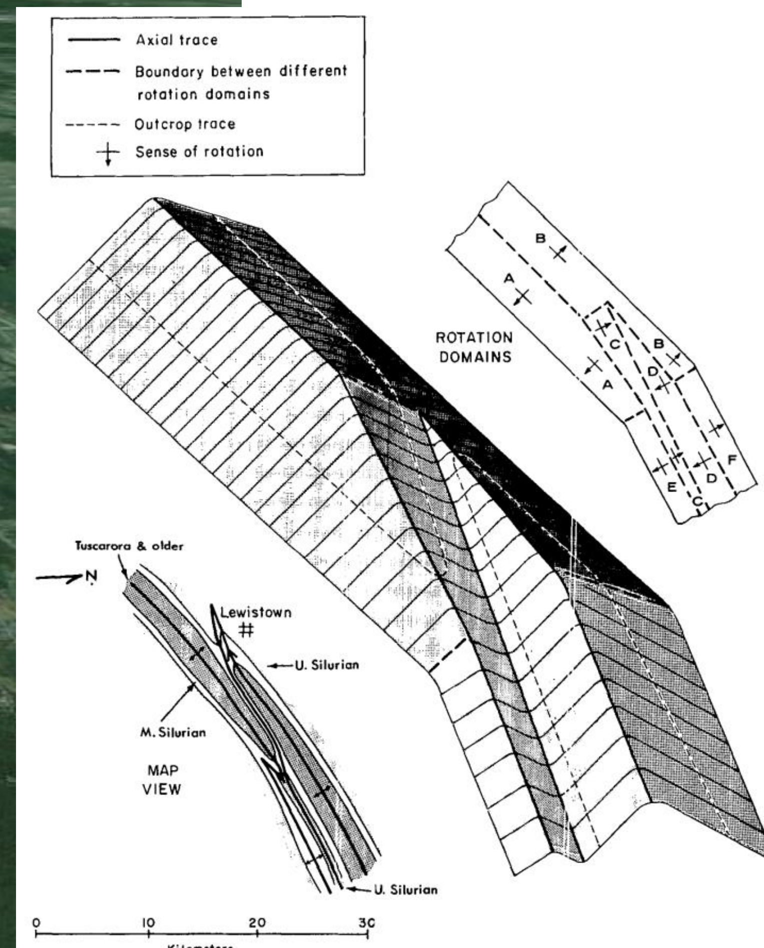

Faill, 1973

Explanation for the original dip-domain model as first put forward by Faill (1973)

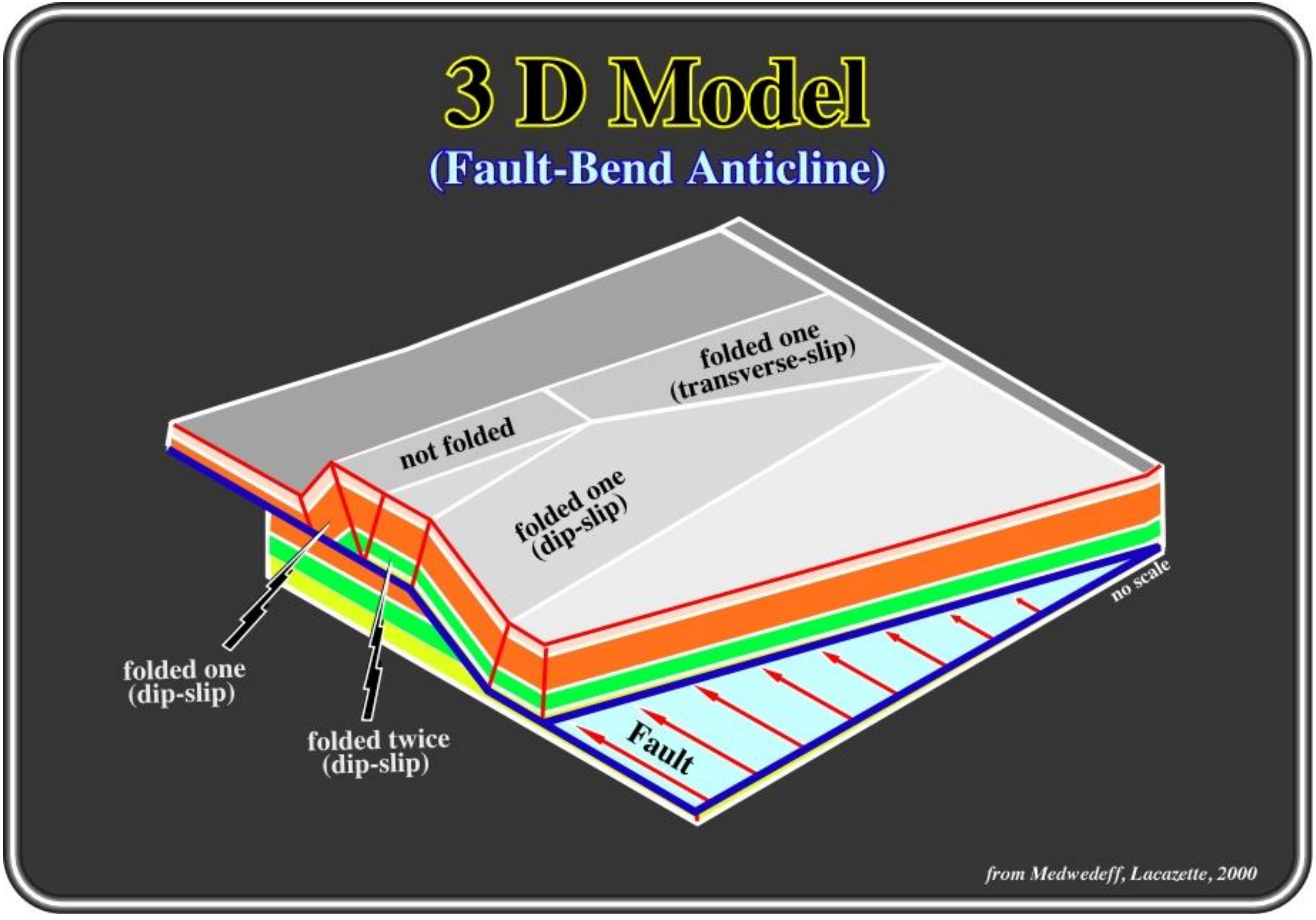

Fault bend fold

Pine Mountain Thrust Sheet, Cumberland Plateau, Tennessee, USA

Suppe's (1983) original study of fault-bend folds gave the Powell Valley Anticline as a 'type' example of such folds.

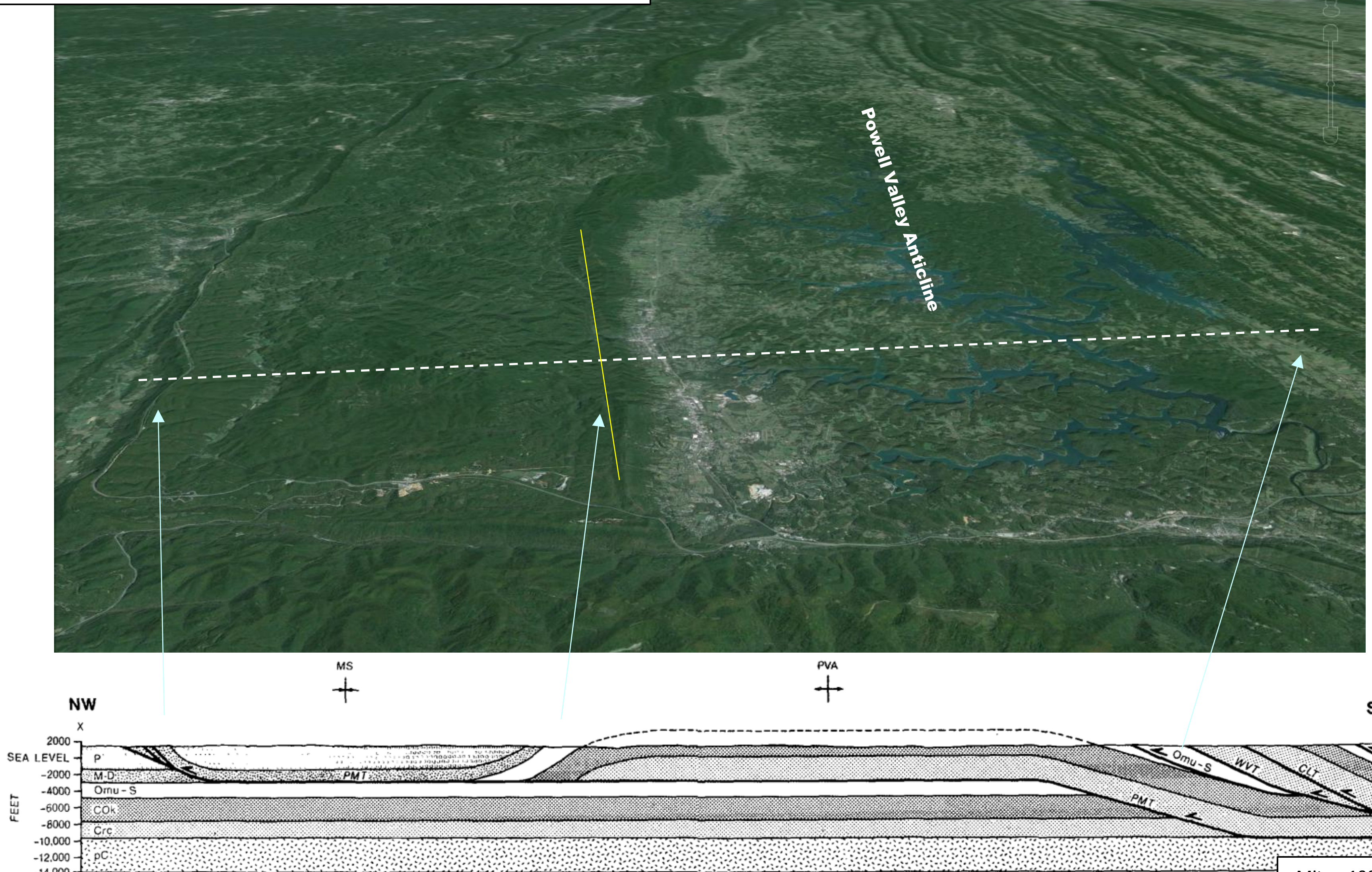

Mitra, 1988

Fault-related fold
Cumberland Plateau, Southern Appalachian Mtns, Tennessee, USA

Ohlmacher & Aydin, 1997

As early as the first survey of Pennsylvania, geologists realized that the anticlines of the state were asymmetric with the dip of the foreland limb being more that twice as steep as the dip of the hinterland limb (Rogers and Rogers 1843).

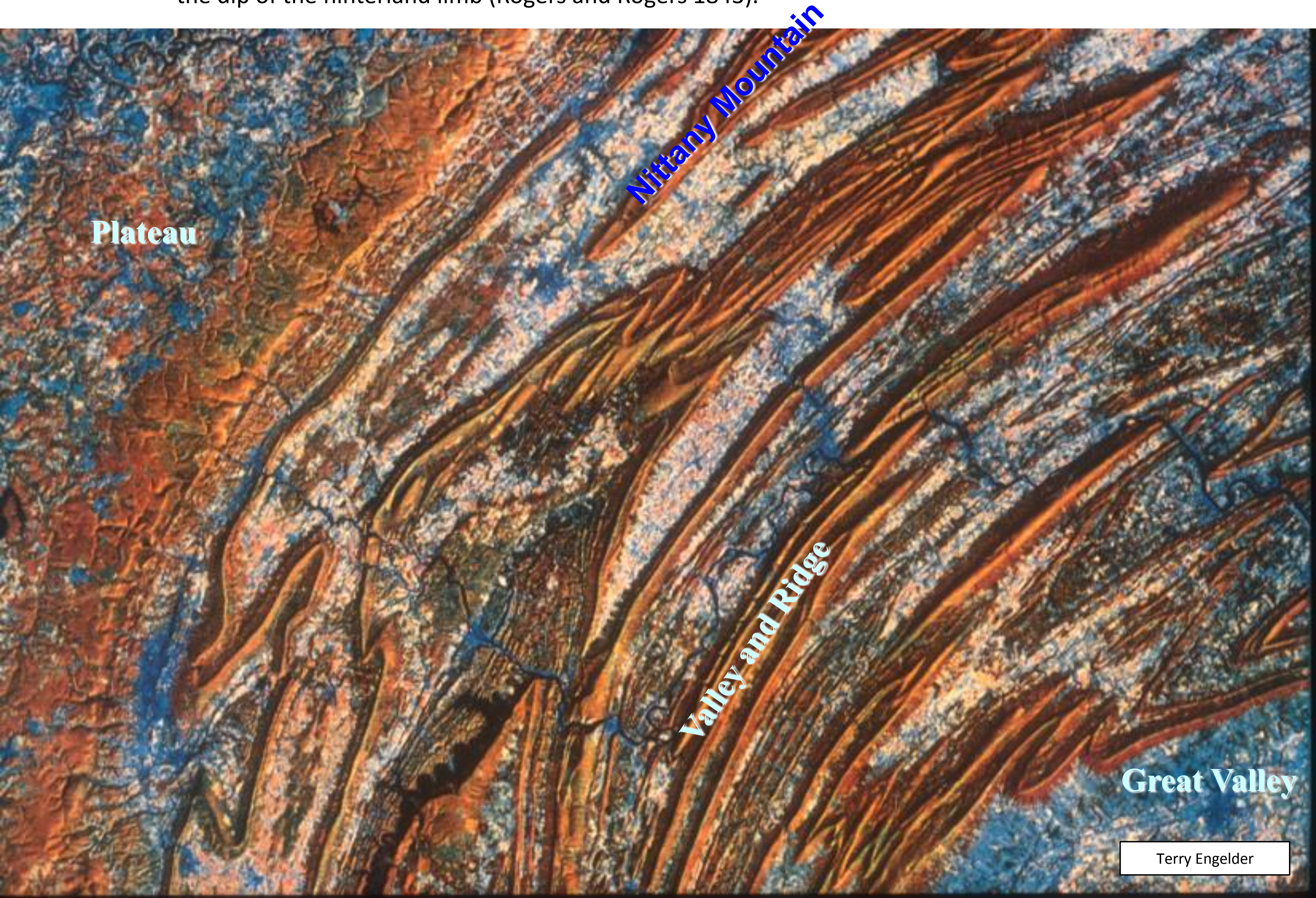

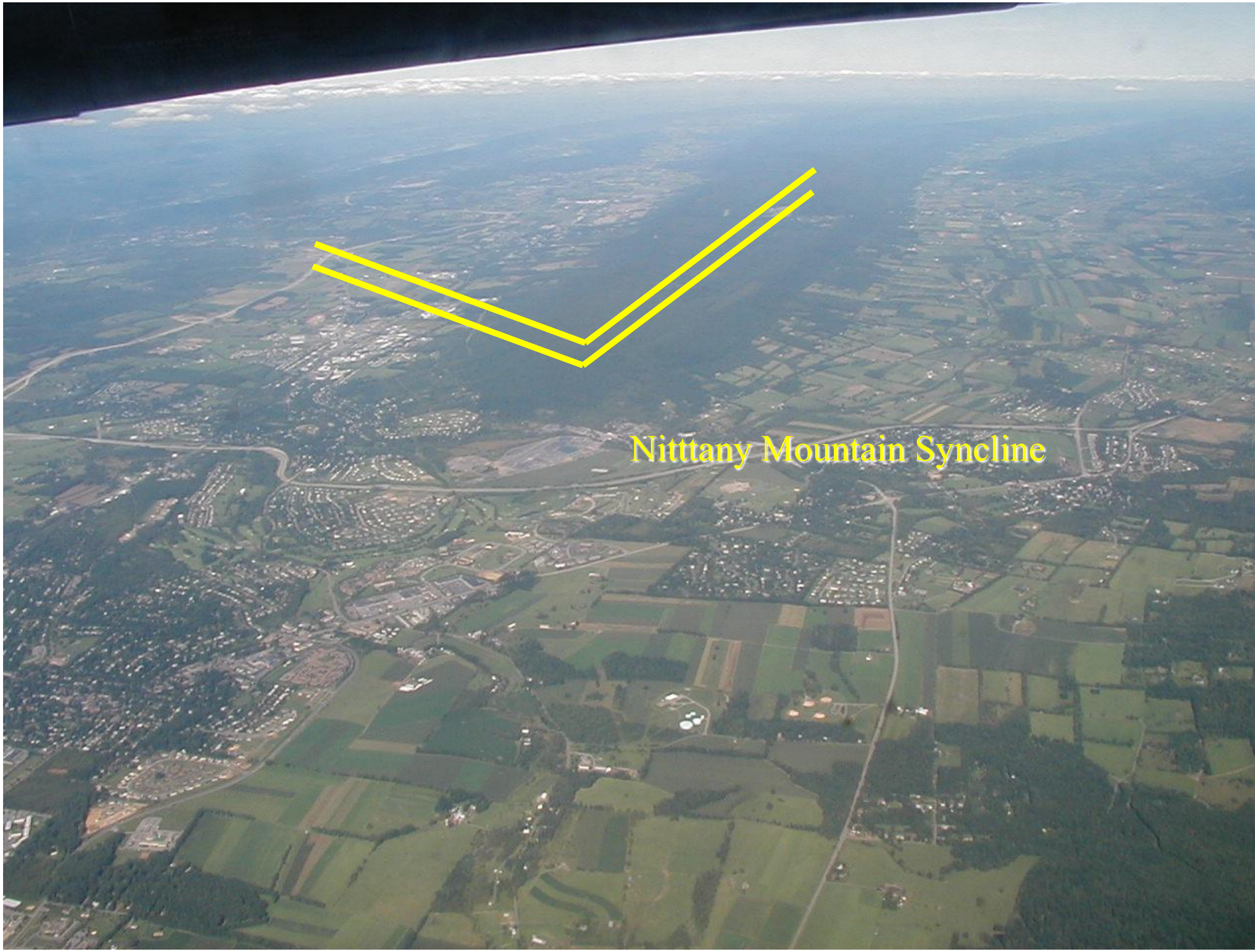
Nitttany Mountain Syncline

Foreland Limb, Nittany Mountain Syncline

Hinterland limb – Nittany Mountain syncline

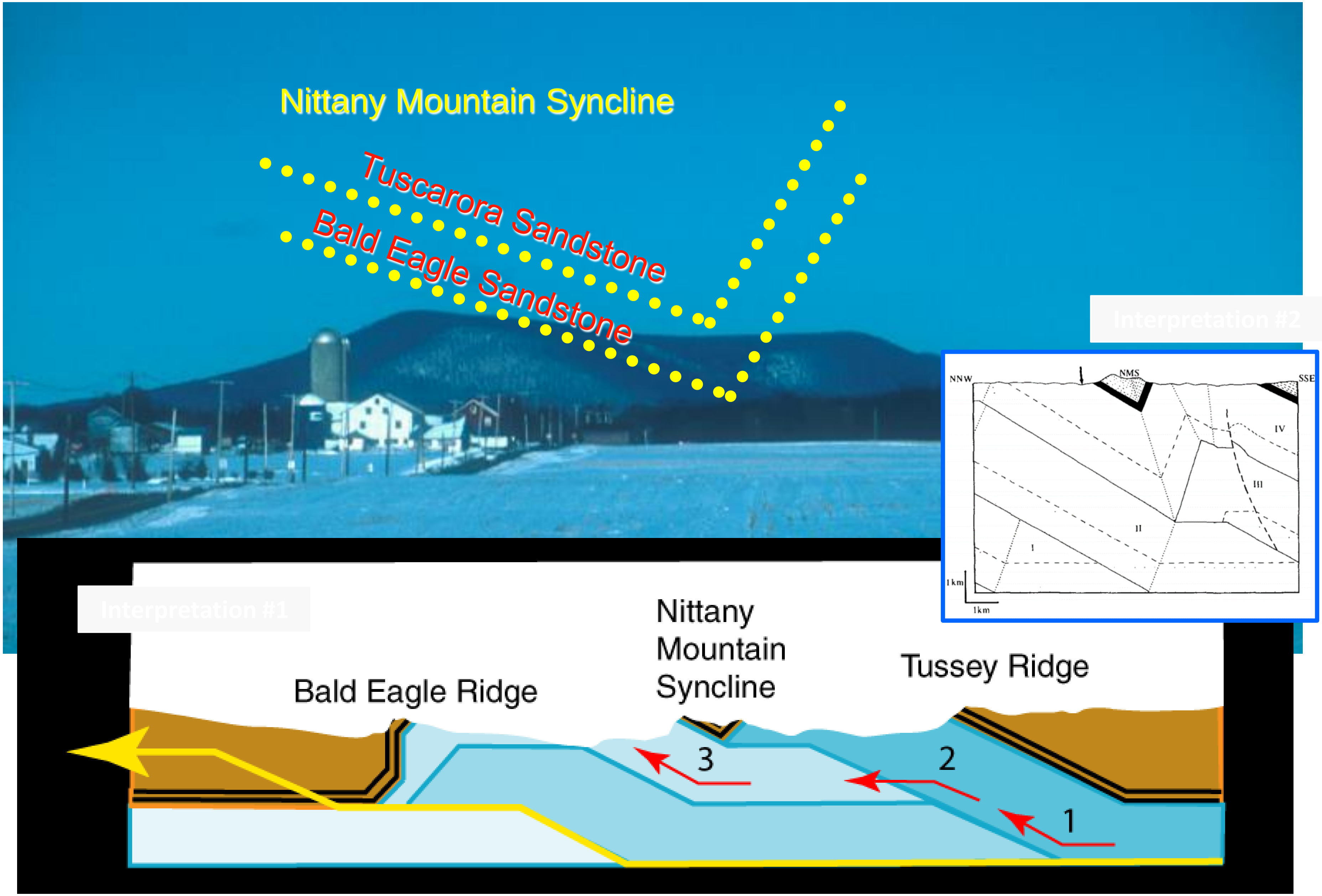

Nittany Mountain Syncline
Tuscarora Sandstone
Bald Eagle Sandstone
Interpretation #2
NNW
NMS
SSE
IV
III
II
I
1 km
1km
Interpretation #1
Bald Eagle Ridge
Nittany Mountain Syncline
Tussey Ridge
3
2
1

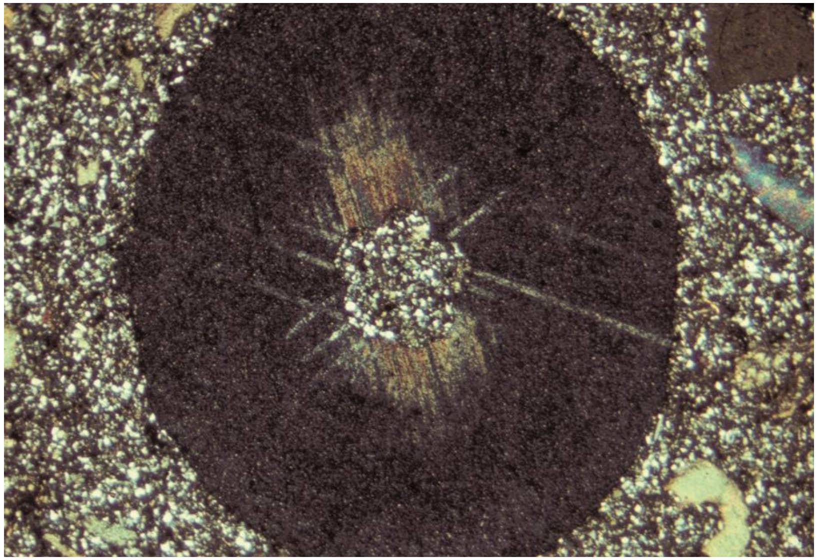

4.2.3 – Structural Validation

An AAPG Short Course by
Terry Engelder
Professor of Geosciences
The Pennsylvania State University

Structural Validation

Validating structural interpretations is necessary to extract additional information, such as the shape of the structure between wells and seismic lines, predicting the presence of structures too small to be seen at the resolution of seismic lines and surface outcrops, and determining the structural evolution over time. Most of the techniques of structural restoration, balance and prediction are related to one another by use of a common set of kinematic models.

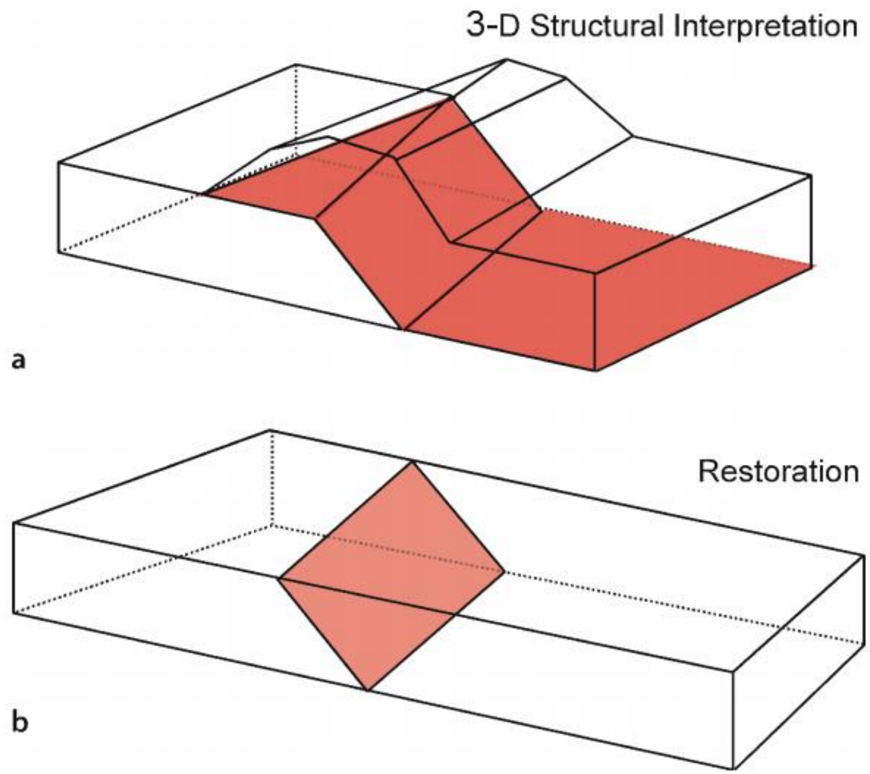

A restorable structure can be returned to its original, pre-deformation geometry with a perfect or near-perfect fit of all the segments in their correct pre-deformation order. Restoration is a fundamental test of the validity of the interpretation. A restorable structure is internally consistent and therefore has a topologically possible geometry. An unrestorable structure is topologically impossible and therefore is geologically not possible (Dahlstrom 1969). An interpretation based on a large amount of hard data, such as a complete exposure, many wells, or good seismic depth sections controlled by wells, is nearly always restorable, whereas interpretations based on sparse data are rarely restorable. This is the empirical evidence that validates restoration as a validation technique.

Groshong, 2006

Structural Validation

Kinematic models represent simplified descriptions of the mechanical processes that form structures. The deformation in some structures is more complex than can be fit by one of the simple kinematic models. For these structures the more general area balancing methods can be appropriate. Using the relationship between displaced area and depth, a structure can be tested for area balance and its lower detachment predicted without performing a restoration or a model-based prediction. Layer-parallel strain is treated here because it is an intrinsic part of both the kinematic models and the area-depth relationship and because it provides a tool for predicting sub-resolution structure (i.e., folds and faults too small to be seen at the resolution of the data) and is another tool for validating the structural interpretation.

One of the most common kinematic behaviors in layered rock is flexural slip. There are a number of validation models that assume that bed lengths do not change during deformation, particularly involving flexural slip. Given the evidence for layer-parallel shortening in forelands, especially the Appalachian Plateau, this assumption may be questioned. Never-the-less a first cut at restoration can assume constant bed length so that a pin line and loose line remain intact during restoration. Below are examples of both a perfect and imperfect restorations.

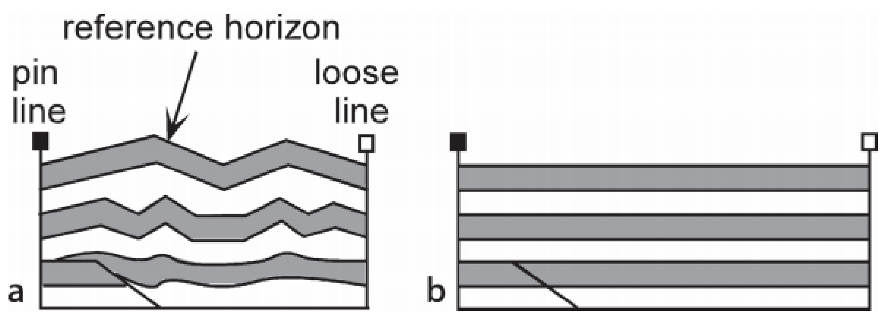

Perfect restoration

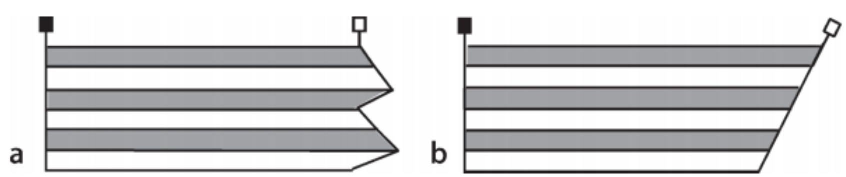

Imperfect restoration

Groshong, 2006

Structural Validation

Flexural-slip restoration is based on the model that bed lengths do not change during deformation (Chamberlin 1910; Dahlstrom 1969; Woodward et al. 1985, 1989). Internal deformation is assumed to occur mainly by layer-parallel simple shear (Fig. 11.3b). For the area to remain constant, the bed thicknesses must be unchanged by the deformation as well. This is the constant bed length, constant bed thickness (constant BLT) model. Flexural-slip restoration is particularly suitable where the beds are folded and structurally induced thickness changes are small, the style of deformation in many compressional structures.

Restoration may be used for fault-shape prediction. Based on the assumption of constant BLT on a cross section bounded by vertical pin lines, there is a unique relationship between the hangingwall shape caused by movement on a fault and the shape of the fault itself. In the technique developed by Geiser et al. (1988), a complete deformed-state cross section is constructed while simultaneously producing a restored cross section. The method is based on: (1) constant bed length and bed thickness, (2) slip parallel to bedding, (3) fixed pin lines in the hangingwall and footwall of the fault, and (4) the hangingwall geometry is controlled by the fault shape. The pin lines are chosen to be perpendicular to bedding. The data required to use the method are the location of a reference bed and the hangingwall and footwall fault cutoff locations of the reference bed. The original regional of the reference surface is not required. The method produces a cross section that is length balanced, has constant bed thickness and has bedding-normal pin lines at both ends. The technique is as follows:

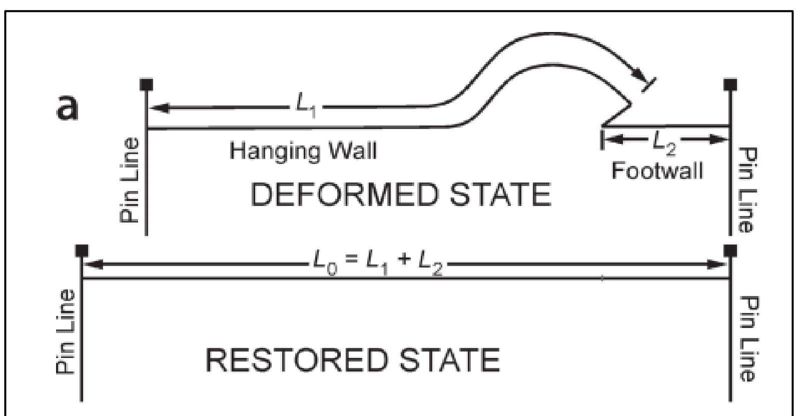

1….. Define the reference bed, its fault cutoffs, and the shape of the fault between the cutoffs (top).
2….. Place the pin lines in the deformed-state cross section. Usually they are chosen to be perpendicular to bedding and beyond the limits of the structure of interest (top).
3….. Measure the bed length of the reference horizon between the pin lines and draw therestored-state section (bottom).

Groshong, 2006

Structural Validation

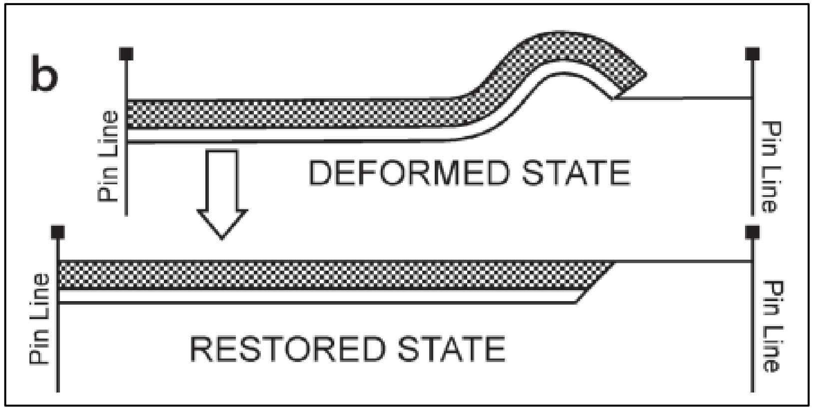

4….. Construct one or more constant thickness beds in the hangingwall between the hangingwall pin and the fault (top).
5….. Measure all the bed lengths in the hangingwall between the hangingwall pin and the fault and place them on the restored-state cross section (Fig. 11.36b, bottom). This defines the shape of the footwall beds in the restored state.

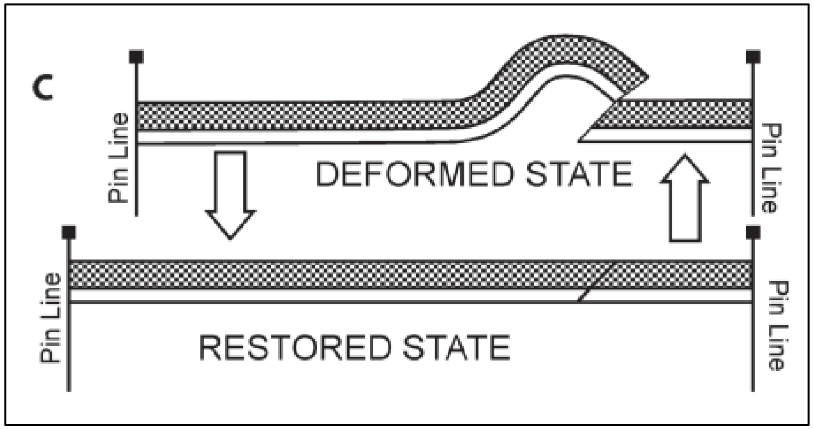

6…. Draw the restored-state footwall on the deformed-state cross section (top). This gives a new hangingwall cutoff.

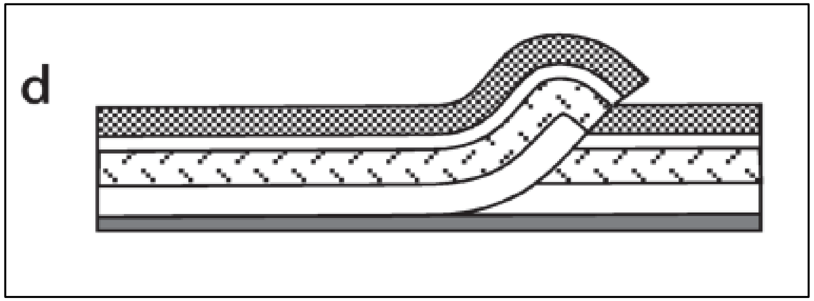

7….. Continue the cycle of steps 4–6 until the section is complete.

Groshong, 2006

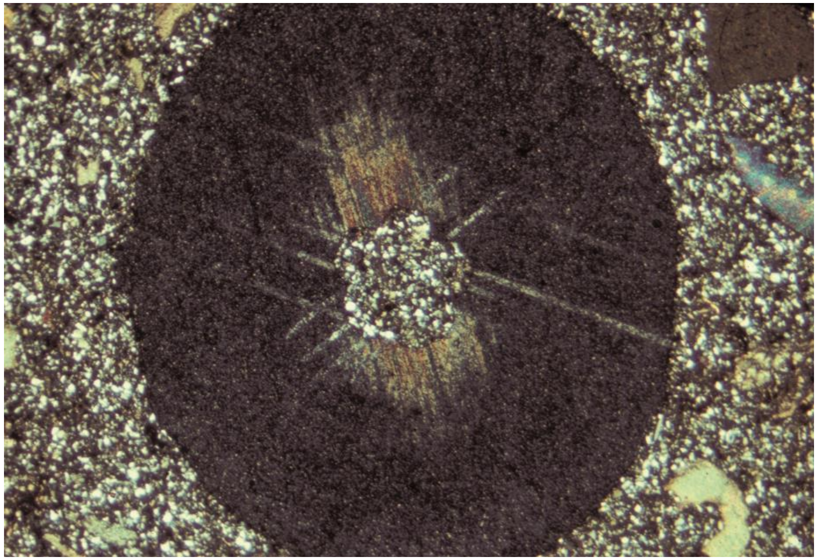

4.2.4 – Fault-related Folding Models

An AAPG Short Course by
Terry Engelder
Professor of Geosciences
The Pennsylvania State University

A small thrust in the Chilean Andes, showing a classic footwall ramp and flat geometry, overlain by a hangingwall flat.

From Rick Allmendinger, Cornell

Chevron fold – Fault-bend folds

Three types of rotation can be distinguished in association with a chevron fold. The rotation #1 is an external rotation as indicated by the change in orientation of the bedding. This is φ in the our analysis of kink folds. Rotation #2 is an internal rotation and is shown on the strain ellipse by θ. Rotation #3 develops off of beds of limestone that have been shortened by cleavage development. Each block of limestone is bounded by pressure solution cleavage that dissolves the beds and permits shortening without the total rotation shown as #1 for the sandstone beds.

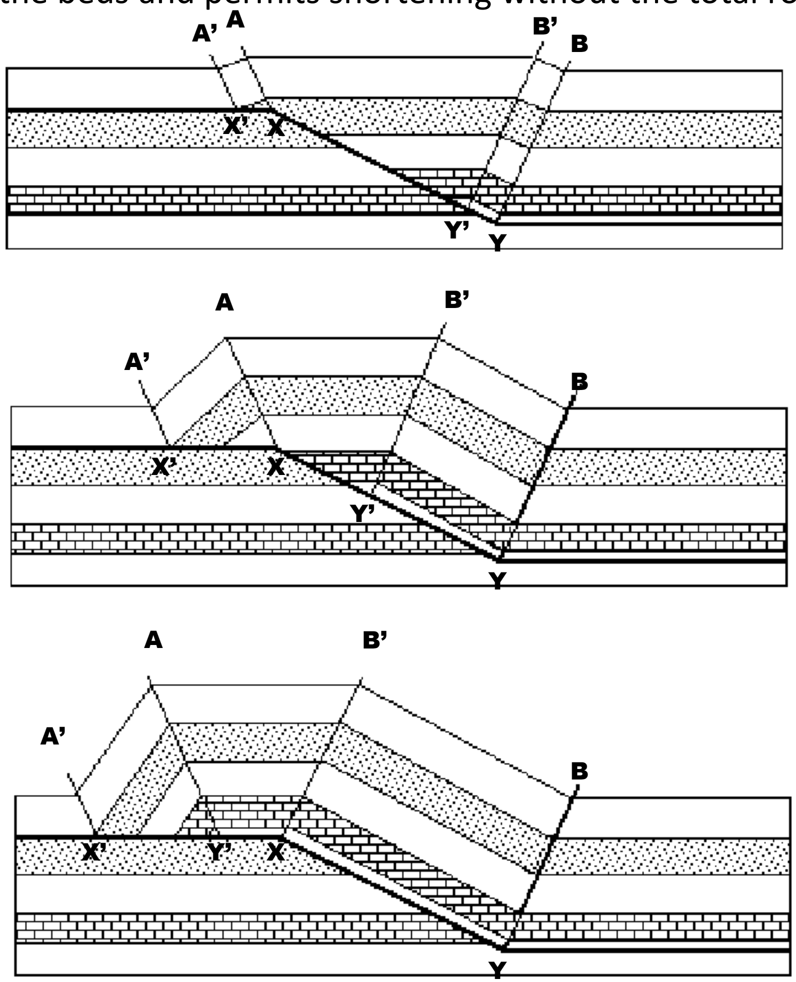

Fault-bend folds, versions of kink folds, are a consequence of décollement tectonics where bedding parallel detachments climb section by cutting across several beds (Suppe, 1983). A model of fault-bend folding involves a detachment fault where the thrust plane comes from the right, cuts upward across bedding, and continues parallel with bedding off to the left. Upon the initiation of the fault across bedding two kink bands develop at the bends in the footwall because these bends cause folding in the upper sheet of the thrust system. The axial surfaces A and B terminate at the bends in the detachment where it changes from bedding parallel to cross cutting. The axial surfaces A' and B' terminate at the transitions between crosscutting and bedding-plane fault segments in the hanging wall at points X' and Y' which match points X and Y in the footwall. As slip continues kink bands A-A' and B-B' grow in with and the anticline above the crosscutting fault grows in height.

Terry Engelder

Fault-propagation folds

Axial surfaces A' and B' move with the thrust sheet because they are fixed to the hanging wall cutoffs. Because the axial surfaces A and B are fixed to the footwall cutoffs X and Y, the beds must move through the axial surfaces, first bending and then unbending.

The motion of the fault-bend fold is complex because when the hanging-wall cutoff, Y', reaches the footwall cutoff, X, the fold has reached its maximum amplitude, which is the height of the step in décollement. At this point the deformation, axial surface A, which has been fixed to the footwall is suddenly released to move with the hanging-wall cutoff, Y', whereas axial surface B', which has been moving with the hanging wall, is suddenly locked to the footwall cutoff, X.

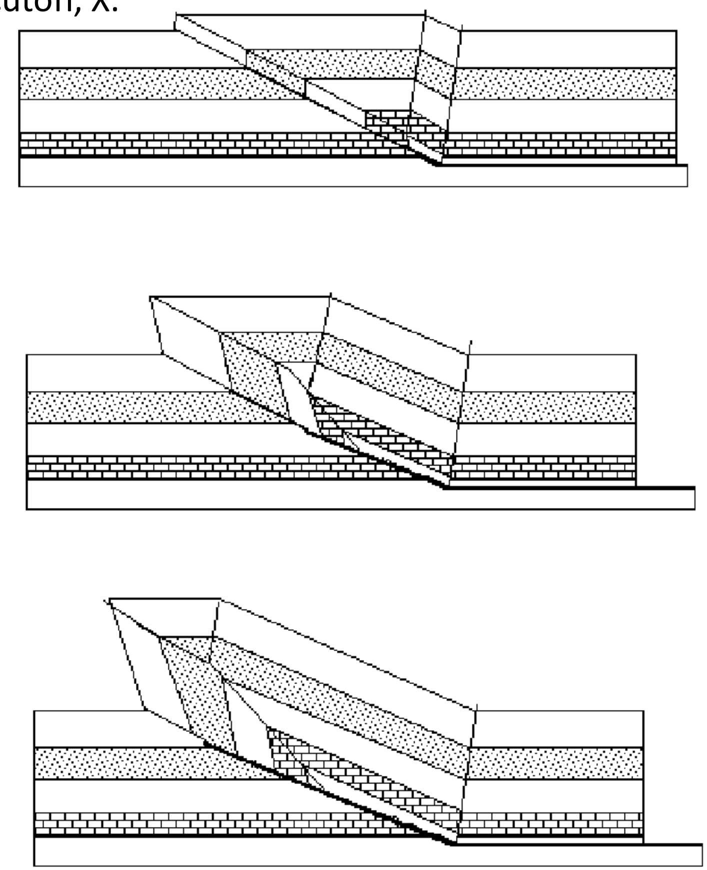

Fault-propagation folds form as a part of the process of fault propagation. In such a fold the thrust fault cuts across section but does not extend in the subsurface in front of the fold as was the case for a fault bend-fold. Like the fault-bend fold, as the thrust starts to step up through the section two kink bands immediately develop. One axial surface is pinned to the footwall cutoff and the beds roll through the fold by first folding and then unfolding. Another axial surface is pinned to the tip of the fold and beds roll through it was the fault propagates forward. A third axial surface touching the fault plane moves with the velocity of the thrust sheet and is the surface where the two initial kink bands have merged below the surface. Commonly, fault-propagation folds will become locked because the bending resistance of some formation may be too great. In this case the fault may propagate along the anticlinal or synclinal axial surfaces or somewhere in between.

Terry Engelder

Fault-related folding

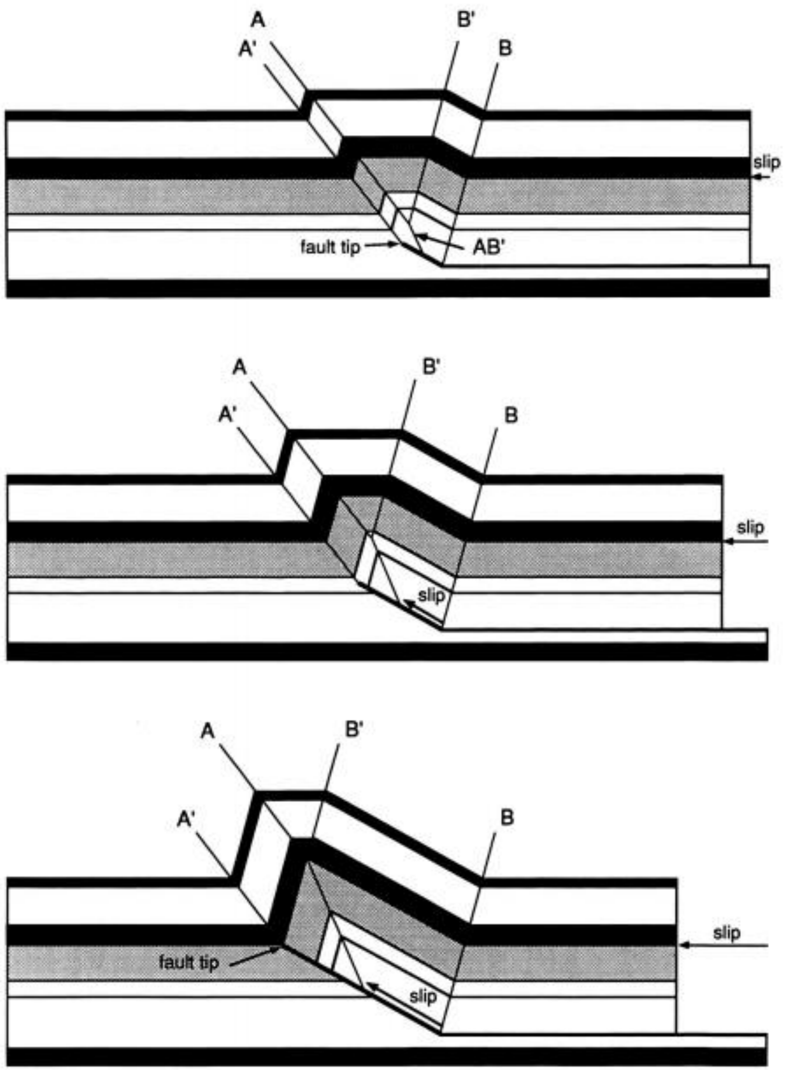

Retrodeformable model of the progressive development of a simple-step fault-propagation fold (from Suppe & Medwedeff, 1990). The drawing is for a step-up angle of 29°, for which axial-surface A is fixed relative to the material. Under these conditions the constant-thickness and fixed-axis theories predict identical foldshapes.

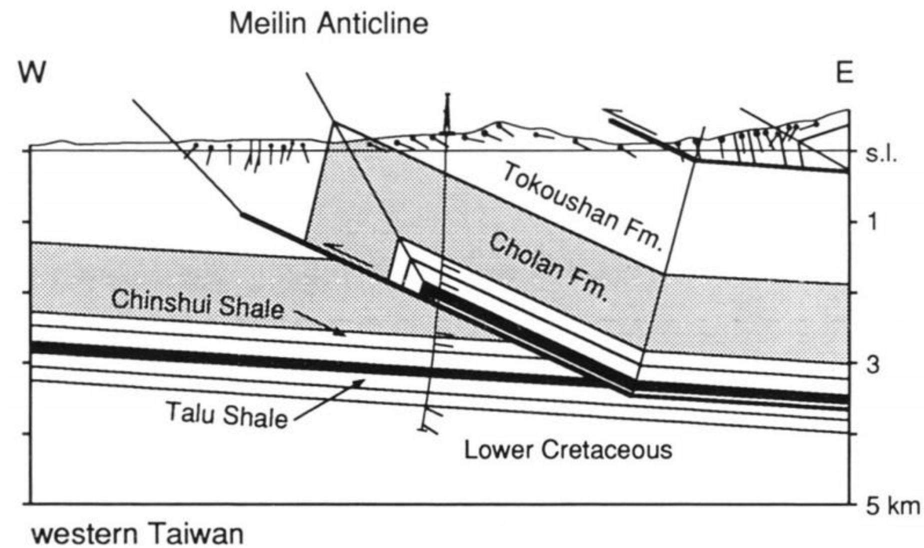

Cross-section of Meilin anticline, western Taiwan overthrust belt near Chiavi, a fault-propagation fold.

Suppe, 1983, 1986

Fault-related folding

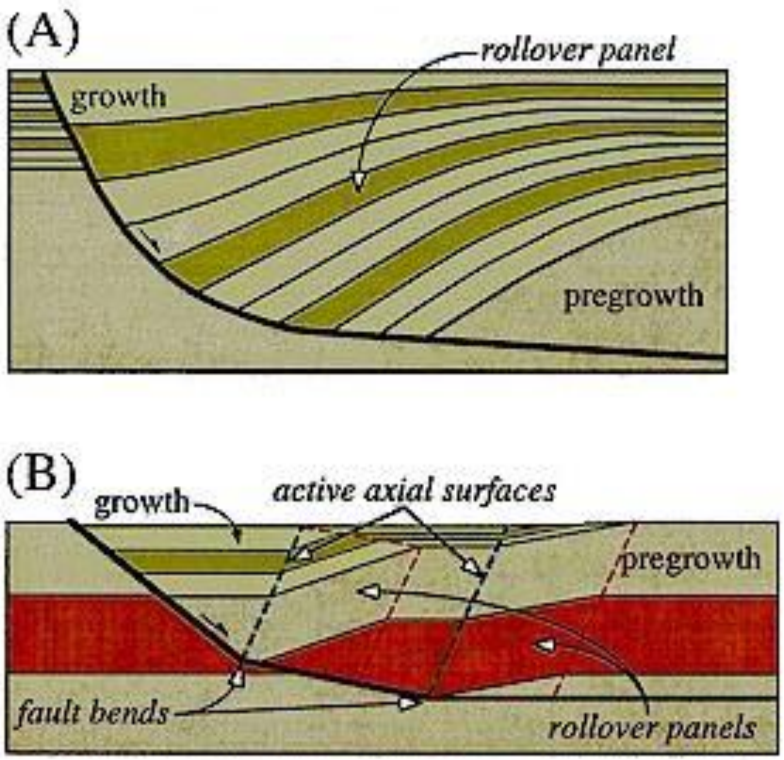

Planar rollover panels above a normal fault that is composed of planar segments. Rollover panels are bounded on the left by active axial surfaces, which are pinned to fault bends (from Shaw et al., 1997).

Fault-related folding

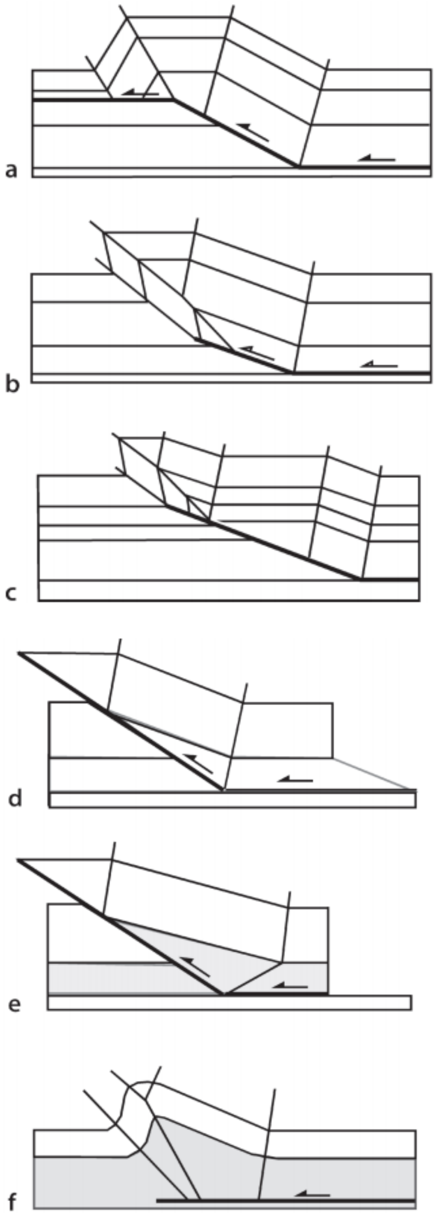

Fault-related fold models. Unshaded: constant-thickness units; shaded: variable-thickness unit.

a…. Fault-bend fold (after Suppe 1983).
b…. Fault-propagation fold (after Suppe 1985; Suppe and Medwedeff 1990).
c…. Fault-propagation fold at the tip of a long ramp (after Chester and Chester 1990).
d…. Simple-shear fault-bend fold (after Suppe et al. 2004).
e…. Pure-shear fault-bend fold (after Suppe et al. 2004).
f…. Detachment fold (after Jamison 1987)

*Numerous models have been developed that relate fold shape to fault shape for various flexural-slip structural styles related to fault-related folding. Many of these have adopted planar or ramp-flat fault shapes, leading to **dip-domain cross-section styles**. Models like the fault-bend fold, fault-propagation fold and fault-tip fault-propagation fold are based on the assumption of constant bed length and constant bed thickness (BLT) throughout and so yield unique relationships between the fold shape and the fault shape. Such models can be used to predict the entire structure from a very small amount of hard data. Other models, like the simple-shear, pure shear, and detachment folds maintain constant BLT in the upper part of the structure but are area balanced in the decollement zone at the base. The latter style of model admits a wider range of geometries and so more must be known before the complete structure can be predicted. Other variants allow thickness changes in the steep limb, which creates even more degrees of freedom in the interpretation. A discussion of all the models and their variants is beyond the scope of this book. The objective here is to introduce the basic concepts and provide a guide to additional sources of information.*

Groshong, 2006

Fault-related folding

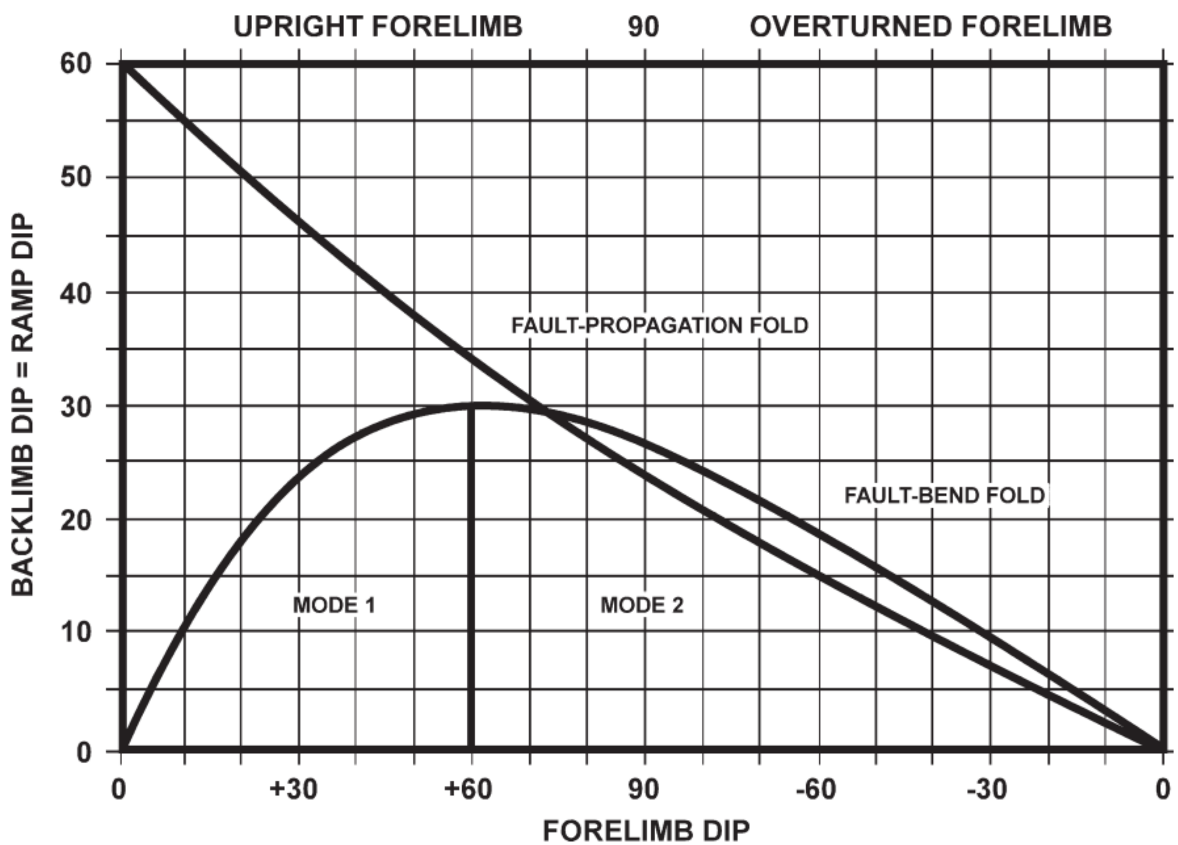

The starting point for a model-based interpretation is to determine which model is appropriate. Constant BLT fault-bend and fault-propagation folds have analytical relationships between forelimb and backlimb dips that can be expressed graphically. This graph is a plot of forelimb dip versus backlimb dip, with the dips being measured relative to the regional dip outside the fold. A field example (next page) can be plotted on the graph to see if falls on either the fault-bend or fault-propagation fold curve. If the point falls on one of the lines, then there is a high probability that the fold fits the model and the model can be used to predict the fold geometry.

Groshong, 2006

Fault-related folding

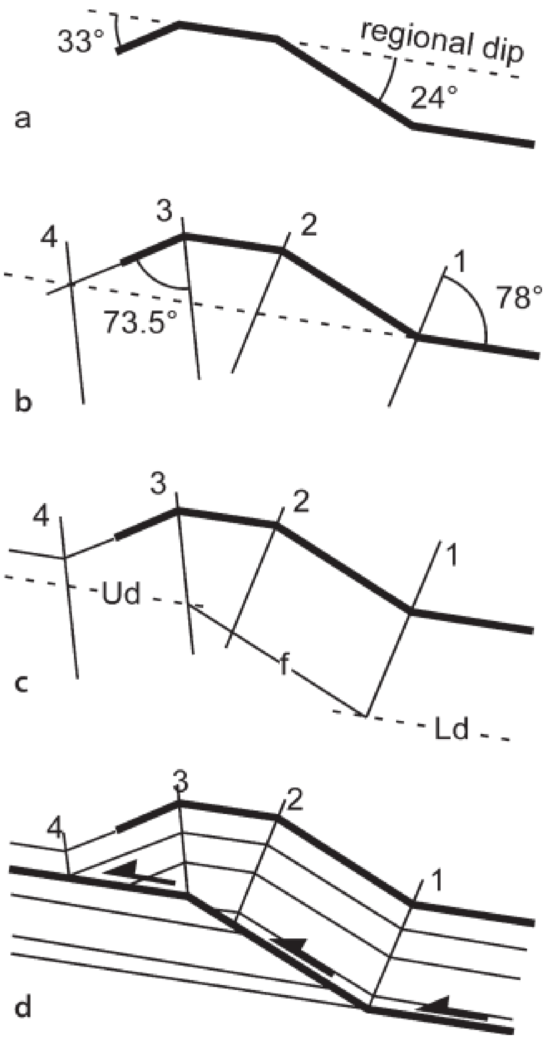

Construction of a complete fault-bend fold starting with a single horizon.

a…. Starting fold geometry with dips measured from regional dip.

b…. Axial surfaces bisect hinges.

c Location of the fault. Ud: upper detachment; f: fault ramp; Ld: lower detachment.

d Final geometry

As an example of the methodology, the deep structure of this fold is interpreted. The regional dip is inferred to be parallel to the planar domain between the two limbs and is confirmed because the same dip is seen outside the structure. The limb dips are measured with respect to regional and plotted. The points fall on the fault-bend fold curve, indicating the model to be used. The interlimb angles are measured and bisected to find the axial-surfaces. The backlimb axial surfaces (1 and 2) are parallel, as are the forelimb axial surfaces (3 and 4). Beds must return to regional dip outside the anticline, allowing the location where the forelimb flattens into regional dip (axial surface 4) to be determined. The fault ramp must be below and parallel to the backlimb. The exact location of the fault requires additional information about the position of the lower and upper detachments. Bed truncations in the forelimb of the hangingwall or against the ramp in the footwall may serve to locate the detachments. Alternatively, the stratigraphic section may contain known detachment horizons that can be utilized in the interpretation. Additional controls from the model are that axial surfaces 1 and 2 always terminate at the upper detachment, and axial surface 1 always terminates at the base of the ramp. Axial surface 3 can be on the ramp or at the top of the ramp. Having determined the best location for the fault, the dip domains can be filled in with the appropriate stratigraphy and the interpretation is complete.

Groshong, 2006

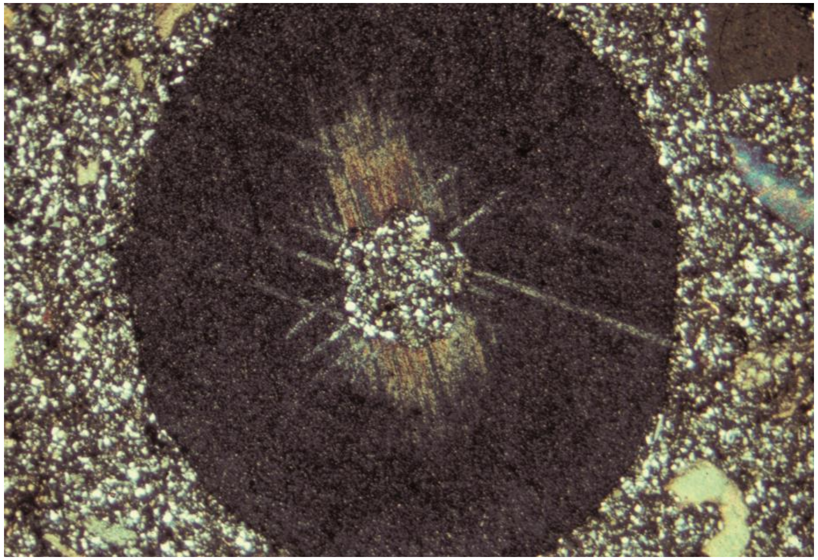

4.2.5 – Fold-related Stresses during Fault Bend Folding

An AAPG Short Course by
Terry Engelder
Professor of Geosciences
The Pennsylvania State University

Fault-bend fold
Nittany Valley Syncline, Appalachian Valley and Ridge, Pennsylvania, USA

Bedding-parallel (BPV), strike (SV), and cross-fold (CFV) veins represent a sequence of polyphase fracturing during the development of a fault-bend fold in lower Paleozoic carbonate beds in the Appalachian Valley and Ridge province, Pennsylvania. Brecciation and layer-parallel shearing played important roles in the development of the earliest vein set (BPV) which propagated prior to folding. Fluid inclusions in calcite BPV are highly saline brines (23.4 wt% NaO) trapped at conditions close to lithostatic (P < 180 MPa, T < 267°C). While passing through the lower kink plane of a fault-bend fold, strike joints propagated in dolomitic beds located on the extensional side of neutral surfaces. Stylolitization of strike joint surfaces accompanied slip of the hanging wall up a ramp. Renewed extension upon passing through a second kink plane led to propagation of antitaxial SV along the stylolitized joints by the crack-seal process. Slightly less saline fluids (22.4 wt% NaO) were trapped in SV at fluid pressures < 144 MPa and temperatures < 217 °C. With the concurrent formation of lateral ramps, the carbonates moved to the upper Oat and were subjected to strike parallel extension as manifested by the propagation of antitaxial CFV. Due to further mixing of fresh waters, the salinity of fluids forming CFV decreased (20.5 wt% NaO) with trapping conditions at p < 116 MPa and T < 179°C. The fluid evolution path from BPV to CFV through SV shows a modest decrease in salinity with a sharp decrease in possible trapping pressures.

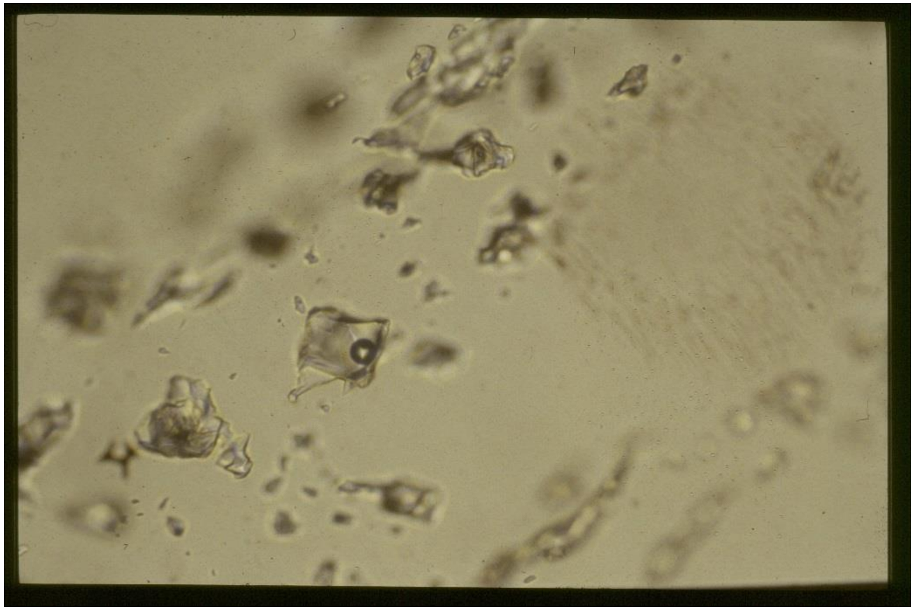

Two-phase fluid inclusions in calcite

Srivastava & Engelder, 1990

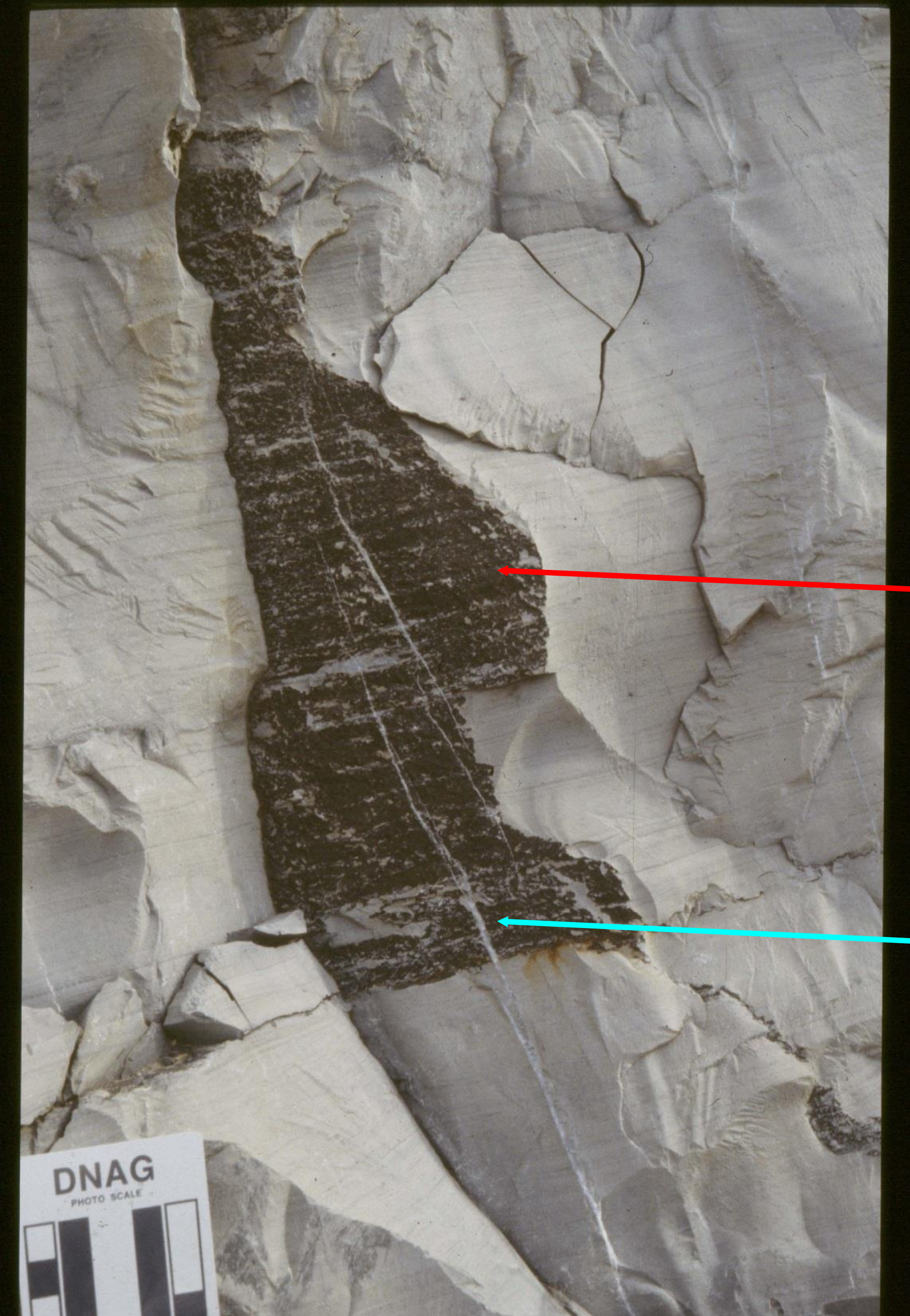

strike vein with
insoluble residue

cross-fold vein cuts
strike vein

Srivastava & Engelder, 1990

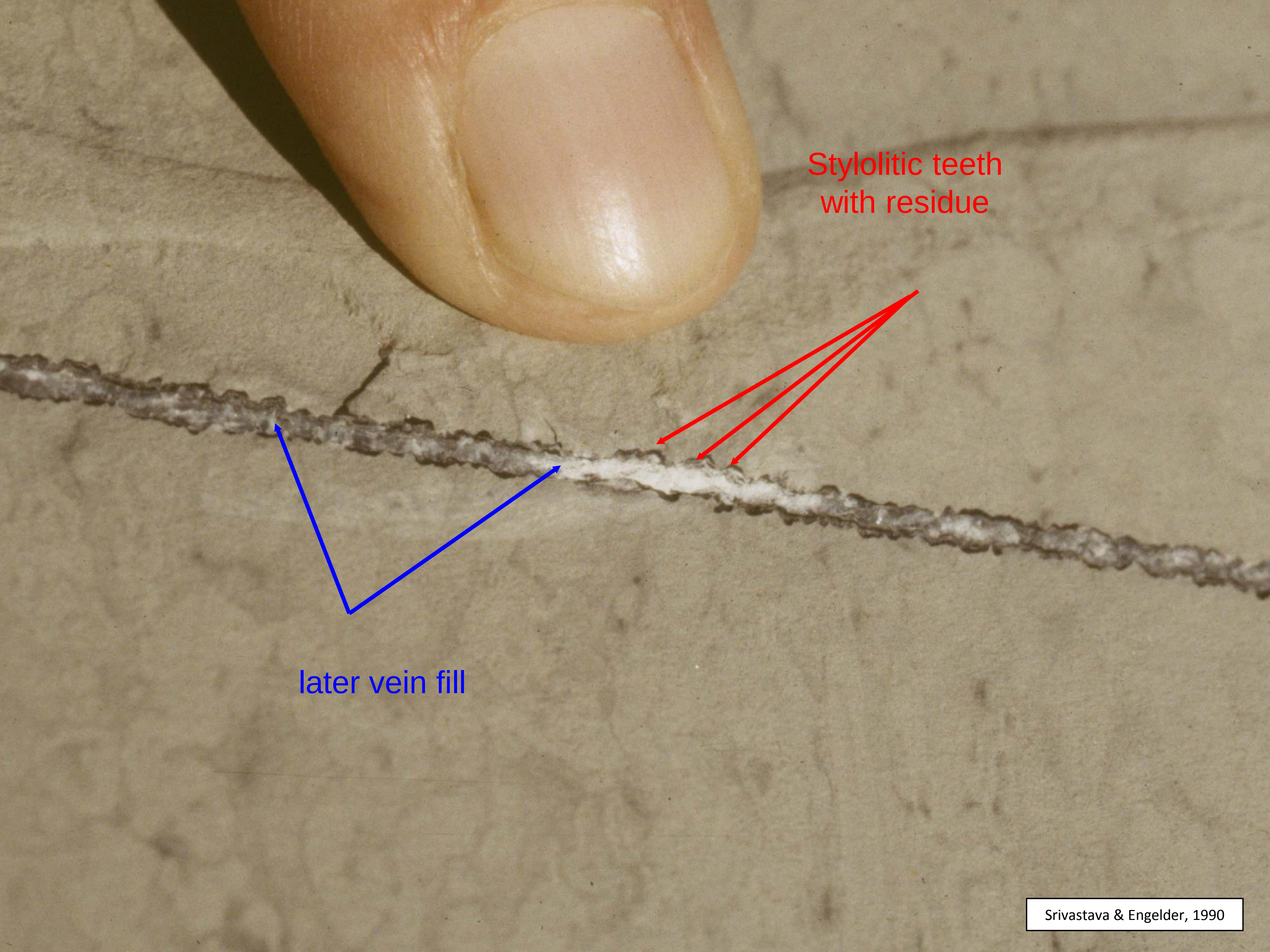
Stylolitic teeth
with residue
later vein fill
Srivastava & Engelder, 1990

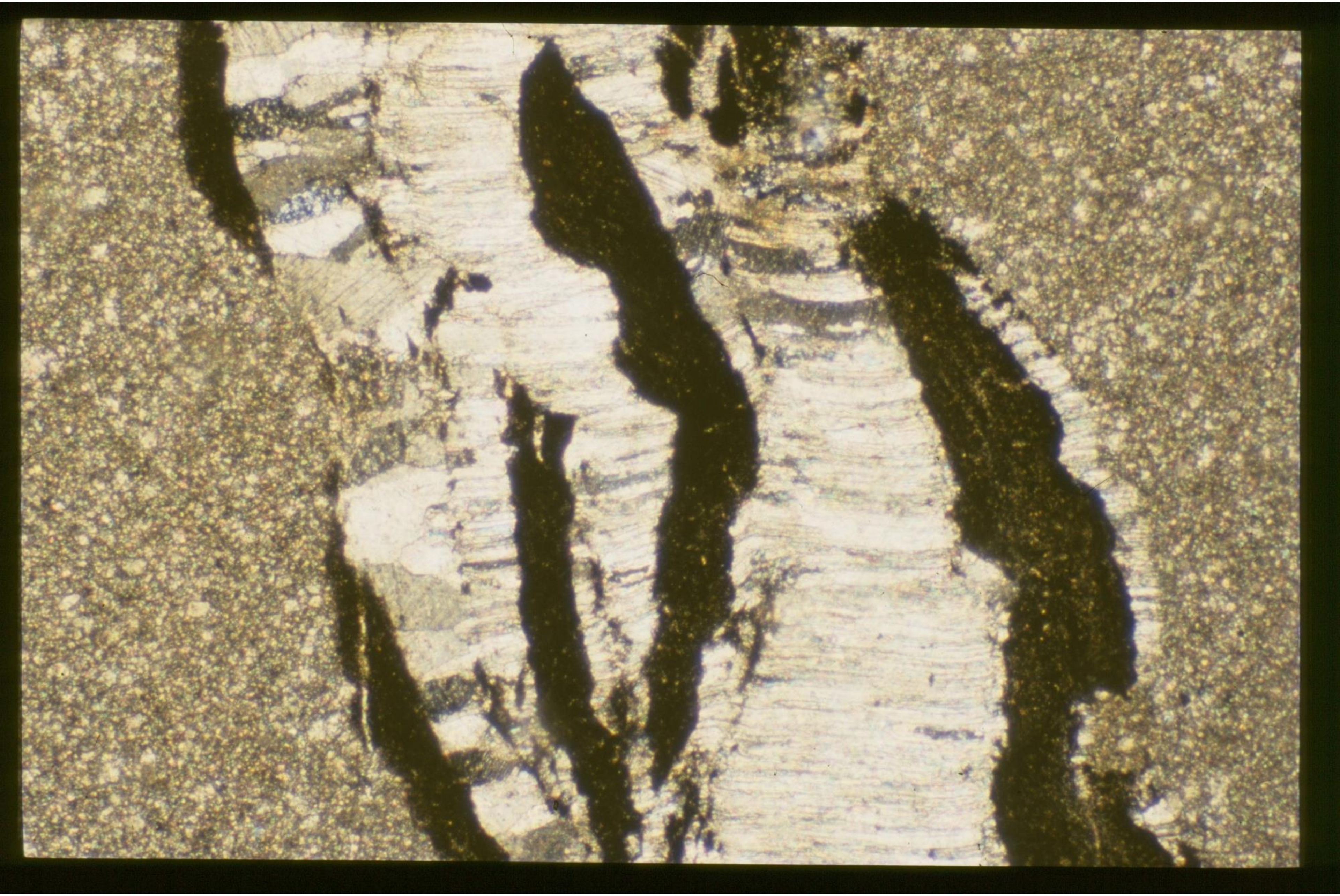

Srivastava & Engelder, 1990

ory

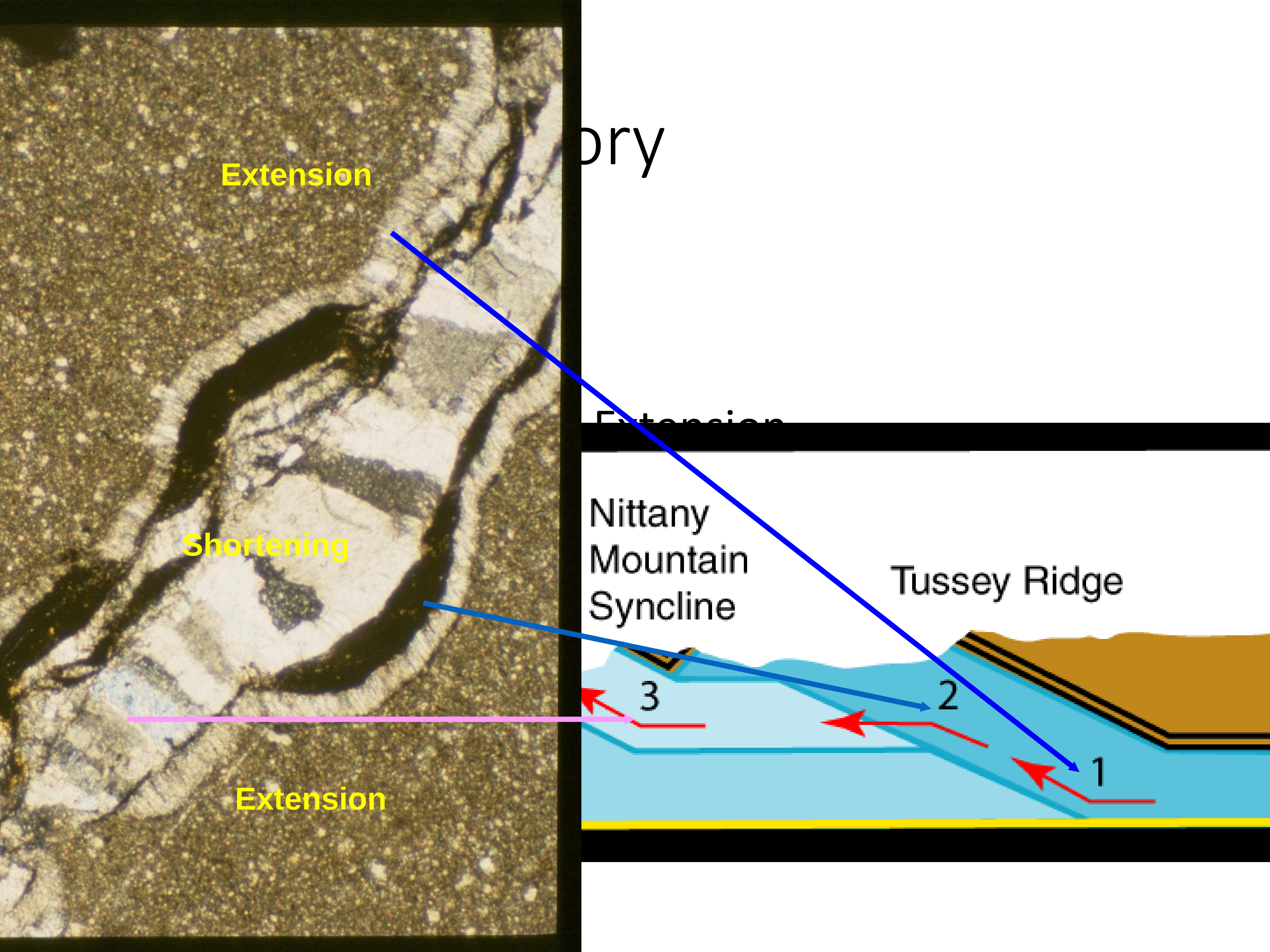

Extension
Shortening
Extension
Nittany
Mountain
Syncline
Tussey Ridge
3
2
1

Fluid Inclusions: Frozen methane with crystal face shrinkage crack with frozen CO_2

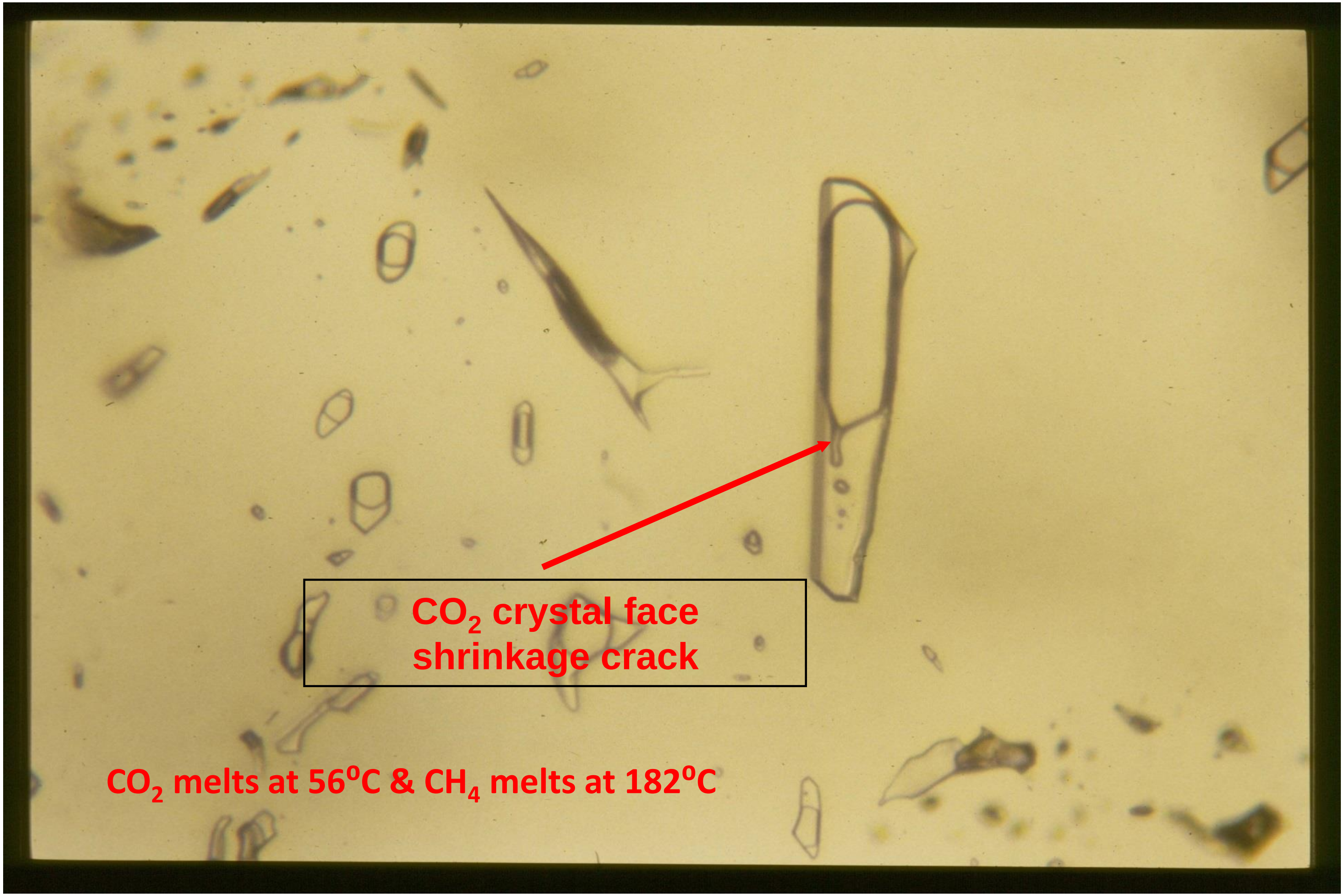

Srivastava & Engelder, 1990

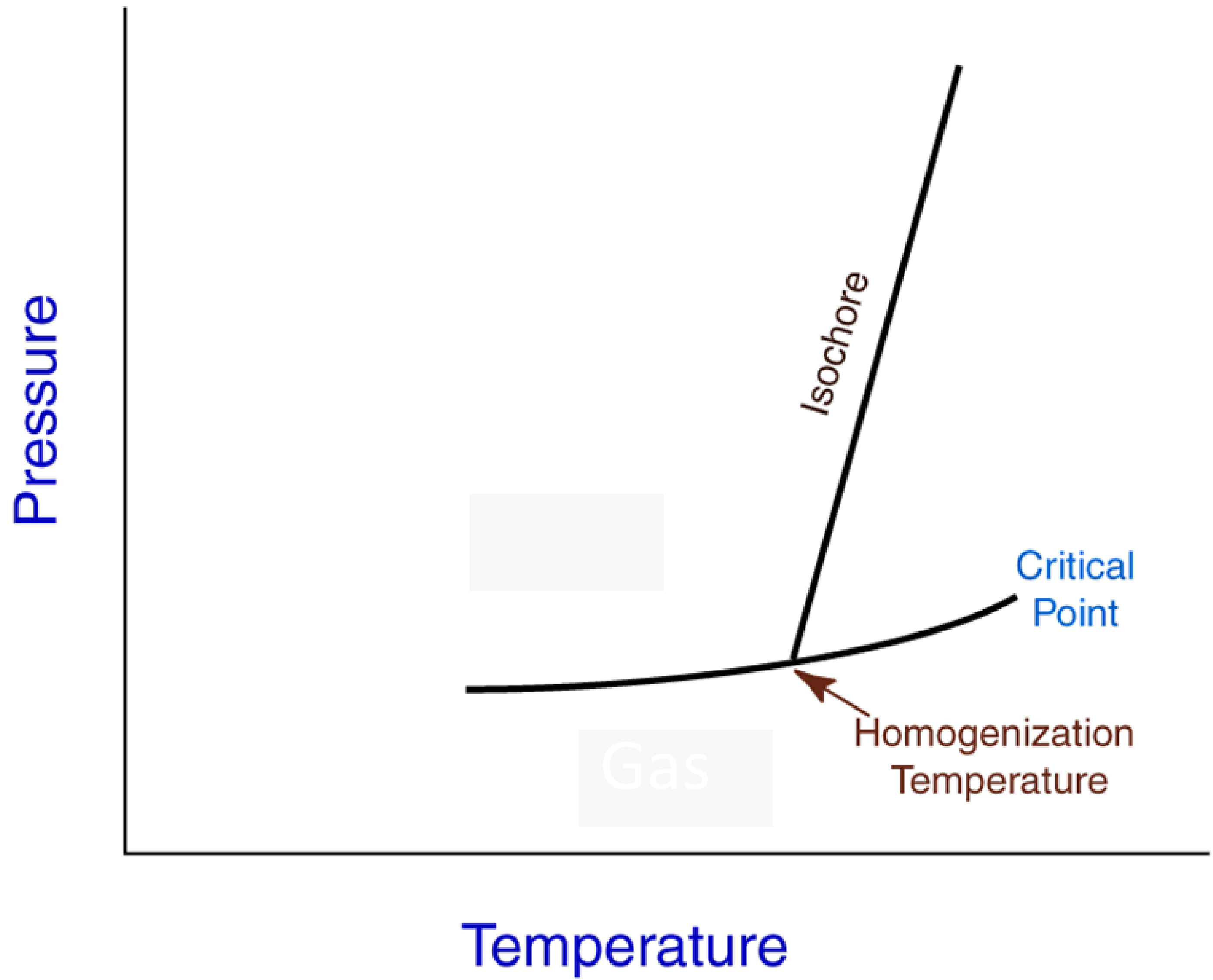

Srivastava & Engelder, 1990

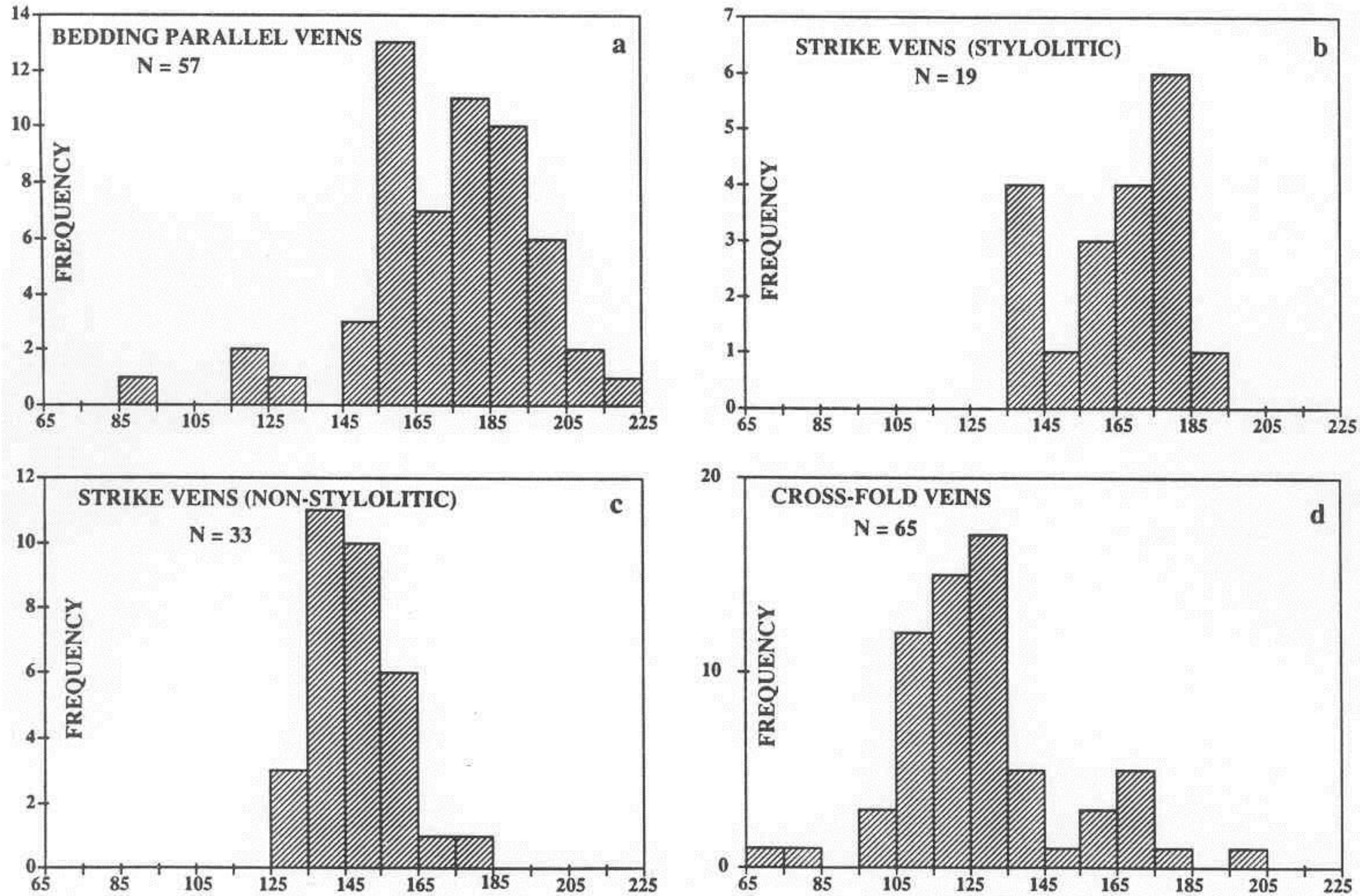

Srivastava & Engelder, 1990

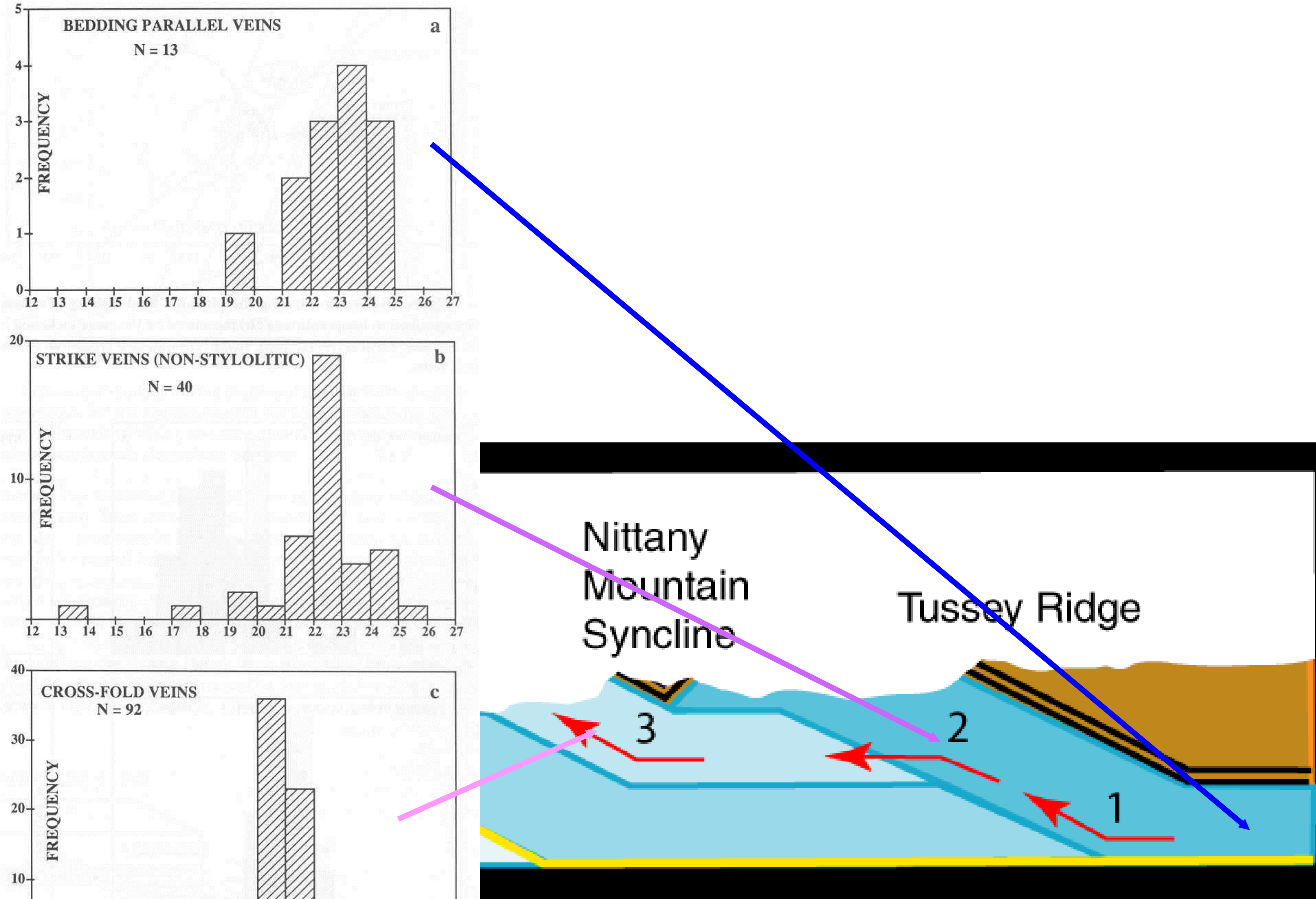

Srivastava & Engelder, 1990

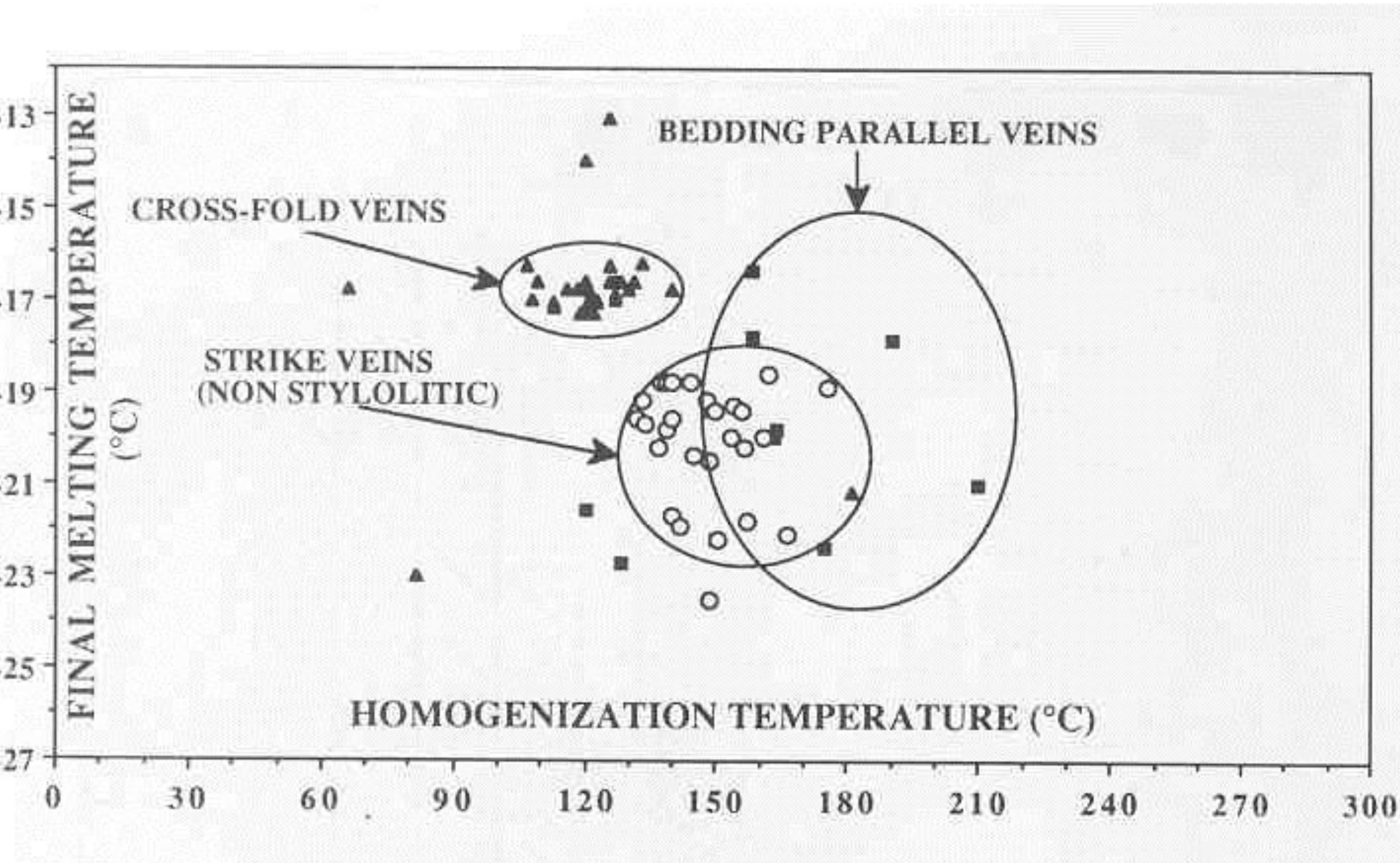

Srivastava & Engelder, 1990

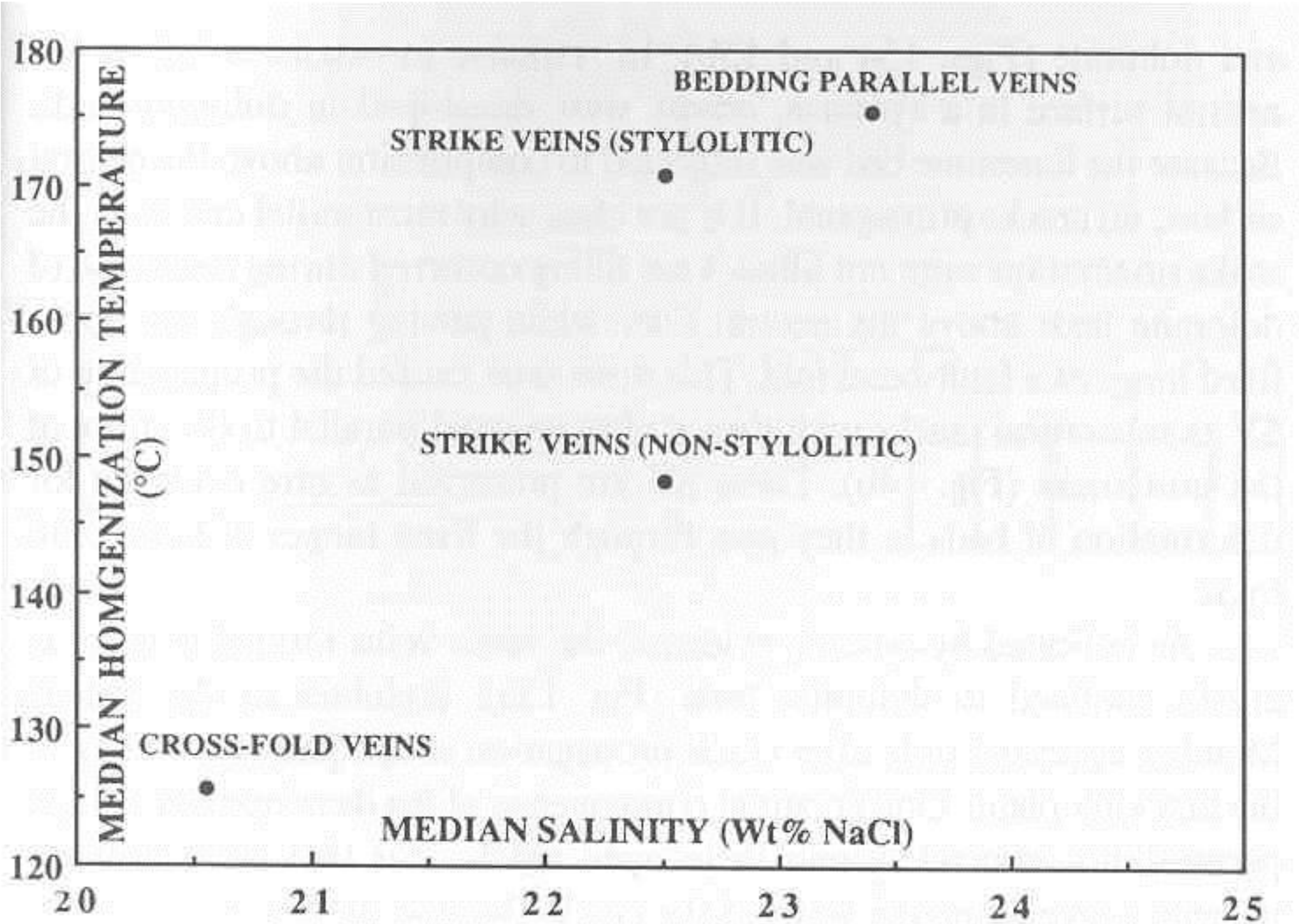

Srivastava & Engelder, 1990

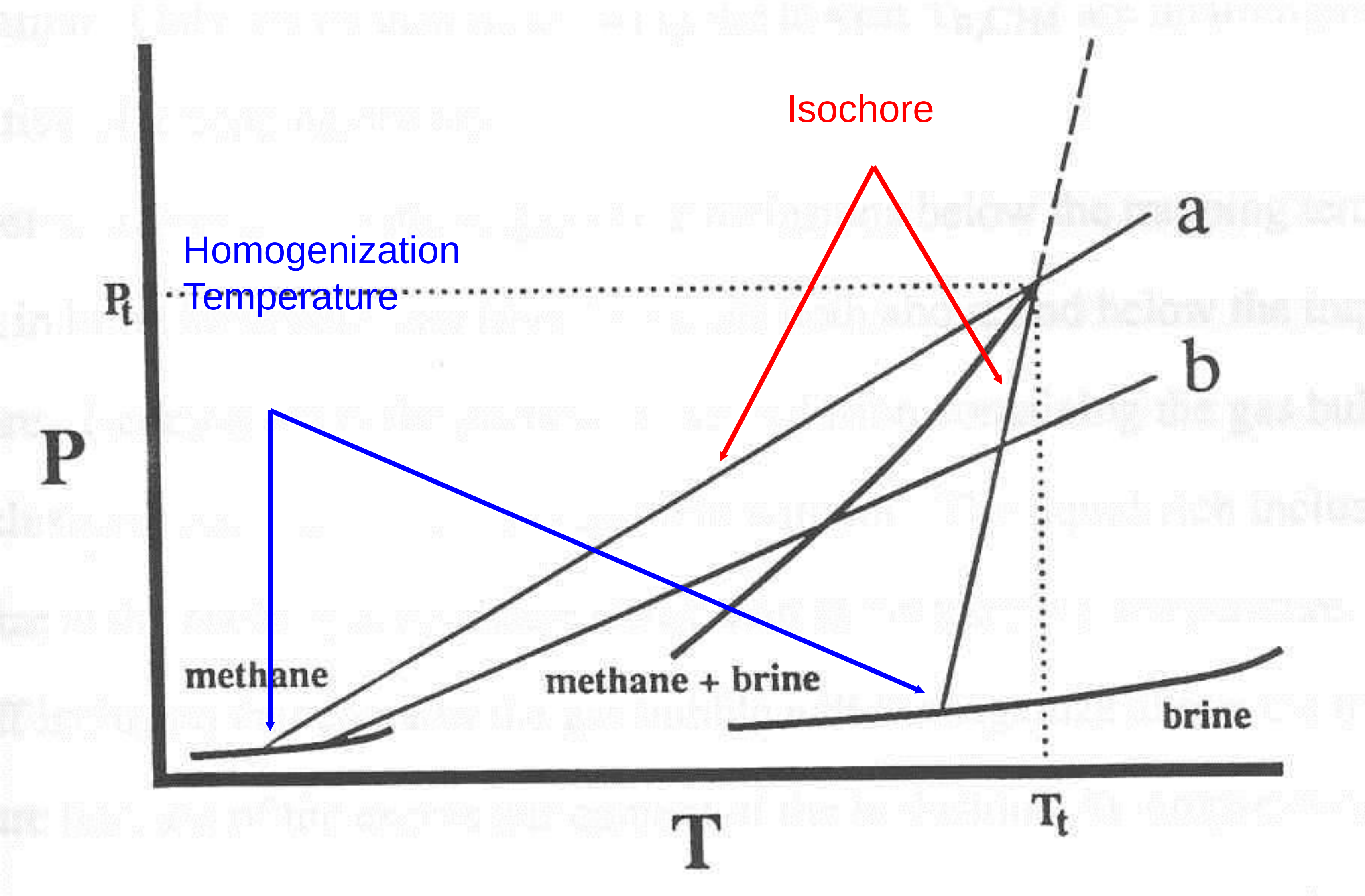

Srivastava & Engelder, 1990

- LOCHT provide constraints on trapping conditions and hence fluid pressure at the time of crack propagation.

Lines of Constant Homogenization Temperatures

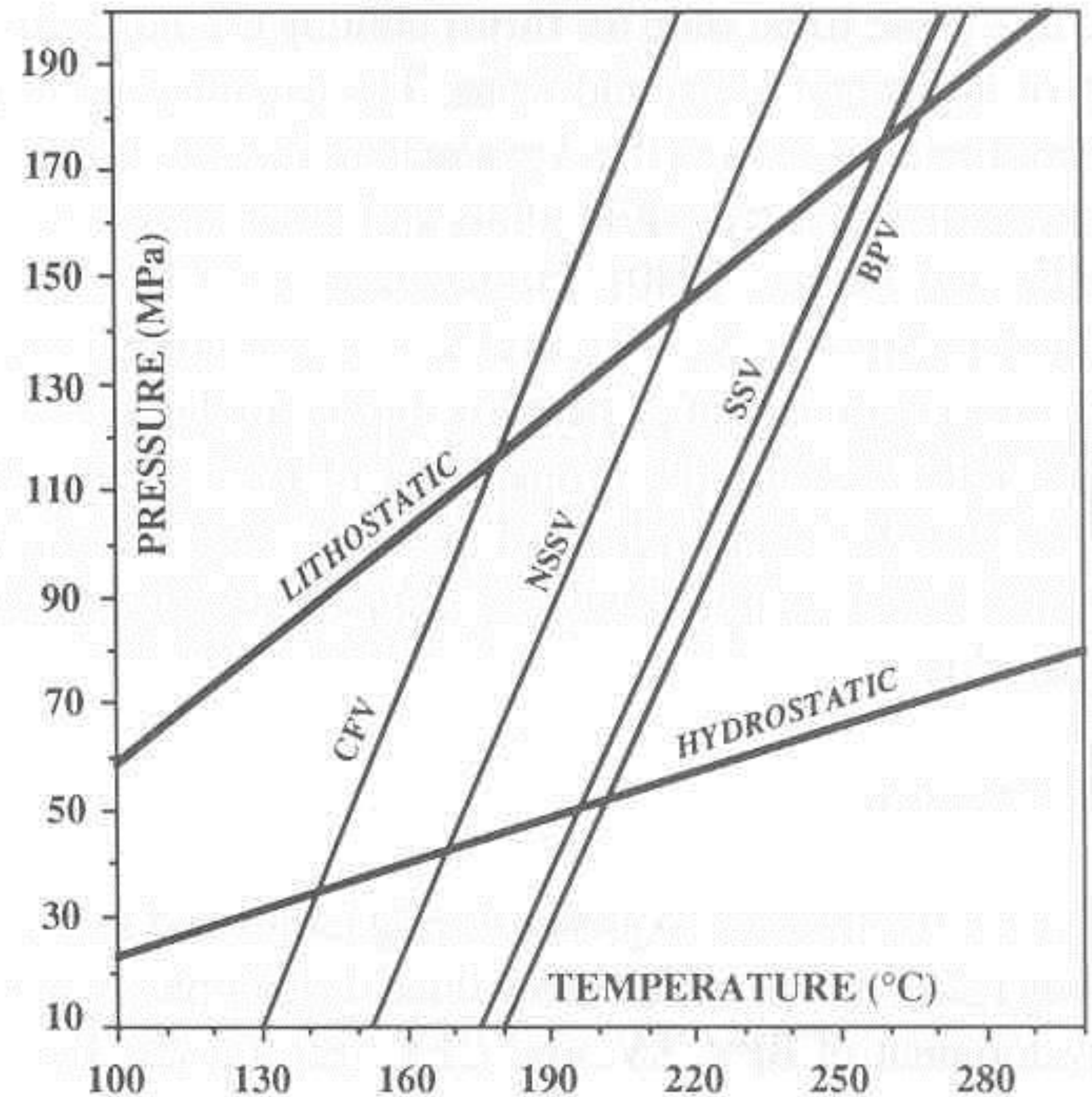

Srivastava & Engelder, 1990

[Click to View Session 5.1.1 (13.9 MB)]

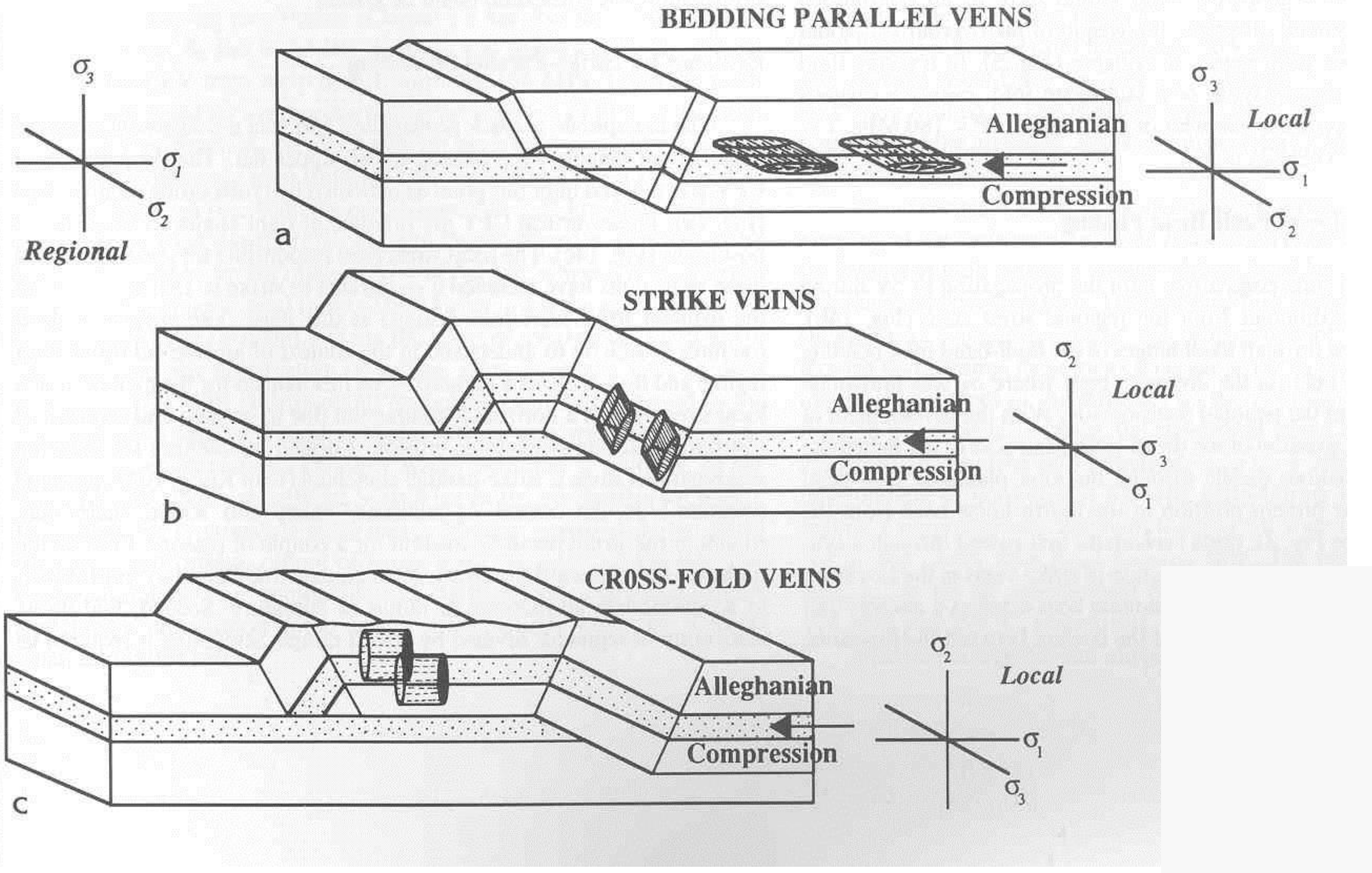

Srivastava & Engelder, 1990